APPLICATIONS OF HYBRID GROUND

SOURCE HEAT PUMP SYSTEMS TO

BUILDINGS AND BRIDGE DECKS.

By

MAHADEVAN RAMAMOORTHY

Bachelor of Engineering

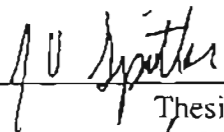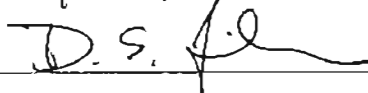Government College of Technology

Coimbatore, India

1996
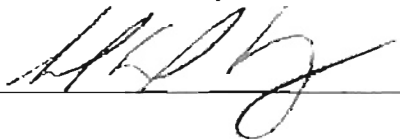
APPLICATIONS OF HYBRID GROUND

SOURCE HEAT PUMP SYSTEMS TO

BUILDINGS AND BRIDGE DECKS.
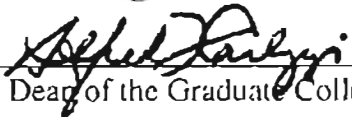
Thesis Approved:

_____

Thesis Advisor

_____

D. S.

_____

_____

Dean of the Graduate College

ACKNOWLEDGEMENTS

Last but not the least, I would like to extend my thanks to all those people especially my friends, the unsung heroes, who contributed to this work in a direct or indirect way.

TABLE OF CONTENTS

LIST OF TABLES

LIST OF FIGURES

NOMENCLATURE

C_p = specific heat capacity (kJ/kg °K)

d = diameter (m)

EFT = entering fluid temperature (°C)

ExFT = exit fluid temperature (°C)

GLHE = ground loop heat exchanger

GSHP = ground source heat pump

h = convection coefficient

HGSHP = hybrid ground source heat pump

k = thermal conductivity (W/m²/°K)

$\dot{m}$ = mass flow rate (kg/s)

Nu = Nusselt number (-)

Pr = Prandtl number (-)

Q = heat transfer rate (kW)

QSguess = heat pump source side heat transfer rate (kW)

QLguess = heat pump load side heat transfer rate (kW)

r = radius (m)

R = thermal resistance (°K per W/m)

Re = Reynolds number (-)

T = temperature (°C)

TL = heat pump load side temperature (°C)

TS = heat pump source side temperature (°C)

UA = overall heat transfer coefficient

ε = effectiveness

β = borehole shape factor coefficient (-)

ΔP = pressure drop (kPa)

Subscripts

b = borehole

c = condenser

cond = conductive

conv = convective

e = evaporator

i = inlet, inner

l = load side

o = outer

s = source side

Chapter 1

Introduction

1.1.Overview of Hybrid Ground Source Heat Pump Systems

Increasing energy demand and rapid depletion of non-renewable resources have forced mankind to search for alternative energy resources. Over the recent decades, there has been a shift towards energy efficient renewable sources of energy as compared to conventional resources. The use of ground source heat pumps (GSHPs) in commercial and residential facilities is one excellent example. GSHP systems, also known as ground coupled heat pump (GCHP) systems, use the earth as a heat source/sink to extract heat during summer for cooling applications and to reject heat during winter for heating applications. High first cost and lack of design guidelines have been two major deterrent factors in their applications to commercial facilities.

Cooling dominated buildings, having larger annual cooling loads than annual heating loads, reject more heat to the ground than they can absorb. This creates an imbalance between the heat extracted from the ground and the heat rejected to the ground. Over the years of use, the heat build up in the ground due to the imbalance causes the fluid in the ground loop to run at higher temperatures. High entering fluid temperature to the heat pump adversely affects its performance. This leads to much longer ground loop length for cooling dominated buildings than that required to meet balanced load. Hence, the GSHP systems may not be economically attractive in such cases due to the higher first costs associated with longer bore lengths. If the bore length

is sized to meet the heating requirements and an equivalent amount of cooling load, and the excess heat is rejected to the supplemental heat rejecter, significant savings in first cost can be achieved. Such systems are called hybrid ground source heat pump systems (HGSHP). Hybrid ground source heat pump systems are GSHP systems with an additional supplemental heat rejecter such as a closed-circuit liquid cooler, a cooling tower with a plate frame heat exchanger, or a shallow pond. HGSHPs may be most advantageous when compared to conventional systems due to their capital cost considerations or available surface area. Although this appears to be a good alternative, to date there has only been a limited amount of published research that addresses application of HGSHP systems.

A somewhat different type of HGSHP may be used for bridge deck de-icing applications. The preferential icing of the bridges during snow, sleet, and freezing rain conditions causes a number of accidents during winter. The conventional method of de-icing bridges using chemicals has resulted in deterioration of the bridge deck due to its corrosive nature. In this case, the system will only extract heat, and the ground temperature would naturally decrease from year to year. By using the bridge deck as a supplemental heat source, storing heat in the ground in the summer, the bore length can be reduced significantly.

1.2. Literature Review

Only a small number of published reports on hybrid ground source heat pump systems for commercial/institutional applications can be found in the literature. A summary of the available literature is discussed below.

2

The *Commercial/Institutional Ground Source Heat Pump Engineering Manual* (ASHRAE, 1995) discusses the design and sizing procedure of supplemental heat rejecters. It is suggested that the ground loop heat exchanger be sized for maximum heat extraction during the design heating hour and the supplemental heat rejecter be sized for meeting the cooling heat rejection requirements in excess of the ground loop heat exchanger capacity. The recommended sizing method is based on monthly average heating and cooling loads rather than peak loads. It also recommends the usage of supplemental heat rejecter during night hours for cooling the ground when the vertical boreholes are closely spaced. The manual also suggests guidelines for installation of supplemental heat rejecter illustrating recommended piping methods, and a few options on its operation such as set point control, operation during night hours for cold storage, and year round operation of the system in warm climates. The use of a plate heat exchanger with cooling tower for isolating the ground loop and the usage of three-way valve to bypass the ground loop are also recommended.

Kavanaugh and Rafferty (1997) suggest a few alternatives for HGSHP design based on the peak block load at the design condition. The authors emphasize the need for hybrid ground source heat pump systems due to the high first cost of excessively long ground loop lengths. The peak block load at design condition is used as a criterion for sizing supplemental heat rejecters. The capacity of the supplemental heat rejecter is calculated based on the cooling capacity of ground loop heat exchanger equal to the difference between the ground loop heat exchanger lengths required for cooling and

3

heating. The text also recommends that the supplemental heat rejecter be piped in parallel to the ground loop when the flow rate in the rejecter is much higher than the ground loop.

The design method described above is revised and extended by Kavanaugh (1998). The revisions to the design practices discussed in ASHRAE (1995) and Kavanaugh and Rafferty (1997) include the consideration of heat buildup in the ground on an annual basis. A method for balancing heat extraction from the ground with heat rejection to the ground on an annual basis to prevent the heat buildup in the ground and thereby avoiding performance degradation of the heat pump is suggested. The method assumes the use of a supplemental heat rejecter at ground loop temperatures above a set point (typically 27°C - 32°C; 80.6°F – 89.6°F) to compute the required operating hours of the supplemental heat rejecter to balance the heat flow to the ground. The design procedure is adopted for HGSHP design for a multi story office building requiring 100 tons (350 kW) of cooling for three different climatic conditions: Mobile, AL; Louisville, KY; and Minneapolis, MN. Economics of the design procedure are analyzed for the three different climates. The author concludes that HGSHP systems are most suitable for warm and hot climates due to the smaller bore length required than that for moderate and cold climates.

Phettepace and Sullivan (1998) present a performance study from data collected over a period of 22 months of a HGSHP system at a 24,000 ft^2 (2,230 m^2) military base administration building at Ft. Polk, La. The HGSHP system described in their study consisted of 70 vertical closed-loop boreholes, each 200 ft (61 m) deep and 10ft (3 m) apart. The ground loop was sized to meet the peak heating requirements of the building.

A 274 kW (78 ton) closed circuit cooling tower is used as the supplemental heat rejecter. The fan and the sump pump of the cooling tower are activated when the heat pump entering fluid temperatures exceed 36°C (96.8°F) and are shut off when the temperature falls below 35°C (95°F). The authors report that during the monitoring period, heat rejection to the ground was approximately 43 times the heat extraction. The loop temperatures during the test period are also high (peak of 40.9°C, 105.6 °F) due to the heat buildup in the ground caused by the imbalance in heat flow to the ground. Relative energy consumption of the major system components over the study period is 77% from heat pump, 19% for circulating pump, 3% for cooling tower fan, 1% for cooling tower pump as reported. The study reports an annual duty factor of 30% for the cooling tower.

Gilbreath (1996) presents design suggestions for hybrid GSHP systems using the Paragon Center as an example and attempts to establish methods for monitoring system performance through the measurement of energy consumption, demand and loop temperatures. The impact of various control options based on the percentage assistance of the heat rejecter is investigated. Effects of heat recovery and fluid flow control are also discussed. An installation and operating cost analysis is provided comparing the hybrid application to the conventional GSHP to assess and quantify potential cost savings.

Singh and Foster (1998) report on the savings in first cost of hybrid ground source heat pump systems as compared to the conventional closed loop water source heat pump systems in their study. The study was conducted on 80,000 ft^2 (7,432 m^2) Paragon Center building located in Allentown, PA, and an 85,000 ft^2 (7,897 m^2) elementary school building located in West Atlantic city, New Jersey. An HGSHP system was chosen for

the Paragon Center due to the drilling difficulties at the site that prevented from the required ground loop length being used. The system consists of 88 boreholes, each 125 ft (38 m) deep for 281 kW (80 tons) of cooling and the closed circuit cooler was sized to meet the remaining 422 kW (120 tons) of the buildings requirement. In the case of elementary school building, insufficient land area for accommodating 100% closed loop geothermal system to meet the buildings heating and cooling requirements led to the installation of HGSHP systems. The hybrid system consists of 66 boreholes, each 400 ft (122 m) deep and 468 kW (133 tons) capacity to meet the required heating and most of the cooling requirement and the closed circuit cooler of 411 kW (117 tons) is used. The report indicates savings in ground loop cost and a decrease in pay back time in both cases. The use of supplemental heat rejecters reduces the ground loop length by 40% for Paragon Center and 12 % for the elementary school building.

Yavuzturk and Spitler (2000) use a short time step simulation model to study the performance and hourly energy consumption of a 14,205 ft^2 (1,320 m^2) office building that uses a hybrid GSHP system. The merits and demerits of various control strategies for the hybrid system are analyzed for two different climatic conditions based on a 20-year life cycle cost analysis. The hybrid system reported in the study consists of an open cooling tower and a plate heat exchanger to couple two fluid loops in the system. A set point control, a differential control, and a scheduled control have been investigated in the study. The set point control activates the cooling tower when the heat pump entering or exiting temperatures exceeds 35.8°C (96.4°F). The differential control is based on a temperature differential between heat pump entering and exiting fluid temperatures and ambient wet bulb temperature. The scheduled control depends on the season and/or time

of the day during the year. The scheduled control is augmented with set point control to prevent high temperatures in the ground loop. The system simulation results indicate significant savings in first cost due to the reduced ground loop lengths for all of the operating strategies when compared to conventional GSHP systems. The authors' suggest that significant savings can be realized when the supplemental heat rejecter is operated under the most favorable conditions and the differential control strategy is used to reject heat to air at maximum efficiency. The authors' conclusion is in agreement with that of Phetteplace and Sullivan (1998) in that the heat rejecter operates at an increased efficiency when operated under the most favorable conditions.

The literature survey on applications of hybrid ground source heat pump systems to bridge deck de-icing yielded few results. A brief overview of related texts are discussed below.

Wadivkar (1997) report a study conducted on an experimental facility to analyze the feasibility of using GSHP systems for bridge deck deicing. The experimental facility consisted of an 8 inch (0.2 m) thick, 3 ft (0.9m) by 10 ft (3m) concrete slab to represent a scaled model of the bridge deck. Six 10 feet long polybutylene pipes of ¾ inch (19.05 mm) nominal diameter are buried 2.5 inches (63.5 mm) below the surface across the 3 foot width. A water source heat pump of 18,000 BTU/hr(5.3 kW) nominal capacity is used in the experimental facility. The ground loop consisted of a horizontal 500 ft (152.4 m) pipe divided into four sections, each 125 (38.1 m) ft long, and ¾ inch nominal diameter and were buried 6 ft (1.83 m), 5 ft (1.52 m), 4 ft (1.22 m), and 3 ft (0.91 m) deep in the same trench. The slab is insulated on all sides leaving only the top surface of the

7

slab exposed for heat transfer with the surroundings. The results from a detailed numerical model have been validated against the data collected from the experimental setup over a period of 8 days. The reported study suggests idling of the system prior to the snow events for effective melting of snow/ice over the slab surface. Although the numerical model predicts the transient response of the system, the predicted performance of the bridge deck reportedly was not in agreement with ASHRAE recommended guidelines. Convection and radiation losses computed by the numerical model were much higher than that computed using ASHRAE guidelines. The heat flux calculated by the ASHRAE model was much lower than the heat input predicted by the numerical model to keep the surface temperature above freezing.

Iwamoto et al. (1998) discuss the applications of underground thermal energy storage in snow melting systems in Japan. The experiment conducted over a period of 74 days at Hokkaido University is introduced and the results compared with the similar systems at Hiroshima. The system consisted of one 328 ft (100 m) vertical ground heat exchanger, heat dissipation pipes embedded in the 280 ft^2 (26 m^2) concrete pavement and a circulating pump. The circulating pump was the only component that had an electrical consumption. The "recharge" of the ground, with the heat collected using solar collectors, is employed during summer. The study reports a balance in heat extraction from the ground and the heat rejection to the ground. Though initial cost of the system is twice that of a conventional system according to the study, the operating costs were reportedly 1/8 to 1/20th that of the conventional system.

The use of passive geothermal heating systems for de-icing bridge decks dates

back to early 1970's. Considerable research on employing the heat pipes for bridge de-

icing applications have been done since their introduction in early 1940's. Heat pipes are

passive geothermal heating systems in the sense that they do not require any external

power for their operation. The circulation of the fluid depends upon the gravity return of

the condensed fluid to the high temperature end (evaporator) where it vaporizes and

returns to the low temperature end (condenser). A brief review of some of the related

texts on using heat pipes for de-icing applications are discussed below.

Ferrara and Haslett (1975) describe an experimental facility to analyze the

performance of bridge deck preferential deicing systems. The system reportedly uses 2 in.

(51 mm) diameter heat pipes installed 30 to 50 feet (9.1 m-15.2 m) deep in the ground.

Donnelly et al. (1982) suggest bridge deck heating systems using heat pipes in their

feasibility study. Different evaporator designs and various condenser spacing have been

investigated in the experimental setup to study the performance of such systems. Lee et

al. (1984) presents an experimental study conducted on a bridge deck heating using heat

pipes to transfer heat from 100 ft (31 m) vertical boreholes. The authors' report that the

heated surface is 2°C (3.6°C) to 4°C (7.2°C) higher than the unheated portion. The report

also suggest a computer model validated against data collected from two experimental

facilities.

Although passive geothermal heating systems, in the form of heat pipes, operates

without the need for pumps, controls, or external power, it has some inherent

disadvantages. The pipes should be oriented in such a way as to allow the heat exchange

9

fluid (like ammonia) to circulate due to gravity. The evaporation and condensation cycle takes place whenever the bridge deck is cooler than the earth. Even though the system does not have any operating costs, the excessive heat loss from the ground have to be compensated by an increased pipe size and/or depth which increases the first cost of the system. The plumbing in the deicing system must have enough gradient to allow the condensed fluid to flow back to the evaporators. This increases the installation cost of heat pipes into the bridge deicing system (Nydahl et al., 1984). If the pipes are not properly cleaned or if the gradient of a few condenser pipes is not sufficient, ice may form near the pipes. It takes lot of cost and effort to repair such heating systems. Moreover, the recharge of the ground during summer is not possible since the condensate from the ground loop cannot flow against gravity to the evaporator pipes in the bridge deck.

1.3. Thesis Objective and Scope

This study aims at applying and revising a detailed simulation methodology to predict the performance of hybrid vertical-loop ground source heat pump systems that are used to meet building heating and cooling requirements and bridge deck heating systems. This study coupled with earlier research attempts to achieve better understanding of such systems to establish better design guidelines in future. The three main objectives of this study can be summarized as follows:

1) To determine an optimum size for the ground loop heat exchanger and shallow heat rejecting pond of a hybrid GSHP system using a control strategy that operates the heat rejecter at most favorable conditions.

2) To make the ground loop heat exchanger, bridge deck, and heat pump models sturdy and robust and suitable for use, and create new component models in the HVACSIM+ simulation environment.

3) Finally, use the component models in various system configurations to develop a model for studying the heating and recharge strategies for bridge deck heating systems that use hybrid GSHP systems.

Chapter 2 of this thesis deals with the first objective mentioned above. The power of system simulation in analyzing different control strategies and evaluating the associated economics is evident in this chapter. System performance is evaluated by a life cycle cost comparison, determined through hour-by-hour system simulations with TRNSYS (SEL, 1997). Typical meteorological year (TMY) weather data is used for the system simulations. Building loads are determined using the Building Loads Analysis and System Thermodynamics (University of Illinois at Urbana-Champaign, 1986) simulation software.

Chapter 3 aims at exploring the structure, merits and demerits of two simulating environments, TRNSYS and HVACSIM+ (NBS, 1986). Alterations have been made to the water-to-air heat pump, water-to-water heat pump, ground loop heat exchanger, and slab model models to make them compatible with HVACSIM+. Some new models such as "gang of heat pumps", controller, and simple pump are discussed. Also, some of the models have been updated for robustness and accuracy. The simulation results of the component models have been compared with their respective simulation results from TRNSYS modeling environment.

Chapter 4 discusses the challenges faced during the intermediate steps in system modeling and the steps taken to circumnavigate them. Modifications done in the nonlinear simultaneous equation solver are discussed in detail. Finally, a workable configuration of bridge deck heating system is presented.

Chapter 5 describes the system configuration of a bridge deck heating system and its predicted performance under several strategies. During summer, the system circulates the fluid directly through the ground loop heat exchanger to reject heat to the ground. The system simulation is mainly used to study control strategies for winter heating and summer recharge. Results from the system simulation showing operation both in the winter heating mode and summer recharge mode are presented.

Chapter 2

Optimal Sizing of Hybrid Ground Source Heat Pump Systems that use a Cooling pond as a Supplemental Heat Rejecter – A system Simulation Approach

2.1. Introduction

Ground source heat pump (GSHP) systems offer an attractive alternative for both residential and commercial heating and cooling applications because of their higher energy efficiency compared with conventional systems, but their higher first cost has been a significant drawback to wider acceptance of the technology. This is especially true in commercial and institutional applications where the vertical closed-loop configuration is commonly preferred. These types of buildings are generally cooling-dominated, and therefore reject more heat to the ground than they extract on an annual basis. As a result, the required ground-loop heat exchanger (GLHE) length is significantly greater than the required length if the annual loads were balanced. One option to reduce the size of the GLHE, and therefore the first cost of the system, is to effectively balance the ground thermal loads by incorporating a supplemental heat rejecter into the system. GSHP systems that incorporate a supplemental heat rejecter have been referred to as "hybrid GSHP systems".

Supplemental heat rejection can be accomplished with a cooling tower, fluid cooler, cooling pond, or pavement heating system. Currently suggested design methods for hybrid GSHP systems attempt to size the GLHE based on the annual heating load and then size the supplemental heat rejecter to balance the annual ground loads. However, the

design of the system components also depends on the strategy used to control the supplemental heat rejecter. A smaller supplemental heat rejecter operated for more time may reject the same amount of heat as a larger supplemental heat rejecter operated for less time. Hence, a balance between the size of ground loop, size of the supplemental heat rejecter, and the control strategy is required to achieve the best economic alternative.

The work presented in this chapter is a follow-up study to that presented by Yavuzturk and Spitler (2000), where various operating strategies of a cooling tower in a hybrid GSHP system were compared by simulating the system with TRNSYS (SEL, 1997). The purpose of the Yavuzturk and Spitler (2000) work was not to find the optimum size of the system, but to compare different control strategies for the supplemental heat rejecter, assuming the GLHE had been economically sized. The objective of this paper is different in that it uses the best supplemental heat rejecter control strategy found by Yavuzturk and Spitler (2000), and then uses system simulation to determine an optimum size for the ground loop heat exchanger and shallow heat rejecting pond of a hybrid GSHP system. System performance is evaluated by a life cycle cost comparison, determined through system simulations with TRNSYS (SEL, 1997). An example small office building is chosen and the hybrid GSHP system is optimized for two climatic regions.

2.2. Methodology for System Simulation and Analysis

2.2.1. Building Description and Loads Calculation

A small office building was chosen for simulating the performance of hybrid GSHP systems. The total area of the building is approximately 14,205 ft^2 (1,320 m^2). The annual building loads are determined using Building Loads Analysis and System Thermodynamics (BLAST, 1986) simulation software. The following assumptions have been used to determine the annual building loads:

1) The building is divided into eight different thermal zones.

2) For each zone, a single zone draw through fan system is specified. The total coil loads obtained from system simulation are equal to the loads to be met with ground source heat pump system.

3) The office occupancy is taken as one person per 100 ft^2 (9.3 m^2) with a heat gain of 132 W (450 BTU/hr), which is 70% radiant.

4) A 1.1 W/ft^2 (11.8 W/m^2) of office equipment plug load as suggested by Komor (1997) is used.

5) The lighting loads are assumed to be 1 W/ ft^2 (10.8 W/m^2).

6) A thermostat set point of 68.0 °F (20.0 °C) during the day (8am-6pm) and 58.0 °F(14.4 °C) during the night is used for all zones in the building. Only heating is provided during the night, depending on the requirement.

7) Schedules for office occupancy, lighting, equipment, thermostat controls are specified.

The example building was simulated for two different climatic regions using
Typical Meteorological Year (TMY) weather data. The regions selected were Houston,
TX for its hot and humid climate and Tulsa, OK for its moderate climate. The annual
building loads determined on an hourly basis are shown in Figure 2.1.
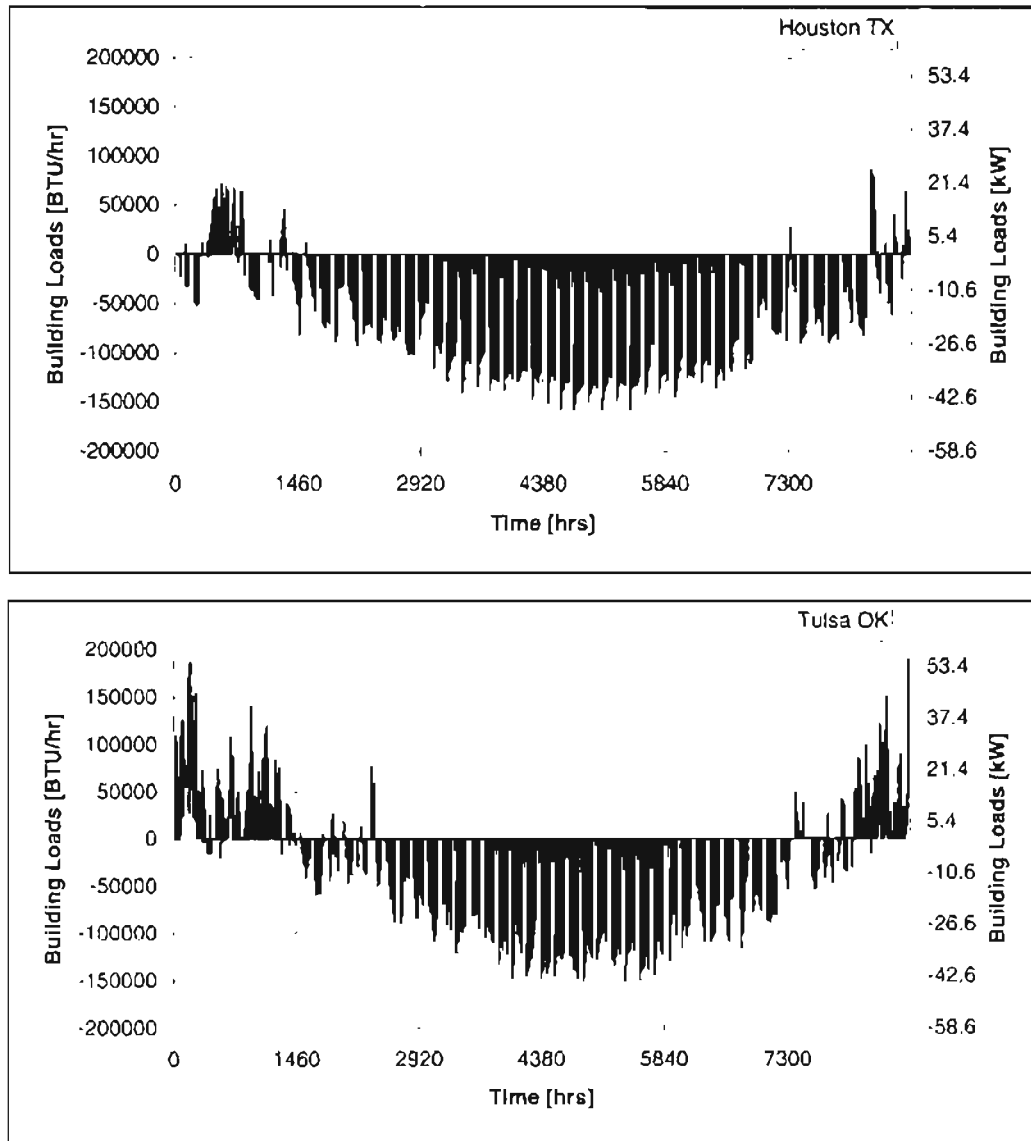
Figure 2.1. *Annual building loads for climatic conditions typical of Houston, TX and
Tulsa, OK (cooling loads are negative and heating loads are positive).*

2.2.2. Hybrid System Configuration and Component Model Description

A schematic of the hybrid GSHP is shown in Figure 2.2. The system uses two fluid circulation pumps to reduce pumping energy when the cooling pond is not being used for heat rejection. The system has been constructed in the TRNSYS modeling environment using standard and non-standard component models. The standard TRNSYS component models for components such as pumps, t-pieces, flow diverters, and the differential controller are described by SEL (1997). The non-standard component models are described below.
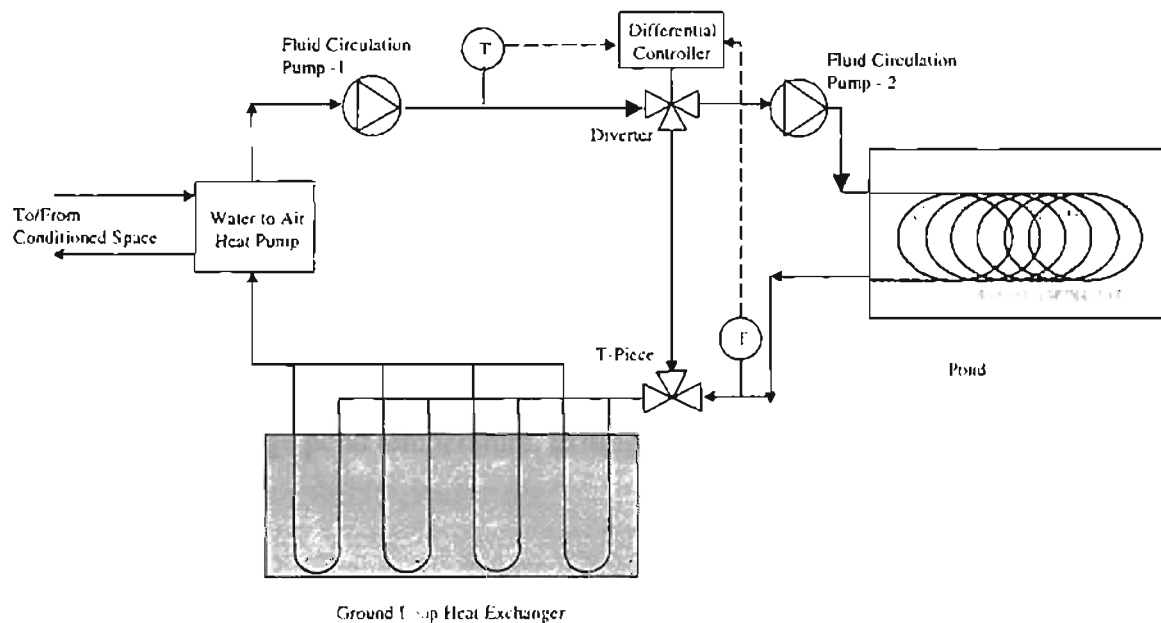
Figure 2.2. *Schematic diagram of the hybrid system component configuration*

The building is not modeled explicitly in this application. The hourly building thermal loads described previously are read from a file and passed to the heat pump subroutine, which is a simple water-to-air heat pump model that has been developed for this and other GSHP system simulations. Inputs to the heat pump model include sensible

17

and latent building loads, entering fluid temperature, and fluid mass flow rate. The model uses quadratic curve-fit equations to manufacturer's catalog data to compute the heat of rejection in cooling mode, heat of absorption in heating mode, and the heat pump energy consumption. Outputs provided by the model include exiting fluid temperature, energy consumption, and fluid mass flow rate.

The shallow pond model used in this study is that described by Chiasson et al. (2000). The model accounts for several natural heat transfer mechanisms within a shallow water body plus convective heat transfer from a closed-loop heat exchanger coil. Environmental heat transfer mechanisms that are simulated by the model include solar radiation heat gain, heat and mass transfer due to evaporation, convection heat transfer to the atmosphere, thermal or long-wave radiation heat transfer, conduction heat transfer to the surrounding soil or fill material, and ground water discharge contributions. A lumped-capacitance approach is taken and the resulting first-order differential equation describing the overall energy balance on the pond is solved numerically. Outputs provided by the model include average pond temperature, exiting fluid temperature, and heat rejected to the pond.

The GLHE model used in this study is that described by Yavuzturk and Spitler (1999), which is an extension of the long-time step temperature response factor model of Eskilson (1987). It is based on dimensionless, time-dependent temperature response factors known as g-functions, which are unique for various borehole field geometries. In order to compute the average temperature of the borehole field for each time step, the time-dependent ground loads profile is decomposed into unit pulses and superimposed in

18

time using the corresponding temperature response factors. The model includes a flexible load aggregation algorithm that significantly reduces computing time. The main output provided by the model includes the exiting fluid temperature.

2.2.3. Ground and Pond Loop Sizing

The peak entering fluid temperature (EFT) to the heat pump is one of the critical factors in the sizing of any GSHP system. The ground loop is sized to maintain the heat pump entering fluid temperature between approximately 25 °F and 105 °F (-3.4°C and 40.6°C). The design peak EFT usually varies from 85.0 °F to 95.0 °F (29.4°C to 35.0°C) depending upon the manufacturer and make of the heat pump. The peak EFT can be as high as 110.0 °F (43.3 °C) for high efficiency rated heat pumps. Similarly, the heat pump entering fluid temperature is also constrained by a lower limit depending on the heat pump and the heat exchanger fluid used in the ground loop. For colder climates, antifreeze is required to prevent the working fluid from freezing. Hence the sizing of the ground loop and shallow heat rejection pond are bound by the upper and lower limits of the heat pump entering fluid temperatures.

The study of Yavuzturk and Spitler (2000) showed that the best control strategy for the supplemental heat rejecter (in that case, a cooling tower) was to reject heat under the most favorable conditions. More specifically, the best results were achieved when the cooling tower was operated when the difference between the ambient wet bulb temperature and the heat pump exiting fluid temperature exceeded a set value. In this present study, we adopt a similar control strategy, which is to reject heat to the pond

19

when the difference between the average pond temperature and the heat pump exiting fluid temperature exceeds a set value. For Tulsa, an additional set point control based on the heat pump exiting fluid temperature is used to prevent operation of the pond heat exchanger when there is a danger of freezing the heat exchange fluid. The ground and pond loop sizing method is described below for each simulation case. In all cases, the simulation time was 20 years.

Case 1 (base case): For this case, the ground loop heat exchanger was sized for use without any supplemental heat rejecter. The system simulation for this case included the heat pump, GLHE, and the circulation pump for the main loop. The optimal ground loop size for each climatic condition was found by adjusting the borehole depth such that the peak EFT was kept below 96.6 °F (35.8 °C). The borehole field for Houston for the base case consisted of 36 boreholes in a 6x6 configuration with a borehole depth of 250 ft (76.2 m) and a bore spacing of 12.5 ft (3.8 m). The borehole field for Tulsa for the base case consisted of 12 boreholes in a 3x4 configuration with a borehole depth of 240 ft (73.2 m) and a bore spacing of 12 ft (3.7 m).

A larger loop was required for Houston because of the greater imbalance in cooling load with respect to the heating load. The heat transfer fluid for both cases was water with a flow rate of 3.0 gpm (0.1893 m³/s) per borehole. Undisturbed ground temperatures of 73 °F (22.8 °C) for Houston and 63 °F (17.2 °C) for Tulsa were chosen for the system simulation. Other parameters included a constant thermal conductivity of 1.2 BTU/hr-ft-°F (2.8 W/m-K) for the ground, borehole radius of 3.5 inches (88.9 mm), U-tube pipe nominal diameter of 1.25 inches (31.75 mm), and conductivity of the

.

thermally enhanced grout at 0.85 BTU/hr-ft-°F (1.47 W/m-k) for both climatic conditions.

Cases 2, 3, 4, and 5: For these cases, the borehole field was reduced from 36 (6x6 configuration) boreholes to 12 boreholes (3x4 configuration) for Houston and from 16 (4x4 configuration) to 9 boreholes (3x3 configuration) for Tulsa. The shallow heat rejection pond loop circuit was tied to the reduced size GLHE loop circuit as shown previously in Figure 2.2. Heat was rejected to the pond by operating the circulation pump (pump 2 as shown in Figure 2.2) using the differential control strategy as described above for Houston. For Tulsa, in addition to the differential control strategy, a set point control was used. The set point control shuts off the pond when the heat pump exiting fluid temperature falls below 50 °F (10 °C). This ensured that the loop circulating fluid temperature did not fall below freezing and thereby avoided the use of antifreeze solutions. The temperature differential selected was 14.4°F (8°C) with a dead band range of 9°F (5°C). The pond model was set up to simulate a 2-feet (0.61-m) deep pond with a series of horizontally positioned, 500 ft (152.40 m) long, ¾ in. (19.4 mm) nominal diameter, high-density polyethylene "slinky" heat exchanger coils. Each slinky was configured such that the resultant coil was 40 ft (12.19 m) long with a diameter of 3 ft (0.91 m), thus occupying an area of 120 ft^2 (11.1 m^2).

For each increasing case number (2 through 5), the pond area and the number of slinky coils were progressively increased, keeping the control strategy constant. The number of slinky heat exchanger coils that occupy the pond dictated the pond area. As the pond area was increased, the borehole depth was decreased so that the peak entering

fluid temperature to the heat pump determined after a 20 year simulation was within acceptable limits. For the Houston case, the critical design temperature was the <u>maximum</u> heat pump EFT because of the predominant cooling load. However, for the Tulsa case, once a pond was added, the critical design temperature was the <u>minimum</u> heat pump exiting fluid temperature (ExFT) because of the relatively higher peak heating loads. Therefore, borehole depths were adjusted for the Houston case to keep the maximum heat pump EFT below 96.6 °F (35.9 °C), and for Tulsa to keep the heat pump minimum ExFT above 35.6 °F (2 °C).

Table 2.1 summarizes the pond surface area, the number and depth of boreholes, and the differential control strategy for each case for Houston and Tulsa respectively.

Table 2.1. Summary of Design Parameters for each Simulation Case

Houston, TX

Case	No. of Pond Slinky Coils	Pond Area ft² (m²)	No. of Boreholes (arrangement)	Borehole Depth ft (m)	Differential Control (HP ExFT-T Pond) Dead Band Temperature, F (C) High	Low	Set Point Temperature F (C)
Case 1	None	N/A	36 (6x6)	250 (76.2)	N/A	N/A	N/A
Case 2	2	240 (22.3)	12 (3x4)	258.7 (78.9)	14 4 (8)	5.4 (3)	N/A
Case 3	4	480 (44.6)	12 (3x4)	170 0 (51.8)	14 4 (8)	5.4 (3)	N/A
Case 4	6	720(66.9)	12 (3x4)	101.96 (31.1)	14 4 (8)	5.4 (3)	N/A
Case 5	8	960 (89 2)	12 (3x4)	85.6 (26.1)	14 4 (8)	5 4 (3)	N/A

Tulsa, OK

Case	No. of Pond Slinky Coils	Pond Area ft² (m²)	No. of Boreholes (arrangement)	Borehole Depth ft (m)	Differential control (HP_ExFT-T_Pond) Dead Band Temperature, F (C) High	Low	Set Point Temperature F (C)
Case 1	None	N/A	16 (4x4)	240 (73.2)	N/A	N/A	50 (10)
Case 2	1	120 (11 2)	9 (3x3)	300 8 (91.7)	14 4 (8)	5 4 (3)	50 (10)
Case 3	2	240 (22.3)	9 (3x3)	304 7 (92.9)	14 4 (8)	5 4 (3)	50 (10)
Case 4	4	480 (44.6)	9 (3x3)	322 4(98.3)	14 4 (8)	5.4 (3)	50 (10)
Case 5	6	720(66.9)	9 (3x3)	340.2 (103.7)	14 4 (8)	5 4 (3)	50 (10)

Note. N/A = not applicable

2.3. Result and Discussion

2.3.1. Analysis of system performance

Table 2.2 summarizes the borehole depths, operating hours, operating temperatures, and energy consumption for each case. The details are further discussed below.

Table 2.2. Summary of the System Performance for All Cases

Houston TX

		Case 1	Case 2	Case 3	Case 4	Case 5
Number of boreholes (arrangement)		36 (6x6)	12 (3x4)	12 (3x4)	12 (3x4)	12 (3x4)
Depth of boreholes, ft[m]		250 (76.2)	258.7 (78.9)	170.0 (51 8)	102.0 (31.1)	85.6 (26 1)
Pond area, ft² [m²]		N/A	240 (22.3)	480 (44.6)	720 (66.9)	960 (89 2)
Max. flow rate [gpm]	GLHE	108	36	36	36	36
	Pond	N/A	8	16	24	32
Operation of the pond [hrs]	Year 1	N/A	3800	3308	2497	2273
	Year 20	N/A	4549	3472	2451	2209
	Average	N/A	4422	3447	2452	2212
Average Annual Energy consumption [kWh] 1. Main circulation pump		11996	4092	3146	2420	2246
2. Pond circulation pump		N/A	299	466	497	598
3. Heat pump		24245	23101	22198	21583	20452
Heat Pump EWT, F [C] during 20 year operation	Max.	96.6 (35 9)	96.6 (35.9)	96.6 (35.9)	96.6 (35.9)	96.8 (36.0)
	Min	71.3(21 8)	59.4(15.2)	48.95(9.42)	38.62(3.68)	35.58(1.99)
Heat Pump ExWT, F [C] during 20 year operation	Min.	N/A	56.9(13 8)	46.6(8 1)	36.7(2.6)	35.9(2.0)

Tulsa OK

		Case 1	Case 2	Case 3	Case 4	Case 5
Number of boreholes (arrangement)		16 (4x4)	9 (3x3)	9 (3x3)	9 (3x3)	9 (3x3)
Depth of boreholes, ft[m]		240 (73.2)	300.8 (91.7)	304.7 (92.9)	322 4(98.3)	340.2 (103 7)
Pond area, ft² [m²]		N/A	120 (11.2)	240 (22.3)	480 (44.6)	720 (66.9)
Max flow rate [gpm]	GLHE	48	27	27	27	27
	Pond	N/A	4	8	16	24
Operation of the pond [hrs]	Year 1	N/A	3002	2861	2475	2173
	Year 20	N/A	4177	3434	2589	2089
	Average	N/A	3940	3315	2569	2102
Average Annual Energy consumption (kWh) 1. Main circulation pump		5190	3405	3436	3578	3720
2. Pond circulation pump		N/A	133	224	347	426
3. Heat pump		19927	19160	18080	17041	16664
Heat Pump EWT, F [C] during 20 year operation	Max.	96.4 (35.8)	93.7 (34.3)	87.7 (30.9)	81.9 (27.7)	80.3 (26.7)
	Min	50.2 (10.1)	44.8 (7.1)	44.8(7 1)	43.8 (6 7)	41.2 (5.1)
Heat Pump ExWT, F [C] during 20 year operation	Min	N/A	35.6 (2.00)	35.6 (2.00)	35.6 (2 00)	35.6 (2.00)

N/A: Not applicable

23

Case 1 (base case): The heat pump EFTs for the 20-year simulations are shown in Figure 2.3. The gradual increase in the maximum peak EFT from year to year is typical of cooling-dominated buildings. For the Houston case, the maximum peak EFT to the heat pump was 96.8 °F (36.0 °C), occurring at the end of the 20th year and the minimum EFT is 71.2 °F (21.8 °C), which occurred during first year. For the Tulsa case, the peak EFT was 96.9 °F (36.1 °C) and minimum EFT to the heat pump was 50.2 °F (10.1 °C).
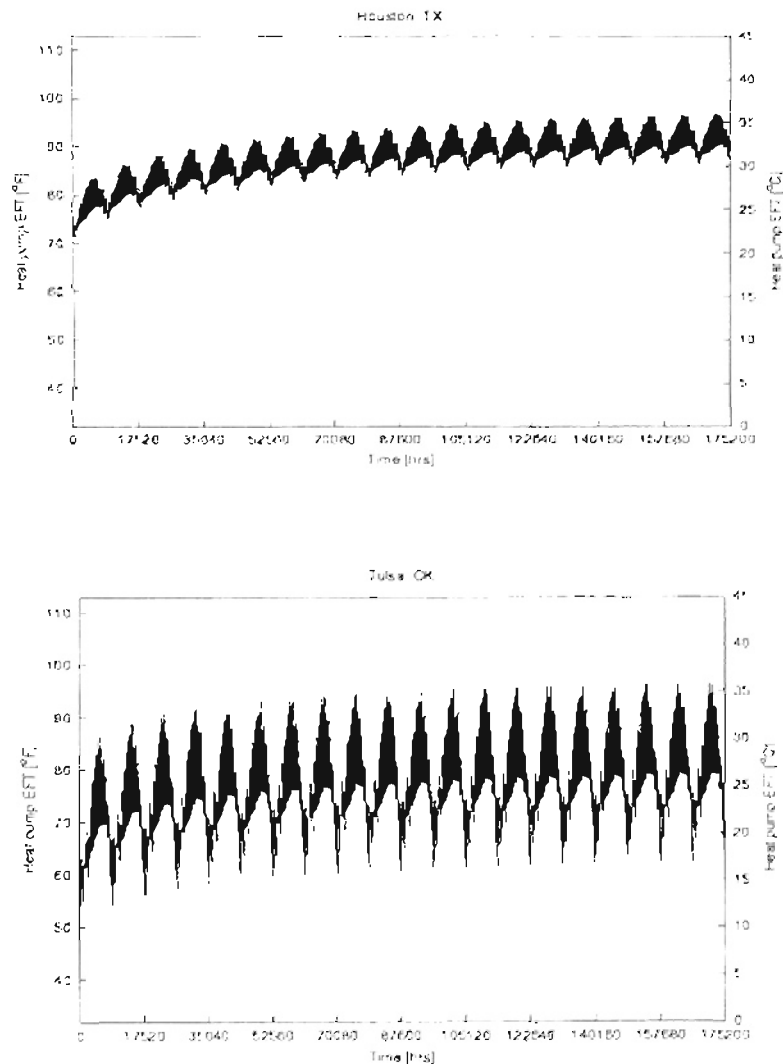
Figure 2.3. *Hourly entering fluid temperatures to the heat pump for Houston, TX and Tulsa, OK climatic conditions- Case 1 (Base Case).*

24

The total power consumed by the heat pump was 67 % of the total energy consumption for the Houston case and 79% for the Tulsa case. The total energy consumption of the main circulation pump for Tulsa was significantly smaller than for Houston due to the shorter length of the Tulsa GLHE.

Case 2: For Houston, a pond of surface area 240 ft² (22.3 m²) with two "slinky" heat exchanger coils was added as the supplemental heat rejecter, reducing the total GLHE length by 65.5%. The pond was observed to operate approximately 50% of the year. The total energy consumption of the system was reduced relative to the base case by 24.2%, mainly due to a reduction in pumping energy caused by the reduction in the GLHE size. A 4.7% decrease in heat pump energy consumption results from lower entering fluid temperatures.

For Tulsa, a pond of surface area 120 ft² (11.2 m²) with one "slinky" heat exchanger coil was added as the supplemental heat rejecter, reducing the total GLHE length by 29.5%. The pond operates approximately 45% of the year. The total energy consumption was reduced relative to the base case by 9.6%. Note that the peak EFT for Tulsa Case 2 was less than the original target limit of 96.6 °F (35.9°C) (Table 2.2). This implies that the GLHE length could be further reduced. However, when the GLHE was further reduced, the heat pump minimum exiting fluid temperature during the heating season was observed to be unacceptable, falling below the freezing point of water. For this reason, the set point control was necessary to limit heat rejection from the pond. Alternatively, it is possible that a more sophisticated control strategy would limit heat

25

rejection from the pond in such a way as to further improve the performance by shifting some of the seasonal heat rejection until after the bulk of the heating season has occurred.

Case 3: For Houston, the number of "slinky" heat exchanger coils was increased to four, reducing the total GLHE length by 77.3% from the base case. The pond was observed to operate approximately 39% of the year. The total energy consumption was reduced relative to the base case by 28.8%, about 4.6% lower than in Case 2.

For Tulsa, the number of "slinky" heat exchanger coils was increased to two, reducing the total GLHE length by 28.6% from the base case. The pond was observed to operate approximately 38% of the year. The total energy consumption was reduced relative to the base case by 13.4%, about 3.8% lower than Case 2. However, note that the GLHE size for Case 3 has increased from that of Case 2 by about 0.9%. This increase in the necessary size of the GLHE was due to the increased amount of heat rejected to the larger pond, which decreased the amount of heat rejected to the ground. With less heat rejected to the ground, a larger GLHE was needed to meet the peak heating load in the winter. At this stage, the point of diminishing returns for increasing the size of the pond has been reached for Tulsa. Figure 2.4 shows the hourly heat pump fluid temperatures for Tulsa for comparison purposes to the base case. The impact of the cooling pond on the heat pump EFT is evident; year-to-year increases in the maximum EFT, as observed in the base case, are eliminated.
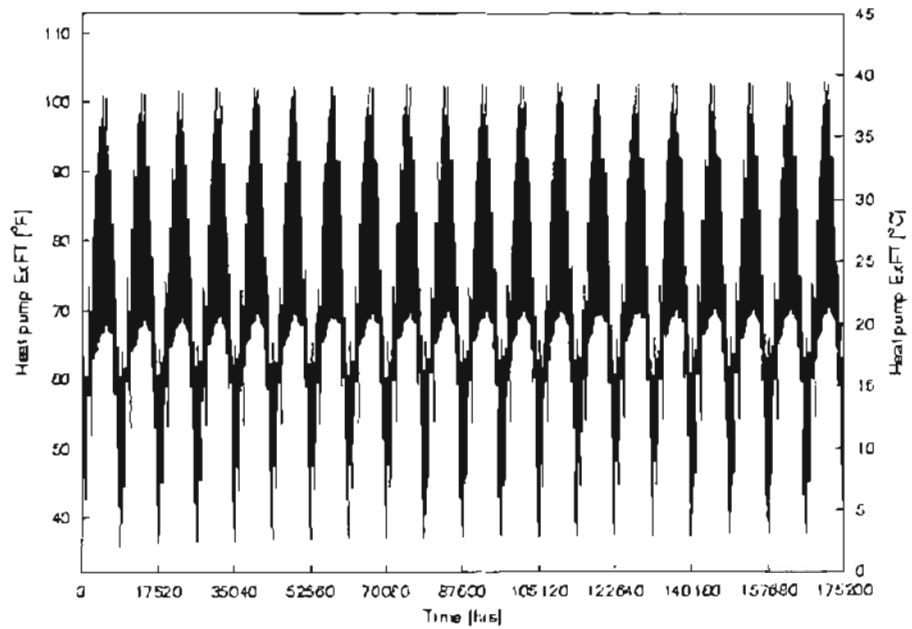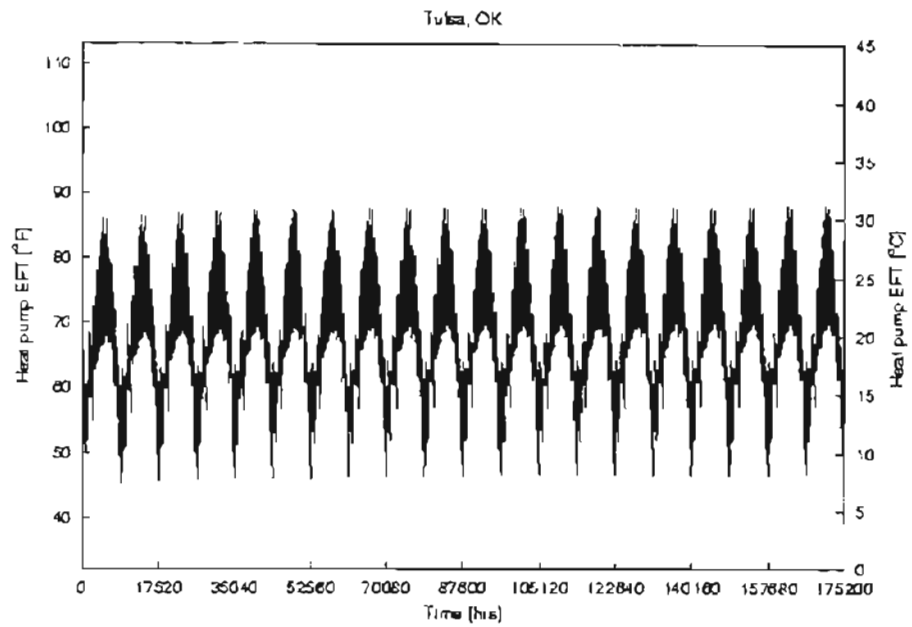
Figure 2.4. *Hourly heat pump entering fluid (EFT) and exiting fluid (ExFT) temperatures for Tulsa, OK climatic conditions-* **Case 3.**

27

Case 4: For Houston, the number of "slinky" heat exchanger coils was increased to six, reducing the total GLHE length by 86.4% from the base case. The pond was observed to operate approximately 28% of the year. The total energy consumption was reduced relative to the base case by 32.4%, about 3.6% lower than in Case 3.

For Tulsa, the number of "slinky" heat exchanger coils was increased to four, reducing the total GLHE length by 24.4% from the base case. For reasons described above, the GLHE size for Case 4 needed to be about 4.2% larger than for Case 3 to meet the heating loads. The pond was observed to operate approximately 29% of the year. The total energy consumption was reduced relative to the base case by 16.5%, about 3.1% lower than Case 3.

Case 5: For Houston, the number of "slinky" heat exchanger coils was increased to eight, reducing the total GLHE length by 88.6% from the base case. The pond was observed to operate approximately 25% of the year. The total energy consumption was reduced relative to the base case by 35.7%, about 3.3% lower than in Case 4. Since the pond loop is connected in series with the ground loop, this case represents the maximum possible size of the pond loop, without either reducing the flow in the individual pond loops or increasing the flow in the GLHE. The number of "slinky" coils results in the total flow rate through the pond loop to be equal to the total flow rate through the ground loop (i.e. all flow is diverted to the pond when the pond circulation pump is operational for this case). Although a larger pond would result in more surface area available for evaporative cooling to occur, increasing the number of "slinky" coils in the pond would result in a decrease in the Reynolds Number of the flow through each coil, thereby reducing the heat

28

rejection rate. Figure 2.5 shows the hourly heat pump fluid temperatures for Houston for comparison purposes to the base case. The impact of the cooling pond on the heat pump EFT is evident; annual temperature increases observed in the base case are eliminated.
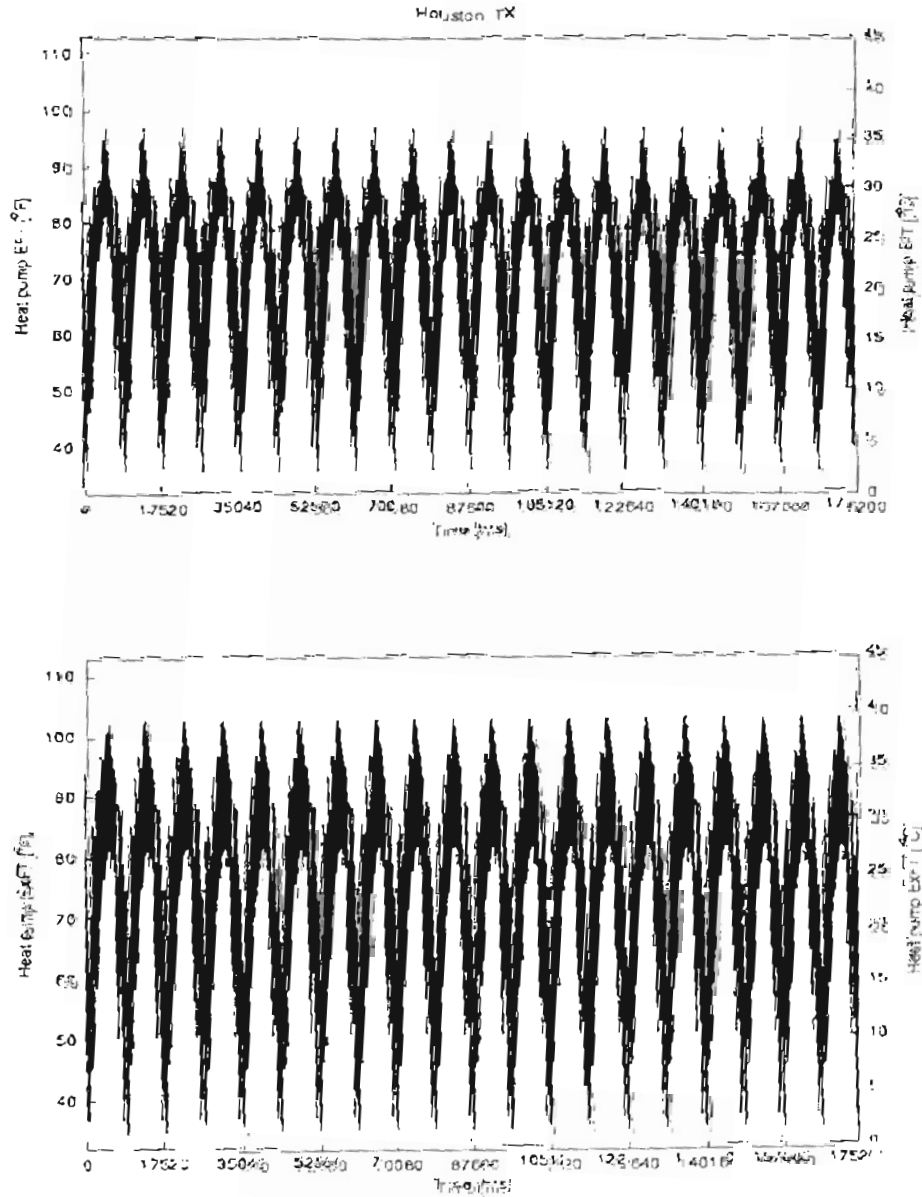
Figure 2.5. *Hourly heat pump entering fluid (EFT) and exiting fluid (ExFT) temperatures to the heat pump for typical Houston, TX climatic conditions. 20-year simulation -- Case 5.*

29

For Tulsa, the number of "slinky" heat exchanger coils was increased to six, reducing the total GLHE length by 20.3% from the base case. For reasons described above, the GLHE size for Case 5 needed to be about 4.1% larger than for Case 4 to meet the heating loads. The pond was observed to operate approximately 24% of the year. The total energy consumption was reduced relative to the base case by 17.1%, about 1.4% lower than Case 4.

2.3.2.Summary of System Performance

The trend of decreased total system energy consumption is observed for all cases as the pond size increases. This decrease is observed because of decreased heat pump energy consumption, which is due to reduced heat pump entering fluid temperatures. For Houston, the pumping energy consumption also decreases with increasing pond size because of the associated decrease in GLHE size. While this was not true for Tulsa, the reduction in heat pump energy consumption still offsets the increases in pumping power beyond Case 2.

Figure 2.6 shows the frequency of the pond usage in the 1st year, the 20th year, and the 20-year average for all cases. For Cases 4 and 5 in both the Houston and Tulsa examples, the annual utilization of the pond remains nearly constant over the years. This constant pond usage means that it was sized in such a way that the annual heat rejection to the ground loop is approximately balanced with the annual heat extraction, ensuring an approximately steady periodic annual fluctuation in GLHE fluid temperatures. An imbalance in the ground loads due to the under- or over-sizing of the pond or due to the control strategy used, is reflected by the imbalanced frequency of pond utilization as

demonstrated by Cases 2 and 3. An undersized pond results in less heat to be rejected to the pond and more heat to be rejected to the ground, therefore increasing the operation of the pond over the years. Conversely, an oversized pond results in less heat to be rejected to the ground loop, thereby decreasing the pond utilization over the years.
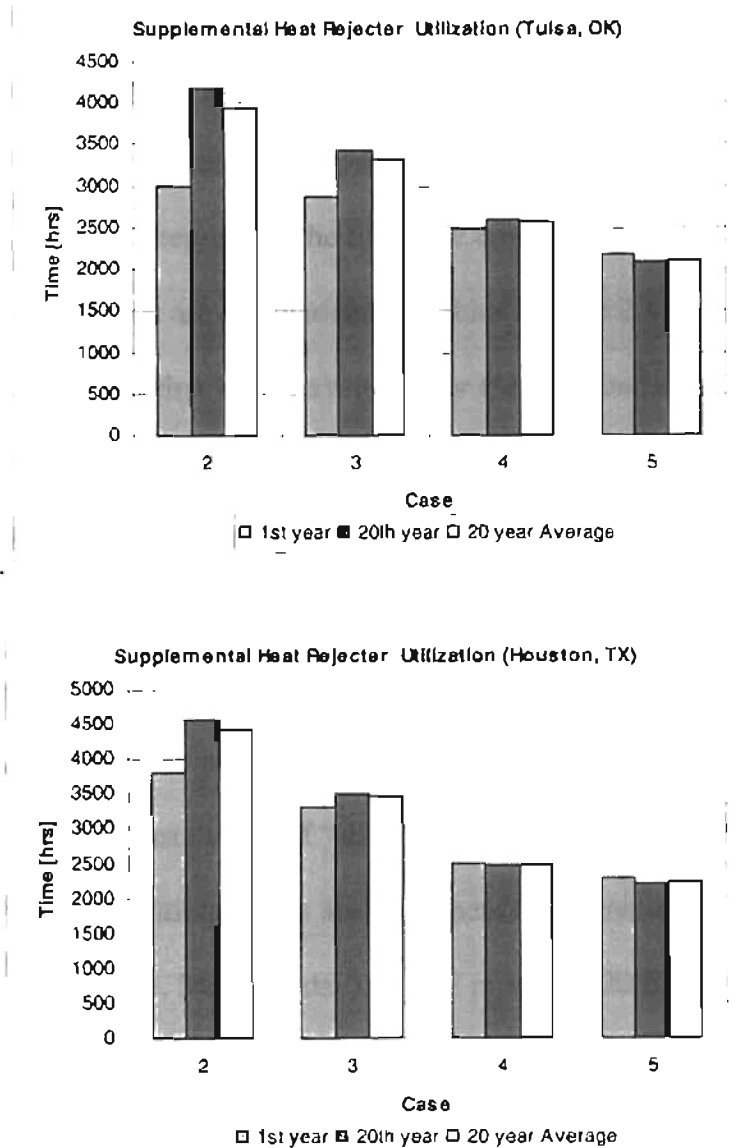
Figure 2.6. *Annual operating hours for the pond supplemental heat rejecter for Houston, TX and Tulsa, OK.*

Given the above, it would appear that the larger pond sizes are the best design options in both climatic regions. However, as further economic analysis shows, the economics of the system are dominated by other factors.

2.3.3. *Life Cycle Cost Analysis*

A life cycle cost analysis was performed to evaluate the economics of the various cases that were simulated. A present value approach was selected to compare the alternatives—the present value represents the life cycle cost in present dollars. The results of the economic analysis are summarized in Tables 2.3 and 2.4. One major assumption in the analysis was that land is available for the pond construction at no cost, and that the resale value of the property is not diminished by the pond construction. Additional assumptions are as follows:

a) Ground loop costs: $6.00/ft ($19.69/m) of bore, which includes the material cost of the pipe, horizontal runs and connections, and labor.

b) Pond loop costs: $21/yd^3 of pond volume, which includes costs of excavation, labor, fabrication and installation of "slinky" coils, and assumes an excavation rate of 12.5 yd^3/hr. Additional costs are equipment rental inclusive of pickup and delivery ($350/ half day, $430 full day), HDPE pipes ($0.20/ft, $0.66/m), pond liner ($0.75/ft^2, $8.07/m^2), and pump and controls.

c) Electricity rate cost: $0.07 per kWh.

d) Interest rate: 6% annual percentage rate (compounded annually over the 20 year design period).e) A head loss of 2.67 ft/100 ft (2.67 m/100 m) of pipe length is taken for the ground loop and pond loop.

Table 2.3. Life Cycle Cost Analysis Summary for each Case for Houston, TX

	Case 1	Case 2	Case 3	Case 4	Case 5
Number of boreholes	6x6	3x4	3x4	3x4	3x4
Depth of the boreholes [ft]	250	258.7	170	101.96	85.63
Total bore length [ft]	9000	3104	2040	1224	1028
Ground loop installation cost	$ 54,000	$ 18,626	$ 12,240	$ 7,341	$ 6,165
Savings due to reduced size of the borehole field		$ 35,374	$ 41,760	$ 46,659	$ 47,835
Pond Area [ft^2]		240	480	720	960
Pond Excavation & other costs		$ 975	$ 1,544	$ 2,186	$ 2,751
Number of spools in the pond	0	2	4	6	8
Cost of the Slinky coils		$ 200	$ 400	$ 600	$ 800
Total First cost of the pond		$ 1,175	$ 1,944	$ 2,786	$ 3,551
Annual Operating cost: 1. Main circulation pump	$ 840	$ 286	$ 220	$ 169	$ 157
2. Pond circulation pump		$ 21	$ 33	$ 35	$ 42
3. Heat pump	$ 1,697	$ 1,617	$ 1,554	$ 1,511	$ 1,432
Total annual operating cost	$ 2,537	$ 1,924	$ 1,807	$ 1,715	$ 1,631
Present Value of the operating cost of the system	$ 29,098	$ 22,073	$ 20,723	$ 19,672	$ 18,704
Net Present Value of the system	$ 83,098	$ 41,874	$ 34,907	$ 29,798	$ 28,421

Table 2. 4. Life Cycle Cost Analysis Summary for each Case for Tulsa, OK

	Case 1	Case 2	Case 3	Case 4	Case 5
Number of boreholes	4x4	3x3	3x3	3x3	3x3
Depth of the boreholes [ft]	240	300.8	304.7	322.4	340.2
Total bore length [ft]	3840	2707	2742	2902	3061
Ground loop installation cost	$ 23,040	$ 16,241	$ 16,452	$ 17,410	$ 18,369
Savings due to reduced size of the borehole field		$ 37,760	$ 37,548	$ 36,590	$ 35,631
Pond Area [ft^2]		120	240	480	720
Pond Excavation & other costs		$ 692	$ 975	$ 1,544	$ 2,186
Number of spools in the pond	0	1	2	4	6
Cost of the Slinky coils		$ 100	$ 200	$ 400	$ 600
Total First cost of the pond		$ 792	$ 1,175	$ 1,944	$ 2,786
Annual Operating cost: 1. Main circulation pump	$ 363	$ 238	$ 241	$ 250	$ 260
2. Pond circulation pump		$ 9	$ 16	$ 24	$ 30
3. Heat pump	$ 1,395	$ 1,341	$ 1,266	$ 1,193	$ 1,166
Total annual operating cost	$ 1,758	$ 1,589	$ 1,522	$ 1,468	$ 1,457
Present Value of the operating cost of the system	$ 20,166	$ 18,224	$ 17,455	$ 16,834	$ 16,709
Net Present Value of the system	$ 43,206	$ 35,257	$ 35,082	$ 36,188	$ 37,863

33

An analysis of the data presented in Tables 2.3 and 2.4 shows that Case 5 is the lowest cost alternative for Houston and Case 3 is the lowest cost alternative for Tulsa. It is evident from this economic analysis that the system life cycle cost is mainly dominated by the ground loop first costs, given, of course, that an acceptable control strategy is employed.

It is interesting to note that the ground loop length increases with increase in pond surface area for Tulsa. With the increase in pond area, additional heat is extracted from the ground during winter. As a result, the ground loop temperatures are lowered and a longer ground loop is needed to prevent the temperatures in the loop from freezing during winter. A set point control, with minimum heat pump ExFT as the critical design criteria, has been used in addition to the differential control so that the circulating fluid is maintained above freezing during peak heating conditions. Alternately, the use of an antifreeze (like propylene glycol) solution as a heat exchange fluid or a control strategy that prevents excess heat rejection to the pond would have achieved the same effect without increasing the necessary GLHE lengths and the first costs associated with it.

The system life cycle cost for each case was normalized to the base case and plotted versus the ratio of pond loop length to total loop length in Figure 2.7. A review of this figure demonstrates that the higher the annual demand for cooling in a particular building, the greater the economic benefit can be realized by incorporating a pond supplemental heat rejecter. For the Tulsa example, the lowest life cycle cost alternative (Case 3) has a ratio of 8.5% pond loop length to total loop length and there is a cost savings of 18% relative to the base case. At this same ratio for the Houston example, a

34

much greater cost savings of about 50% is realized. However, the optimum cost savings for the Houston example is 66%, at the point when the ratio of pond loop length to total loop length is at a maximum of 66%.
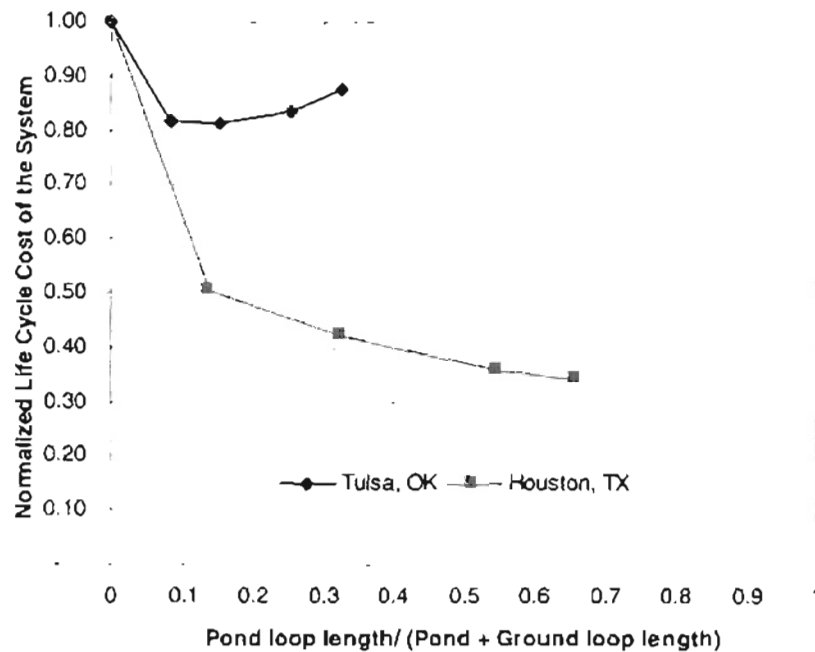
Figure 2.7. Normalized life cycle cost of the GSHP system versus the ratio of pond loop length to total loop length for Houston, TX and Tulsa, OK climatic conditions

Figure 2.8 illustrates the performance of the supplemental heat rejecter for five days in July and December. The pond outlet temperature is shown to be the same as the heat pump exit water temperature when the pond is bypassed. In summer, the pond is used primarily during the day time. During the night, when the heat pump doesn't operate under a high load, the pond is bypassed when the temperature difference drops below 3 °C. During the winter, the first four days are relatively warm, and there exists a cooling load on the building. The heat pump stops operating during the evening. When the temperature difference between the heat pump ExFT and pond temperature is at or above

8 C the system starts rejecting heat to the ... erature difference drops down to 3 C. The fourth day, the pond coo... ond until the te... ...ure to the weather conditions. Hence, the system continues to reject ... ff substantially

Case 2 (Houst...
July 16 - July ...

Case 2 (Houston)
Dec 20 - Dec 24
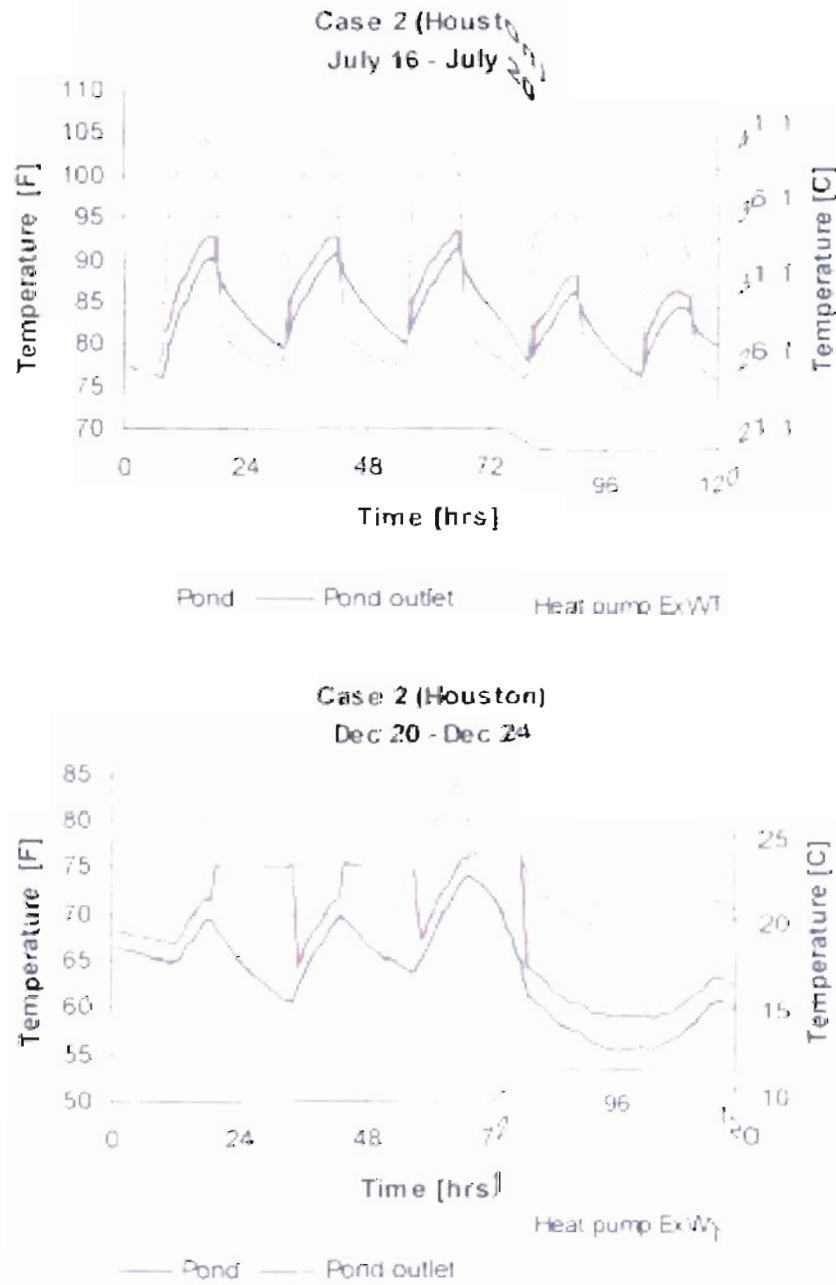
Figure 2.8 *Typical summer and winter perform... ...ental heat rejecter ...or Houston, TX*

The system rejects heat under the most favorable conditions, i.e. when the temperature difference is high under this control strategy. This illustrates that the supplemental heat rejecter operates both under peak conditions as well as in winter to reject heat on a seasonal basis.

2.3.4. Sensitivity Analysis of the Control Strategy

As a limited sensitivity analysis, the impact of varying the differential control strategy on the system performance for Case 5 (Houston) and Case 2 (Tulsa) was examined. The borehole depth and pond size remained unaltered and the system performance was again simulated for 20 years and the economic analysis repeated. Eight simulations were conducted.

The upper dead band was fixed at 14.4 °F (8.0°C) while the lower dead band was increased from 1.8 °F (1°C) to 9 °F (5°C) in steps of 1.8 °F (1°C). Similarly, the dead band lower limit was fixed at 5.4 °F (3°C) while the upper limit is increased from 10.8 °F (6°C) to 18 °F (10°C).

Variations in the dead band temperatures resulted in only marginal differences in the system life cycle cost. These marginal differences were due to the fact that the system cost was governed by the heat pump energy consumption. Changes to the dead band temperatures mainly impacted the cyclic operation of the pond, but had little impact on heat pump performance. The life cycle cost for different control strategies varied within 1% when compared to Case 5 for Houston, and within 0.2% when compared to Case 2 for Tulsa.

2.4. Summary

A system simulation approach to determining the optimum size of a hybrid GSHP system that uses a cooling pond as a supplemental heat rejecter has been presented. Since the design is strongly influenced by the strategy used to control the supplemental heat rejection, the most efficient control strategy from the work of Yavuzturk and Spitler (2000) was adopted for this study. A control scheme was used to operate the pond when the difference between the heat pump exiting fluid temperature and the average pond temperature exceeded a set value.

This study has shown, through system simulation, that the optimum size of a GSHP system with a supplemental pond heat rejecter can be approached by adjusting borehole depths and pond loop lengths until a minimum life cycle cost has been found. This has been done for four configurations of a hybrid pond GSHP system for typical climates of Houston, TX and Tulsa, OK. A sensitivity analysis of the differential control strategy was also conducted.

Some specific conclusions of this study are:

1) The Houston example shows, for highly cooling-dominated buildings, that regardless of the size of the pond supplemental heat rejecter, significant economic benefits on the 20-year life cycle cost can be realized. The savings in the GSHP system cost by including the pond supplemental heat rejecter in this example is approximately 50-65%.

38

2) The Tulsa example shows. in buildings with a dominant demand for cooling but also with a significant heating load. that the most economical design of the hybrid system is dependent on the heating load. There is a point of trade-off in the pond size where too much heat is rejected from the system and hence there becomes an insufficient amount of energy available in the ground for extraction during the winter season. To prevent this from occurring, a more sophisticated control strategy is needed. We adopted a set point control for monitoring the minimum heat pump exiting fluid temperature. Alternatively. it may have been possible to use the pond itself for supplemental heat extraction.

3) The choice of the dead band range used in the differential control strategy appears to have no significant impact on the economics of the system.

This work opens a number of areas for further study. The pond hybrid GSHP systems that were simulated in this work were not truly optimized and there are still some system options that remain to be examined. Some of these include:

a)   Implementation of an optimization routine into the system simulation to find optimal values of desired parameters. In particular, it would be useful to find the optimal balance between the GLHE size and the pond size. This would also allow much more flexibility in the choice of the parameters to be optimized as well as streamline the design process.

39

b)   Examination of variable-speed pumping rates on the system performance. One shortcoming of this study was that a constant pumping rate was assumed. Variable-speed pumping has the potential to significantly reduce operating costs.

c)   A quantitative comparison between the life cycle cost of optimally-designed hybrid GSHP systems with a shallow pond versus hybrid GSHP systems with other supplemental heat rejecters, such as cooling towers and shallow horizontal ground-coupled coils.

d)   Further refinements to the control strategy. For example, consideration of time-of-day electricity rates in the heat rejecter operation strategy may be beneficial.

e)   Life cycle cost comparison of a cooling pond hybrid GSHP system to a pond-only system. This would require additional considerations not currently implemented in the pond model used in this work, such as pond freezing and seasonal stratification of the pond water.

40

Chapter 3

Component Modeling

3.1. Introduction

With the advent of personal computers in the recent past, numerous building

energy simulation packages and thermal system simulation programs have been

developed in order to improve the understanding of system operation. These simulation

packages also serve as a vital tool in design and selection of components that constitute

the thermal system, thereby preventing oversized design and poor energy performance of

thermal systems. It is now possible to design complex systems using computer based

system simulation techniques although it can be frustrating at times. TRNSYS (SEL,

1975) and HVACSIM+ (NBS, 1986) are two such powerful simulation techniques, which

are used to simulate the performance of thermal systems.

This chapter aims at discussing the structure of TRNSYS and HVACSIM+ (NBS,

1986), their relative merits and demerits, steps to convert component models from

TRNSYS to HVACSIM+, and a detailed conversion methodology for specific TRNSYS

component models. The TRNSYS models, previously developed at Oklahoma State

University, that have been made compatible with HVACSIM+ are the simple water-to-air

heat pump, water-to-water heat pump, ground loop heat exchanger, and heated slab

model. A few models among them have been upgraded to improve their robustness and

accuracy. In addition, new components developed in the HVACSIM+ environment are

described. The simulation results for a system comprising of water-to-water heat pump,

ground loop heat exchanger, and slab model in the HVACSIM+ environment are presented for comparison against TRNSYS results for the same set of inputs and parameters. The HVACSIM+ component models can subsequently be used to simulate the performance of a hybrid ground coupled heat pump system or a bridge deck heating system for short-time step (hourly or minutely) system analysis.

3.2 Selection of Modeling Environment

3.2.1. TRNSYS

TRNSYS is a modular simulation program. Systems that are simulated can be separated into discrete components or mathematical models. Thereby, a system can be represented by a combination of mathematical models of all of the system components. The modular nature of the program makes it extremely flexible and it allows the user to specify the components that constitute the system and the way in which they are connected. It also facilitates the addition of component models not available in the TRNSYS library. The modular nature also allows each model to be mathematically described with little regard for the other components. Moreover, the individual components can be used for different simulations with minimal modifications. The TRNSYS environment is suitable for simulation and detailed analysis of transient behavior of systems.

In TRNSYS, the actual implementation of component in a system simulation involves assigning a UNIT number to each "instance" of each component. "Instance" is a term borrowed from object oriented programming. It refers to the fact that a given type of component may appear multiple times in the system e.g. a single system may contain

several circulating pumps. Each pump may have different characteristics, but still represented by the same component model. Each individual pump is referred to as an "instance" of the component model. A UNIT number is a reference number that TRNSYS uses to keep track of the instance of the component in conveying the information about the component to TRNSYS. Several UNITs of the component can be included in a system simulation. The TYPEn subroutine, where n is an integer between 1 and 200 unique to each component, contains the mathematical model of each identifiable kind of system component. The performance of the system is simulated by collectively simulating the performance of individual interconnected components. Thus, the modular structure of TRNSYS simplifies a complex system simulation by reducing it from a large problem into a number of smaller problems.

Table 3.1 gives a summary of the calling arguments used in TRNSYS. These calling arguments communicate between the component subroutine and TRNSYS. For a component model of TYPE number 'n', the FORTRAN statement is

SUBROUTINE TYPEn(TIME,XIN,OUT,T,DTDT,PAR,INFO,ICNTRL,*)

TRNSYS also include some subroutines that perform general utility functions for the component routines. The user can use these in-built capabilities in component formulation or modification. Subroutines TYPECK, DATA, DIFFEQ, ENCL, VIEW, TABLE, INVERT, FIT, PSYCH, LINKCK, RCHECK, FLUIDS are such utility routines.

Table 3.1 Subroutine calling arguments used in TRNSYS component models

Variable	Definition
TIME	Simulation time (seconds)
XIN	Double precision array containing component inputs
OUT	Double precision array containing component outputs
T	Real array containing dependent variables for which derivatives are evaluated
DTDT	Real array containing derivatives of T
PAR	Real array containing the parameters characteristic to the Component
INFO	Array conveying information about the current unit to component subroutines and TRNSYS kernel
ICNTRL	Array conveying the states of the controller variables to component subroutines and TRNSYS equation processor

Differential equations, arising from the component models, are solved either by an approximate analytical solution using the subroutine DIFFEQ or a numerical solution using one of the following three numerical integration algorithms:

1. Modified Euler method

2. Non-self starting Heun's method

3. Fourth order Adam's method

TRNSYS uses a relatively simple successive substitution computational scheme to solve the set of non-linear simultaneous equations. There are inherent problems in solving a set of non-linear simultaneous equations. The convergence of such system of equations depends upon the sequence of arrangement of component models constituting the equation set. This limitation of the simultaneous equation solver is overcome partly using an ACCELERATE command that allows the user to break a selected INPUT-OUTPUT connection and replace it with a single variable Newton's method solution algorithm. Newton's method is more reliable and converges rapidly independent of the

sequence of the component types forming the equation set. Version 14 of TRNSYS also has an option of using SOLVER statement whereby the user can chose the algorithm used for solving the system of equations. In addition to the successive substitution method available with older TRNSYS versions, the user can specify Powell's method (Powell, 1970) for solving simultaneous algebraic and differential equations. The solution method splits the original equation set into smaller set, which could be solved efficiently. One disadvantage of this method is that it computes lot of computation time and effort calculating the Jacobian matrix, for every iteration in a time step, until convergence criteria are met (SEL, 1996).

3.2.2. HVACSIM+

HVACSIM+ employs a hierarchical, modular approach and advanced equation-solving techniques to perform dynamic simulations of systems. The modular approach is based upon the methodology used in the TRNSYS program. HVACSIM+ is hierarchical in the sense that the system is divided into UNITS, BLOCKS and SUPERBLOCKS. One or more units form a BLOCK. One or more BLOCKS constitute an independent subsystem called SUPERBLOCK.

When contrasted to TRNSYS, one main feature of HVACSIM+ is its variable 'freezing' option. Whenever the change in the value of any state variable is less than the user specified tolerance, the variable is 'frozen', i.e. the variable is removed from the simultaneous equation set which solves for the unknown variables. Another attractive feature of HVACSIM+ is the way it handles the variable time step. The user is free to choose a minimum and a maximum time step for simulations. Depending on how the

simulation progresses, the program uses either of the two time steps. If the simulation (as indicated by the simulation work file) does not involve any differential equations, the maximum time step is used. It is possible for the components in a system simulation to have inbuilt differential equations yet the differential equation solver may not be used, in which case the maximum time step is used as the time step for solving the simultaneous equation set. The variable time step algorithm and variable freezing option are discussed in more detail later in this chapter.

HVACSIM+ consists of two large programs – HVACGEN and MODSIM, and a small program- SLIMCON. The main programs that constitute HVACSIM+ have been discussed below in the following sections.

3.2.2.1 HVACGEN

The simulation configuration program, HVACGEN, allows the user to specify specific component models listed in the component library to be included in the system simulation.

The inputs and outputs of the components in the system being modeled are called state variables. The inputs and outputs are read into the respective input and output arrays and passed to a state variable array, which stores these values. Moreover, the inputs and outputs are read into the state variable array depending on their respective 'category'. The user modeling the system specifies the integer identifying input and output 'category' it belongs to. The different 'category' of inputs and outputs and their respective index numbers are given below:

1. Pressure (kPa)
2. Flow rate (kg/s)
3. Temperature (°C)
4. Control signal (any other fraction)
5. Rotation rate (revolutions per second)
6. Energy (kJ)
7. Power (kW)
8. Humidity (kg of water/kg of dry air)

HVACGEN creates the work file (*.sim), which contains the system configuration information. The initial values of state variables, parameter values, and error tolerances are also stored in the work file. Any unit input variables that are not the output of any other unit in the system simulation are taken as boundary variables. The boundary variables retain their initial values throughout if they are not declared as time dependent. However, if they have been designated as time dependent boundary variables then the values of the variables corresponding to the simulation time should be specified in an external boundary file.

The components are grouped into BLOCKs that are in turn grouped into SUPERBLOCKs. Thus, large simulations could be built from already existing pieces of the system. However, this work file cannot be used directly to run the system simulation program. The work file is made readable to MODSIM with the help of a small program called SLIMCON.

3.2.2.2. SLIMCON

The work file created by HVACGEN is not used directly by MODSIM. SLIMCON is a small utility program that converts the work file generated by HVACGEN to a model definition file (*.dfn). The model definition file contains the

preprocessed information derived from the simulation work file. This model definition file containing the complete system description is used by MODSIM to run the system simulation. The program also issues warnings when there are any discrepancies in the system configuration such as a boundary variable being solved for simultaneously or a simulation variable appearing as an output of two or more components.

3.2.2.3. MODSIM

Once the model definition file describing the system is ready, the simulation is run using the core simulation program MODSIM. It contains a built-in non-linear equation solver SNSQ (Heibert, 1982) with its associated subroutines that use a modified Powell's hybrid method as described by Powell (1970). A variable order Gear algorithm (Gear, 1971), which uses backward differentiation formulas and predictor-corrector methods, is coupled with SNSQ for solving stiff ordinary differential equations. HVACSIM+ uses Gear's algorithm to integrate differential equations involving a wide range of time constants.

A system of implicit differential algebraic nonlinear simultaneous equations is solved in HVACSIM+ by SNSQ coupled with the differential equation solver BACKDIF. The derivatives are found in the TYPES subroutine. The subroutine BACKDIF calculates the derivative using the backward difference formulas. The difference between the two constitutes the residual function. Once the derivatives of the variables are found, it is substituted back into the system of simultaneous equation set for being solved by SNSQ. The predicted value for the next time step is found once the order of the backward difference formulae and the step size are determined after the solution

48

has converged. The time interval between the initial and final times used in integrating the differential equation in the backward-difference formula must be specified in the simulation work file. In addition, the model definition file passes the information on the number of differential equations in each UNIT of the simulation. The solution methodology of integrating stiff ordinary differential equations is given in Park et al. (1985).

MODSIM is linked with a library of routines for specific component routines that in turn contains the mathematical model of each component. MODSIM is equipped with a third order Lagrangian interpolator to interpolate values of time varying forcing functions from the 'boundary' file for a particular time step. Even if the boundary variable values have not been specified at equal time intervals, MODSIM interpolates the values for the particular simulation time.

Differential equations introduce additional difficulties in the system simulation. Whenever there is a rapid change in the boundary variable of a SUPERBLOCK or a sudden change in any control variable that might induce sudden transients, the time step is reduced to a user-specified minimum value. A rapid transient in a SUPERBLOCK induces it to take shorter time steps (minimum time step specified by the user), while the other SUPERBLOCK proceed independent of it. The time step is reset to the maximum value when the system has evolved from the transient state to steady state. Such instability particularly occurs in stiff systems with components having widely varying time constants. The variable time step, variable order algorithm for solving differential

equations makes HVACSIM+ capable of handling both short and long-term dynamic processes efficiently.

The variables that have reached steady state are 'frozen' and removed from the set of simultaneous equations. In other words, if the change in variable from its value in the previous simulation time step is within a user specified tolerance limit, it is considered to be 'frozen' and is no longer solved for. The simultaneous equation set is solved for 'unfrozen' variables. This can greatly reduce the computation time of the simulation. 'Frozen' variables are monitored and reinstated into the equation set as soon as the variable changes from steady state to a transient one. Removal of 'frozen' variables from the set of simultaneous equations and separation of subsystems with drastically different time-steps decreases the computation time.

In addition to the component subroutines, the user can also take advantage of the existing utility and property routines of air, water, and refrigerants. MODSIM writes the output of the simulation, final state of the simulation and a summary of the simulation in separate output files. The variables used in TYPES routines are listed in Table 3.2.

Table 3.2 Subroutine calling arguments in HVACSIM+ component models

Variable	Function
XIN	Real array containing component inputs
OUT	Real array containing component outputs
PAR	Real array containing the parameters characteristic to the Component
SAVED	Array for storing the variables required for next time step
IOSTAT	Input/output status vector.

IOSTAT contains the status of the input while entering the component subroutine and contains flags that enable or disable variable 'freezing' for the output variables.

3.2.3. HVACSIM+ Vs TRNSYS

The modular approach is common to both HVACSIM+ and TRNSYS. Nevertheless there are differences in the method of solution, the algorithm for solving the differential equations, and the control strategies used in HVACSIM+, which should make it a more effective tool for dynamic system simulation. However, the solution algorithm does not seem to perform well for all system simulations. The solution algorithm requires good initial guesses for finding a solution for a set of non-linear simultaneous equations. The solutions obtained during start-up transients in system simulation can result in high residuals. The shortcoming of the solution algorithm and convergence problems associated with it will be dealt in detail in Chapter 4. The advantages of HVACSIM+ over TRNSYS can be summarized as follows.

The simultaneous non linear equation solver is supposed to obtain a self-consistent solution for each time step in HVACSIM+, as compared to a relatively simple successive substitution algorithm used in TRNSYS. But, in fact, it failed to obtain a self consistent solution for the problem at hand. There are frequent occurrences of convergence problems, where the program considers the solution to be converged when it is not converged. These issues will be dealt with in more detail in Chapter 4. The successive substitution algorithm used in TRNSYS has inherent pitfalls too. The convergence of a set of simultaneous equations by successive substitution depends on the information-flow diagram of the system, variable initial values and boundary values. It tends to consume greater computation time because of its iterative nature.

51

There is significant difference in the user interface of both the simulation packages. TRNSYS has a menu-driven environment program called TRNSHELL that is equipped with editing, plotting, compiling, linking, and help options. It also houses the TRNSYS program and other utility programs. This enables all the TRNSYS functions to be performed easily from one environment program. TRNSYS also has a general simulation environment program called IIsiBAT (Intelligent Interface for the simulation of buildings). IIsiBAT houses the complete simulation package along with powerful tools and utility programs for graphical connection, plotting, and spreadsheet in one environment making it easy to use for the user. Hence, it is relatively easier to change the simulation time, convergence tolerance, variable and boundary initial values, parameter values, connectivity of the individual components, and direct the output and list files in TRNSYS than in HVACSIM+.

There are some other minor differences between the two simulation packages. TRNSYS is more suited for using hourly time steps or fractions thereof, whereas HVACSIM+ is suited for both shorter (as small as 0.1 seconds) and longer time steps if the variable step algorithm in HVACSIM+ can be effectively exploited. The hierarchical nature and structure of HVACSIM+ makes it difficult to add components to an already existing simulation. Whereas, in TRNSYS, the input file can be edited, to accommodate another component to an already existing simulation, within minutes. Moreover, an error in the connectivity of the individual components in a system simulation can be more easily detected in TRNSYS, because TRNSYS writes the output summary of the simulation run into a data file called 'list' file. It contains a detailed summary of the simulation run. If there are any discrepancies in the information-flow between

52

components or compilation or linking of the component subroutines a summary of errors appears in given in the 'list file'. The TRNSYS error messages in the help option in the TRNSHELL environment are useful in helping the user to detect and diagnose the errors in the input file. In HVACSIM+, the user is notified only on the screen when the convergence progresses badly during a system simulation. The user can however, print a diagnostic report for a specified period of time. The diagnostic report can be made to print the Jacobian, residual information, the "hybrid step" size of the optimization algorithm indicating the progress of the iteration, the limiting convergence criteria, and the intermediate solution vector.

TRNSYS is equipped with a data reader that is used to read data at regular time intervals and supplying it to other component UNITS as time dependent forcing functions. But, most commonly the data reader is used to read user-supplied meteorological data from weather files as inputs to other components. The data reader is a UNIT by itself and there is no limitation on the number of data reader units that can be used in a system simulation. In HVACSIM+, the weather data are read as time dependent forcing functions from a boundary file. However, the weather file cannot be directly read as a boundary file into the simulation, since the order of data in boundary file must correspond to that of state variable index order as it appears in the input file.

An additional feature of HVACSIM+ is the initialization option. If this option is chosen, the final state of one simulation can be used as the initial state of another. With this option, the user has to run a startup transient only once. For proceeding simulation runs, the initialization file of the first run can be used. Thereby, computationally

expensive startup transients can be avoided. Moreover, a long simulation can be broken into a series of short simulation runs, with one run starting from the state where the previous run ended. However, this feature cannot be used conveniently if the subroutines have a built-in history term associated with it. For example, the ground loop heat exchanger model has a history of heat transfer to the ground, and the bridge deck model has a temperature history. With these models, it is not feasible to break a long simulation run into smaller ones.

A summary of the basic differences between the two simulation packages is given in Table 3.3

Table 3.3 Comparison of TRNSYS and HVACSIM+ features

Features	TRNSYS	HVACSIM+
Structure	Modular	Modular, Hierarchical
Solution algorithm	Successive substitution	Non-linear equation solver (Modified Powell hybrid method)
Time Step	Constant, suited for hourly time steps	Variable, suited for large (Hourly) or small (0.1s) time step
Differential Equation solver	Analytical, Numerical integration at constant	Variable time step integration (Gear Algorithm)
Variable freezing option	Not available	Available
User interface	Good	Bad
Data reader	Available	Not Available
Legrangian interpolator for reading time dependent forcing functions	Not available	Available
Error diagnosis	Easy	Difficult
Running the simulation in pieces	Difficult	Easy with Initialization option

These features make it possible to perform detailed simulation of complex dynamic system simulations in HVACSIM+. But some features make it difficult to perform the simulations. The difficulties encountered in using HVACSIM+ for complex simulations will be discussed later in chapter 4.

3.3. Translation of Component Models to HVACSIM+

As mentioned in earlier sections, there is not much difference between TRNSYS and HVACSIM+ in how the TYPES subroutines handle the input and output variables. In order to translate to HVACSIM+, the SAVED and IOSTAT arrays are added to the TRNSYS component routine. The SAVED array is used to store values of variables whose values are to be carried to the next time step. IOSTAT is an input/output vector that is used to enable/disable variable freezing. A state variable is frozen (IOSTAT=0) if it changes less than a user specified tolerance from one time step to the next. When a state variable is unfrozen (IOSTAT=1), the set of simultaneous equations are solved again with the unfrozen variable put back into the equation set. Similarly, the superblock freezing option (IFZOPT) can be used to control the SUPERBLOCK variable freezing and unfreezing when more than one SUPERBLOCK is used in system simulation. There are three modes to control the SUPERBLOCK freezing option if the SUPERBLOCK equation is not frozen:

1. Mode 0 – state variable is not put back into the equation set until next time step.

2. Mode 1 – unfrozen variable is put back into the superblock equation set and the calculation is repeated

3. Mode 2 - all the superblock equations are put back into the equation set and the calculation is repeated.

MODSIM uses common blocks to convey information internally. The common blocks that are mentioned in HVACSIM+ and the information they contain, are discussed below:

CHRONO conveys the following information:

1. TIME: current simulation time

2. TSTEP: current simulation time step

3. TTIME: time interval for integrating differential equations

4. TMIN: minimum allowable simulation time step

5. ITIME: number of time steps since the beginning of simulation

The common block SOSCOM conveys the following information:

1. RTOLX: relative error tolerance

2. ATOLX: absolute error tolerance used as error criteria for differential

   equations and bounds for variable freezing

3. XTOL: error tolerance for simultaneous equation solving

The common block XINIT contains the following information:

1. INIT: flag to determine if the simulation is to be initialized from the initial

   state vector or from initialization file

2. NSAVED: number of saved variables in the entire simulation

The following changes are made to make the TRNSYS component routines
compatible to HVACSIM+:

1. Change the subroutine calling arguments of the component models.

2. State the common variables (TIME, TTIME, INIT etc) available to the subroutine.

3. Assign the input variables and parameters, the values contained in XIN and PAR

   arrays. The order in which the variables are stored in the array should be the same

   as the order followed in extracting the values from the arrays.

56

4. Make necessary changes in the body of the mathematical component model (e.g., the way it handles time).

5. Save the variables required for the next time step.

6. Assign the output array, OUT to the output variables.

3.4. *Component Model Installation*

Once the necessary changes have been made to the TYPES routine of the component model to make them compatible with HVACSIM+, the next step is to install the component model in the component library. The steps for installation of the component model into HVACSIM+ environment are discussed in this section. Prior to running the simulation with the component model, a description of the component model must be added to the file TYPAR.DAT, which is read by HVACGEN for creating the simulation work file. The TYPAR.DAT listing for the ground loop heat exchanger model is included in Appendix B.

The first line in TYPAR.DAT starts with an asterisk to indicate the beginning of a new TYPE description. The second line contains the TYPE number, followed by a brief description of the component. The third line contains information on the number of SAVED variables, differential equations, inputs, outputs, and parameters respectively. Next comes a set of lines describing the inputs, outputs and parameters. The set of inputs is separated from the set of outputs by a "#". The line immediately proceeding the set of output descriptions starts with a "#" to indicate the end of output description. Each of the line describing the set of inputs, outputs and parameters contain an integer followed by a

57

two character fields in quotation marks. The integer identifies the input or output as one among the eight categories as listed in section 3.2.2.1.

Once the component description has been added to the TYPAR.DAT listing, the component TYPE routine is added to the "types.for" file of MODSIM and a CALL statement for the subroutine is added to the subroutine SELECT. Now, the component is ready to be used for simulation.

3.5. HVACSIM+ component models

As discussed in 3.3, a few of the previously developed TRNSYS component models were changed to suit the HVACSIM+ environment. The water-to-water heat pump, ground loop heat exchanger, water-to-water heat pump, and the slab model were translated into HVACSim+. A brief description of these component routines and listing of the TYPAR.DAT file are given in Appendices A and B.

For converting component subroutines in TRNSYS to HVACSIM+, the common blocks specific to TRNSYS (LUNITS, SIM, CONFIG) were removed and common blocks CHRONO, SOSCOM, and XINIT, as described in earlier section, were added to the subroutines. The subroutine calling arguments TIME, T, DTDT, INFO, ICNTRL were removed and IOSTAT and SAVED added to the component subroutines. The XIN and OUT arrays storing the input and output variable values were declared REAL in HVACSIM+. The CALL statement for each of the component subroutines is added to the subroutine SELECT. The component description is added to the TYPAR listing according to the procedure mentioned in previous sections. The mass flow rates in

HVACSIM+ are directly read into the component subroutines in 'kg/s' instead of being read in 'kg/h' and then converting it into 'kg/s' as in TRNSYS. The mass flow rates being supplied as outputs for the component subroutines are also in 'kg/s'. Also, the time dependent variables for which the simultaneous equation is solved for are monitored. The IOSTAT array is used to identify time dependent variables and monitor their 'freezing' and 'unfreezing'. Hence, the input/output status vector of time dependent variables is assigned a value (IOSTAT=0 or 1) at the end of the component subroutines. This is to ensure that the time dependent variables are not removed from the set of simultaneous.

3.5.1. Water-to-Air Heat Pump

This component model simulates the performance of a water-to-air heat pump. Chiasson (1999) provides a detailed description of the model. The model takes total heating or cooling load on the heat pump, entering fluid temperature, and fluid mass flow rate as inputs and computes the exit fluid temperature, the heat of rejection in cooling mode, heat of absorption in heating mode, and the heat pump power consumption using quadratic curve-fit equations to manufacturer's catalog data.

For a given heating or cooling load, entering fluid temperature, and mass flow rate the model determines the heat of absorption or rejection of a heat pump for each time step in a system simulation. This model uses a quadratic curve fit of catalog data to find the heat of absorption or heat of rejection as a function of inlet fluid temperature.

The hourly building loads are intended to be read as boundary variables. By convention heating loads are given as positive and cooling loads are given as negative. If

59

the building loads are positive, the heat pump model uses the first six parameters as curve-fit coefficients to compute the heat of absorption. Parameters seven through twelve are used as the curve-fit coefficients to compute the heat of rejection during the cooling mode. Other component models supply entering fluid temperature and fluid mass flow rate. Outputs provided by the model include exiting fluid temperature, power consumption, and fluid mass flow rate (for availability to the next component).

The parameters LOWERC, UPPERC, LOWERH, UPPERH, and MINFLOW which signify the lower and upper limits of the inlet fluid temperature in cooling and heating mode and the minimum allowable flow rate respectively were added to the model to prevent it from computing a value for heat of absorption, heat of rejection or power consumption of the heat pump beyond the limits of the catalog data. If the inlet fluid temperature is above or below these limits, the model fixes the output temperature equal to the inlet temperature and heat of absorption/rejection and power consumption to zero. This mimics shutting off of the heat pump when the temperature or flow rate goes beyond its operating range. The component description of the heat pump as it appears in the TYPAR.DAT listing is given in Table 3.4.

60

Table 3.4. Description of simple heat pump model (TYPE 92)

Inputs	Outputs	Parameters
1. Total load, kW	1. Outlet fluid temperature, °C	1 through 12- Curve fit coefficients
3. Inlet fluid temperature, °C	2. Outlet mass flow rate of fluid, kg/s	13. Specific heat capacity of the fluid
4. Inlet mass flow rate of fluid, kg/s	3. Power consumption, kW	14 through 17. Upper and lower limits of fluid temperature in heating and cooling modes
		18. Minimum flow rate, kg/s

3.5.2. *Water-to-Water Heat Pump*

The water-to-water heat pump model as described by Jin (2000) is a parameter estimation based steady state simulation model. The parameters describing the overall performance of the heat pump are derived from the manufacturers' data and a optimization algorithm. This model computes the energy consumption of the compressor and exiting water temperature from evaporator and condenser given the entering water temperature and flow rate on both sides. Heat rejected by the condenser is calculated. The model is based on the laws of conservation of mass and energy and uses basic thermodynamic and heat transfer correlations. Since this is a steady state model, converting this model to HVACSIM+ is straightforward and simple. Only the common blocks and the subroutine call arguments are different for both HVACSIM+ and TRNSYS. Changes that were implemented are common to that implemented in all other components as already mentioned.

The component description of the water-to-water heat pump as it appears in the TYPAR.DAT listing is given in Table 3.5.

Table 3.5. Description water-to-water heat pump model (TYPE 71)

Inputs	Outputs	Parameters
1 Load side entering water temperature, °C	1. Load side heat transfer rate, kW	1. Piston displacement, m^3/s
2. Load side entering water flow rate, kg/s	2. Source side heat transfer rate, kW	2. Clearance factor
3. Source side entering water temperature, °C	3. Power consumption, kW	3. Load side heat transfer coefficient, kW/°K
4. Source side entering water flow rate, kg/s	4. Load side leaving water temperature, °C	4. Source side heat transfer coefficient, kW/°K
	5. Source side leaving water temperature, °C	5. Load side heat transfer coefficient, kW/°K
	6. Source side leaving water flow rate, kg/s	6. Electro-mechanical loss factor
	7. Load side leaving water flow rate, kg/s	7. Pressure drop across the suction valve, kPa
		8. Superheat, °C
		9. Minimum flow rate, kg/s
		10. Minimum EFT, °C
		11. Maximum ExFT, °C
		12. Guess value for load side heat transfer rate, kW
		13. Guess value for source side heat transfer rate, kW

A number of challenges were encountered in the water-to-water heat pump model when used in the bridge deck heating system simulation in HVACSIM+. The problems which occurred, when the inputs deviated significantly from the expected range, were as follows. A list of problems encountered is given below.

1. Zero flow rates on the evaporator or condenser sides caused the program to crash due to a divide by zero error.

2. Very small flow rates on the evaporator or condenser side caused very high temperatures which in turn crashed the property subroutines.

3. Very high temperature at condenser inlet caused the program to crash at the refrigerant property subroutine due to negative square root or negative logarithmic errors.

4. Very low temperature at evaporator inlet caused the program to crash at the refrigerant property subroutine due to negative square root or negative logarithmic errors.

To gain insight into the problems encountered in the model, a few equations used in the model are presented below. Equation (3.1) and Equation (3.2) are used to determine the effectiveness on the source side and load side of the heat pump.

$$\varepsilon_s = 1 - e^{\frac{-UA_s}{\dot{m}_s C_p}}$$ (3.1)

$$\varepsilon_l = 1 - e^{(\frac{-UA_l}{\dot{m}_l C_p})}$$ (3.2)

Where, UA_s and UA_l represent the overall heat transfer coefficient of the source and load sides respectively and $\dot{m}_l$ and $\dot{m}_s$ are the mass flow rate of the fluid on the load and source sides and C_p is specific heat capacity of the fluid.

The evaporating and condensing temperatures of the heat pump are computed using the effectiveness calculated using Equations (3.1) and (3.2). The evaporating temperature T_e and condensing temperature T_c are computed using Equation (3.3) and Equation (3.4).

$$T_e = TS_i - \frac{Qguess_s}{\varepsilon_s \dot{m}_s C_p}$$ (3.3)

$$T_c = TL_i + \frac{Qguess_l}{\varepsilon_l \dot{m}_l C_p}$$ (3.4)

TS_i and TL_i indicate the source side and load side entering fluid temperatures. $Qguess_s$ and $Qguess_l$ are taken as the initial guess values of source side and load side heat transfer rates. The heat transfer rates are updated after every iteration until convergence criterion are met. The suction pressure $P_{suction}$ and discharge pressure $P_{discharge}$ of the

compressor is computed from the evaporator and condenser temperatures as shown in Equations 3.5 and 3.6.

$$P_{suction} = P_e - \Delta P_1 \qquad\qquad (3.5)$$

$$P_{discharge} = P_c + \Delta P_2 \qquad\qquad (3.6)$$

Where, ΔP_1 and ΔP_2 represent the pressure drops across the suction and discharge valves of the compressor respectively. The pressure drop is again a predetermined parameter for specific model of heat pump.

The mass flow rates appear in the denominator of a number of equations. Hence, a "zero" mass flow rate results in crashing the computation with a floating-point overflow. Skipping the whole computation part and fixing the exit fluid temperatures equal to the entering fluid temperature avoids this. Also, the power consumption and heat transfer rates are fixed to be zero for the heat pump. This is equivalent to shutting the heat pump down when the conditions become unsuitable for its operation.

A similar problem arises when the heat pump switches from "heat pump off" to "heat pump on" conditions. The problem is evident when time step used in the boundary file is larger than the one used for the system simulation in HVACSIM+. In such cases, the time dependent value of mass flow rate for the current time step is interpolated from the values given in the boundary file. Hence, if it is assumed that the system simulation time step is of the order of 30 seconds and the boundary file changes from 0 kg/s to 1 kg/s in one hour time interval, the flow rate for the current time step would be 1/120 kg/s. This problem is enhanced by choice of large guess values of source side and load side

heat transfer rates. This results in very low evaporating temperature and large condensing temperatures. The problem is compounded by the fact that the refrigerant properties are curve fit models (adapted from R.C. Downing (1980)) with square root and log terms in them. Very low evaporating temperatures result in low evaporating pressure and as a result negative suction pressures. For evaporating temperatures below -273°C (i.e. below absolute zero!), the routine that computes the saturation pressure crashes. Even if it is unrealistic for heat pump to operate at such extreme evaporating and condensing temperatures or pressures, the model should not cause the program to crash. And, the choice of parameters has a pronounced effect on the operating range of the model.

The refrigerant property subroutine, which computes the density of the refrigerant, crashes when the condensing temperature goes beyond the refrigerant critical temperature. This is not an unreasonable failure since the liquid-vapor phase ceases to exist at critical point and evaporation and condensation process cannot occur beyond the critical point.

It would be difficult to force the temperatures and pressures to some reasonable values when such unrealistic operating conditions occur in order to prevent the refrigerant property routines from crashing. Instead, the operating range of condenser and evaporator entering fluid temperatures and minimum mass flow rate that is handled by the heat pump be read as a parameter into the model source code. These checks mimic the real-life behavior of the heat pump, which will be shut off if the pressure is too high under extreme operating conditions.

3.5.3. Ground Loop Heat Exchanger

The ground loop heat exchanger (GLHE) model considered here is that described by Yavuzturk and Spitler (1999), which is an extension of the long-time step temperature response factor model of Eskilson (1987). It is based on dimensionless, time-dependent temperature response factors known as "g-functions", which are unique for various borehole field geometries. In order to compute the average temperature of the borehole field for each time step, the time-dependent building loads profile is decomposed into unit pulses and superimposed in time using the corresponding temperature response factors. The model includes a load aggregation algorithm that significantly reduces computing time.

In the ground loop heat exchanger model implemented in TRNSYS, hourly ground loads and g-function values are stored in an array. Since the algorithm requires a history of ground loads to be considered at each time step, a large number of g-function values are required. The g-function, specific to the borehole geometry used in the simulation, is read from "gfile.dat" as a series of dimensionless time/ dimensionless temperature response factor pairs. G-functions up to 8760 hours are pre-computed (interpolated) and stored in an array, which is passed to the load aggregation and superposition routine. This is done for all time steps. As implemented in TRNSYS, this algorithm only works for time steps of one hour. As currently implemented in HVACSIM+, the subroutine is still unable to handle variable time steps or time steps

smaller than an hour. If the model is to be used for variable time steps, the load aggregation algorithm should be changed accordingly.

The model assumes the heat rejection/extraction per unit length of borehole as the fundamental input variable to compute the average borehole fluid temperature. Therefore, it is necessary for the component model to internally solve for the average fluid temperature, exit fluid temperature and heat rejection/extraction per unit length of borehole simultaneously. The main output provided by the model includes the exiting fluid temperature. As mentioned earlier, the g-function parameters are read into the subroutine from a data file "gfile.dat". The component description of the ground loop heat exchanger as it appears in the TYPAR.DAT listing is given in Table 3.6.

Table 3.6. Description of ground loop heat exchanger model (Type 138)

Inputs	Outputs	Parameters
1. Inlet fluid temperature, $^\circ$C	1. Outlet fluid temperature, $^\circ$C	1. Number of boreholes
2. Inlet mass flow rate of fluid, kg/s	2. Outlet mass flow rate of fluid, kg/s	2. Borehole depth, m
	3. Average fluid temperature, $^\circ$C	3. Borehole radius, m
	4. Ground load, kW	4. Thermal conductivity of the ground, W/(m K)
		5. Volume heat capacity of the ground, J/(m^3 K)
		6. Specific heat capacity of the fluid, J/kg K
		7. Undisturbed ground temperature, $^\circ$C
		8. Borehole thermal resistance, K/(W/m)
		9. Minimum entering fluid flow rate, kg/s

Initially, the model took borehole thermal resistance as a parameter. But, the borehole resistance depends upon the borehole geometry, and the flow rate through the

67

borehole. This inherently poses a problem in system simulation since the flow rate may not be constant throughout the simulation period. To accommodate variable flow rate, a subroutine that computes the borehole thermal resistance is added to the improved version of the ground lop heat exchanger. The model takes into account parameters such as the radius of the U-tube, distance between U-tubes, wall thickness of the U-tube, conductivity of grout, pipe material, and thermo-physical properties of the heat exchange fluid circulated. Thereby, the improved version is capable of predicting the performance with greater accuracy. The procedure for computing the borehole thermal resistance is explained below.

$$R_b = R_{cond} + R_{conv} + R_{grout} \tag{3.7}$$

Where R_b is the borehole thermal resistance ($^\circ$K per W/m). R_{conv} is the convective resistance ($^\circ$K per W/m), R_{cond} is the conductive resistance ($^\circ$K per W/m), and R_{grout} is the resistance of the grout surrounding the U-tubes ($^\circ$K per W/m). The conductive resistance is determined from Fourier's law:

$$R_{cond} = \frac{\log\left(\frac{r_o}{r_i}\right)}{4\pi \ k_{pipe}} \tag{3.8}$$

Where r_o is the outer radius of the pipe, r_i is the pipe inner radius, and k_{pipe} is the pipe thermal conductivity. The convective resistance is computed as follows.

$$R_{conv} = \frac{1}{2\pi \ d_i \ h_{cj}} \tag{3.9}$$

Where d_i is the pipe inner diameter, and h_{cj} is the convection coefficient inside the pipe computed using Dittus-Boelter correlation.

$$h_{cj} = Nu \ K_{fluid} / d_i \tag{3.10}$$

Nusselt number Nu is computed from Prandtl number, Pr and Reynolds number, Re as shown below

$$Nu = 0.23\,Re^{0.8}\,Pr^{0.35} \tag{3.11}$$

Resistance due to the grout, R_{grout} is calculated using the following relation

$$R_{grout} = \frac{1.}{k_{grout}\beta_0\left(R_{borehole}/r_o\right)^{\beta_1}} \tag{3.12}$$

Where β_1 and β_0 are the resistance shape factor coefficients (Paul 1996) whose value depends on the U-tube shank spacing inside the borehole

3.5.4. Bridge Deck

The bridge deck model used is the one described in detail by Chiasson, et al. (2000). This model is used to simulate a hydronically-heated bridge. The conduction heat transfer is modeled using a finite difference algorithm. The heat transfer due to the environmental interactions at the top surface of the bridge include the effects of solar radiation heat gain, convection heat transfer to the atmosphere, thermal radiation heat transfer, sensible heat transfer to snow, heat of fusion required to melt snow, and heat of evaporation lost to evaporating rain or melted snow. Environmental interaction with the bottom surface includes heat transfer due to convection and radiation to the surroundings. Conduction through the pavement material and convection due to the flow of the heat transfer fluid are the two heat transfer mechanisms within the pavement slab. The user supplies weather data as time dependent variables in the boundary variable file.

The variable DELT, which carries the information about the current time step in TRNSYS, is replaced with TSTEP in TRNSYS. For updating and adding the snow/ice

69

layer accumulation in the algorithm before and after each time step, the time step is

changed from DELT to TSTEP. The choice of the time step specified by the user as a

parameter for solving the finite difference problem is limited by the need to maintain the

stability criterion for two-dimensional problems. Moreover, the user specified time step

for the simulation should be greater than the time step chosen for the finite difference

solution.

air temperature | sky temperature | wind direction | solar angle of incidence | rainfall rate | inlet mass flow rate

humidity ratio | wind speed | solar radiation | snowfall rate | inlet fluid temperature

BRIDGE DECK HEATING MODEL PARAMETERS:

1. slab length
2. slab width
3. slab orientation from north
4. thickness of slab + fill
5. pipe spacing
6. pipe diameter
7. pipe depth below surface
8. depth to material 1-2 interface
9. thermal conductivity, layer 1
10. thermal conductivity, layer 2
11. emissivity coefficient
12. absorptivity coefficient
13. volumetric heat capacity, layer 1
14. volumetric heat capacity, layer 2
15. thermal conductivity, pipe material
16. pipe wall thickness
17. flag for fluid type (water or antifreeze)
18. antifreeze concentration if used
19. number of flow circuits
20. pipe length per flow circuit
21. time step for finite difference method
22. flag for bottom boundary condition

slab surface temperature | outlet fluid temperature | mass flow rate | heat rejected/absorbed

Figure 3.1 *Bridge deck heating model component configuration*

The bridge deck subroutine uses psychrometric subroutines in the algorithm to

calculate the humidity ratio of air at the slab surface. This is necessary to compute the

70

heat and mass flux change due to the evaporation of water at the slab surface. Since HVACSIM+ and TRNSYS differ in the utility subroutines they use, the component subroutine was modified to use UTILPSYC, a psychometric subroutine in HVACSIM+ available with its library. The bridge deck heating model component configuration is shown in Figure 3.1

3.5.4.1. Comparison of numerical and analytical solutions under no flow conditions

Initial tests of the bridge deck in a system simulation led to questions about the response of the bridge deck to changes in the fluid inlet temperatures. A step change in the fluid temperature would cause the surface temperature to change nearly instantaneously. Therefore several tests were conducted to compare the numerical solutions of top and bottom surface temperature of the bridge deck model against an analytical solution.

The numerical and analytical solutions for the top and bottom surface temperatures have been compared for two test cases.

1. TC1- Transient conduction –Adiabatic wall

2. TC2-Transient conduction –Step response

The analytical solutions are obtained using the ASHRAE Analytical Test Suite (Spitler and Rees, 2000). The numerical solutions for the bridge deck model are obtained using HVACSIM+ simulation environment. Both the numerical and analytical tests are carried out using the same set of parameters described in the following sections.

TC1: Transient conduction-Adiabatic wall

The responses of the top and bottom surface temperatures of the bridge deck to

step changes in the ambient dry bulb temperature when the bottom surface is adiabatic

are compared to an analytical solution from the ASHRAE Analytical Test Toolkit. The

top surface convection coefficient is fixed at a value of 20. $W/m^2 K$ (3.5 BTU/hr-$^{\circ}$F-ft^2).

The effects of solar radiation, heat transfer from/to the heat exchange fluid, and heat

transfer due to snow/rain/phase change are eliminated in the test.

The driving ambient dry bulb temperature is initially set to 20 $^{\circ}$C (68 $^{\circ}$F). A

temperature step of 50°C (122 $^{\circ}$F) is chosen for the step and reverse step of the ambient

temperature above the chosen datum of 20 $^{\circ}$C (68 $^{\circ}$F) as shown in Figure 3.2. The

thermo-physical properties for the test have been tabulated below in Table 3.7.

Table 3.7. Parameters used for the analytical and numerical
testing of the bridge deck model

1. Thickness of the slab	0.2032 m (8")
2. Thermal conductivity	1.4 W/m K (0.81 BTU/(hr-F-ft))
3. Volumetric heat capacity	2200 kJ/m^3 K (33 BTU/F-ft^3)
4. Convection coefficient	20 W/m^2 K (3.5 BTU/hr-F-ft^2)

70 °C
(158 °F)

20 °C
(68 °F)

-30 °C
(-22 °F)

0   90   180   270

Time [days]
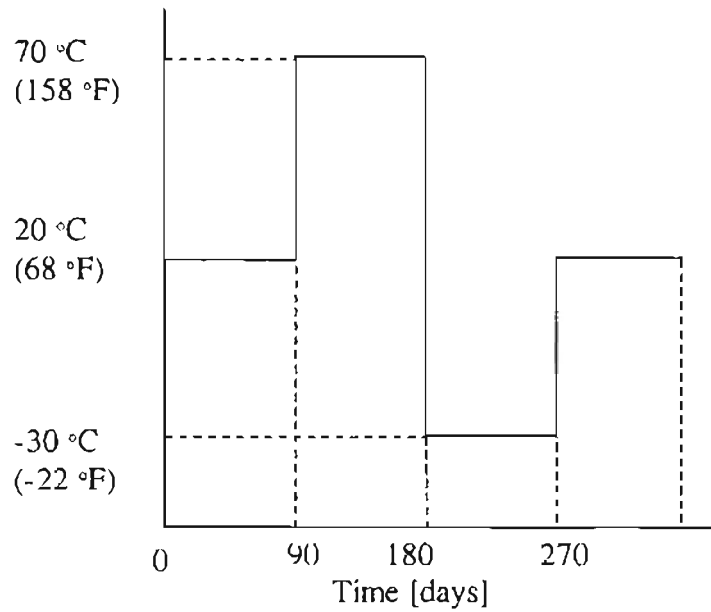
Figure 3.2. *Profile of the ambient air temperature*

The comparison of the analytical and numerical results for both top and bottom surface temperatures are shown in Figure 3.3. As expected, the top surface temperature shows a first order response after each step change in ambient air temperature and reaches a steady state in equilibrium with the ambient temperature. The heat flux at the top surface returns to zero as the surface temperature becomes equal to the ambient air temperature (not shown in the plots). The maximum relative error $|(T_{analytical} - T_{numerical})/T_{analytical}|$ for top surface temperature is 0.7038 % and that for bottom surface temperature is 1.0244 % during the period 2160 –2260 hours.
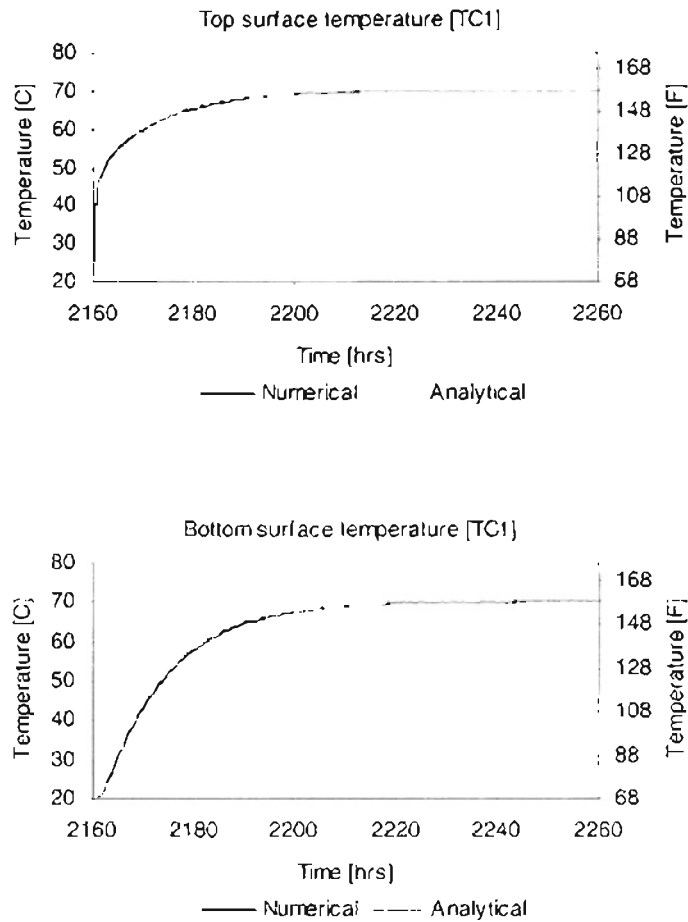
Figure 3.3. *Comparison of numerical and analytical solutions for top and bottom surface temperatures (Test –TC1)*

TC2: Transient conduction-Step response

This test is similar to the test TC1, except that the bottom boundary is convective in this case. The bottom surface is exposed to air at constant temperature of 20 °C(68 °F). The top surface is exposed to ambient air that is subject to the step change as shown in Figure 3.2. A constant convection coefficient of 20 W/m^2 K (3.5 BTU/hr-°F-ft^2) for both surfaces is assumed for both numerical and analytical cases. The thermo-physical properties of the bridge deck are the same as given in Table 3.7.

74
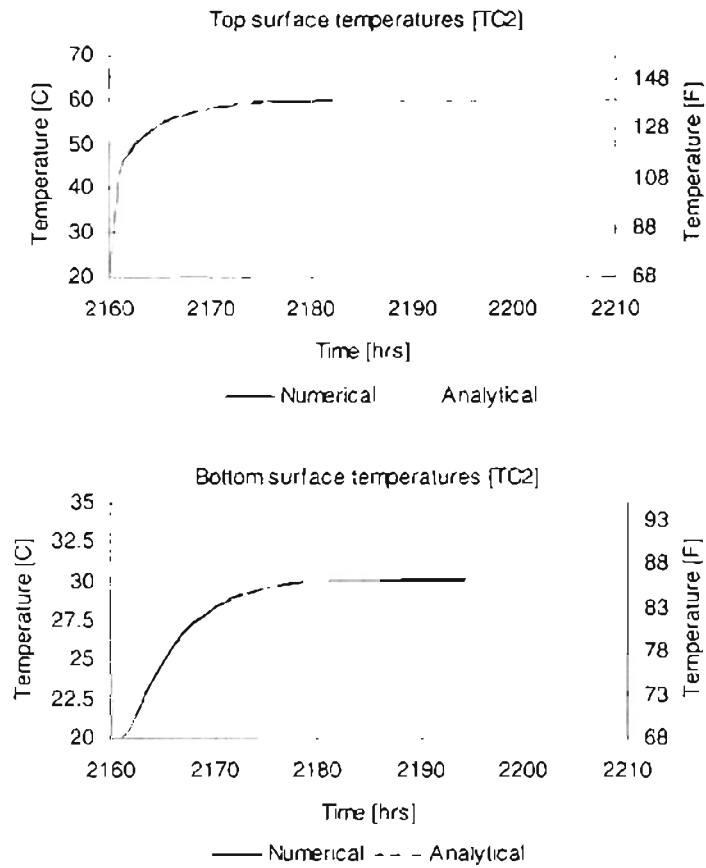
Figure 3.4. *Comparison of numerical and analytical solutions for top and bottom surface temperatures (Test -TC2)*

The results for the test TC2 for the bridge deck top and bottom surface temperatures for bridge deck have been compared against the numerical results in the plot shown in Figure 3.4. The numerical solution is in good agreement with the analytical solution. The maximum relative error in top surface temperatures is 0.7014% and 0.5628% for the bottom surface temperatures during the period 2160-2260 hours.

3.5.4.2. Response to step change in fluid temperature

The afore mentioned tests indicate that the responses of the top and bottom surface temperatures computed numerically by the bridge deck model matches well with their respective analytical solutions. But, the heat transfer to/from the heat exchange fluid circulated in the hydronic pipes embedded in the slab have not been accounted for in the validation of the numerical model against analytical solutions. Going one step further, the effect of heat exchange to/from the circulating fluid is considered in the test case mentioned below.

The numerical model is now simulated with shorter time steps of 30 seconds, which is the same as the time increment used in the explicit finite difference methodology in the model. This was done to obtain output at 30-second intervals. The slab top and bottom surface temperature are initialized to 20 °C (68 °F). Fixing the sky temperature at 20 °C (68 °F) eliminates the effect of radiation heat transfer of the top surface with the sky. Also, the effects of wind speed, wind direction, snowfall, rainfall, and humidity ratio on the bridge deck are eliminated. The mass flow rate of the heat exchange fluid is fixed at a constant value. The fluid inlet temperature, which is initially at 20 °C (68 °F), is stepped up to 70 °C (158 °F) at 2.5 hours and maintained at the same temperature for the rest of the simulation until the 25th hour.

The response of the surface temperatures to the step change in the fluid temperature is analyzed. It is observed from the Figure 3.5, which shows the responses of the surface temperatures, that the top and bottom surfaces respond almost immediately (30 seconds) and reach a steady state in a little over half an hour from time when the

bridge deck is subjected to a step change in fluid temperature. It is highly unrealistic that the top and bottom surface temperatures should almost reach a steady state after a period of 30 seconds.
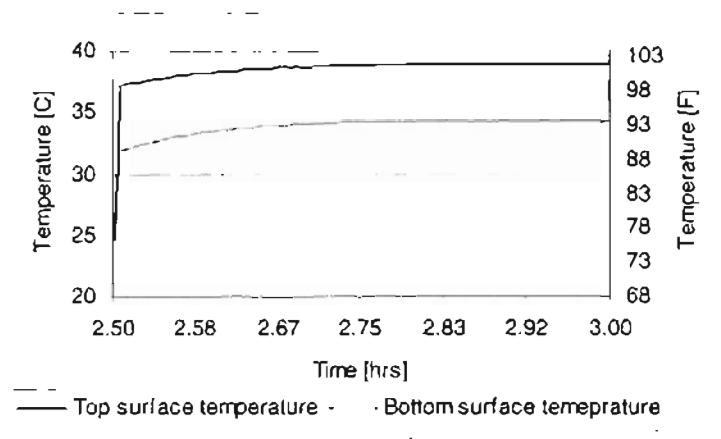
Figure 3.5 *Response of bridge deck surface temperatures to step change in fluid temperature (old version)*

3.5.4.3. Analysis of Result and Correction

The erroneous behavior of the top and bottom surface temperatures is evident. In an explicit finite difference method, the propagation of fluid temperature to the surface cannot occur in a single time step. In an explicit finite difference approach, the temperature passes from one node to the next with each time step. Hence, it would take at least six time steps for a perceptible change in the surface temperatures to occur (the pipe being six nodes away from each surface in this case).

The numerical model of bridge deck matches well with the analytical solution under no flow condition and fails to perform when subjected to a flow in the embedded pipe. If the discretisation equations or the stability criteria of the numerical method used were erroneous, it would reflect in the first two test cases. The problem was finally traced

77

down to the storing of the nodal temperatures for the next time step in the finite difference method. The nodal temperatures of the whole bridge deck grid that should be updated for every time increment in the finite difference method were being updated for every iteration inside the loop used for computing the outlet fluid temperature from the average fluid temperature. Since the convergence criteria for computing the average fluid temperatures is not used when there is no flow in the pipes, the response of the surface temperatures match surprisingly well with the analytical solution.

Having identified the source of the problem, the overwriting of the initial values of the nodal temperatures before each time increment in the explicit finite difference method is corrected. The values of the grid nodal temperatures are updated only after the computation of the average fluid temperature and before each time increment. The response of the surface temperatures to the step change in fluid temperature is presented in Figure 3.6. It is evident that the pipe fluid temperature progresses to the surfaces slowly and the response is similar to the results of tests TC1 or TC2. The surface temperatures take more than 20 hours to reach a steady state condition.
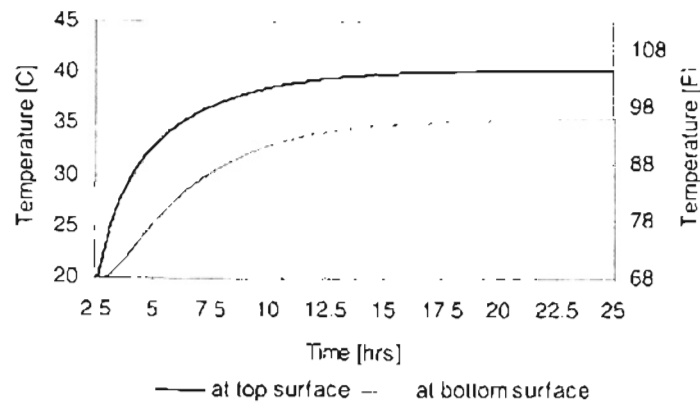
Figure 3.6 *Response of bridge deck surface temperatures to step change in fluid temperature (corrected version)*

3.5.5. Gang of heat pumps

For applications to a full-scale bridge deck, a single water-to-water heat pump is insufficient to meet the heating load requirements. Use of multiple heat pumps would complicate the system simulation by increasing the number of heat pump components, T-pieces and diverters to account for mixing. This implies increase in number of variables in the simultaneous equation set which means more computation time required to solve for them. Since it is highly undesirable to have factors which increase the computation time in such complex system simulations, a model which represents multiple heat pumps is modeled developed by extending upon water-to-water heat pump model (Jin, 2000).

The improved version of the model has been developed to simulate "N" pairs of serially-connected heat pumps as shown in illustration 3.7. The two heat pumps in a pair have their source side in parallel and load side in series. The model takes the number of heat pumps in operation as an additional input. A separate controller controls the number of heat pumps in operation at any given time. The input to the model is the temperature and flow rates to the gang of heat pumps on the evaporator and condenser sides, and the control signal which controls the number of heat pump pairs in operation. The circulating fluid from the heat pumps in operation is mixed with that from the pairs which are not in operation and hence are at the same temperature as inlet, and the outlet temperature computed. In essence, any number of pairs of heat pumps can be represented using the model with much ease. Also, the second heat pump in the pair is turned off when the entering fluid temperature exceeds the user specified maximum depending on the manufacturers' rating.
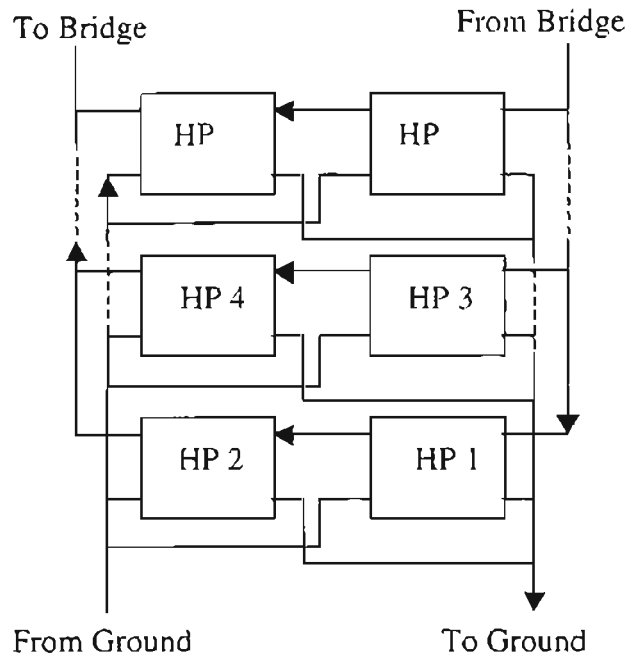
Figure 3.7. *Schematic showing the arrangement of 16 heat pumps in the "gang of heat pumps"*

3.6. Comparison of system simulation results

After having installed the component subroutines into HVACSIM+, as mentioned in earlier in this chapter, a simple hypothetical system as shown in Figure 3.8 consisting of the bridge deck slab model, the water-to-water heat pump model and ground loop heat exchanger model is modeled in HVACSIM+.
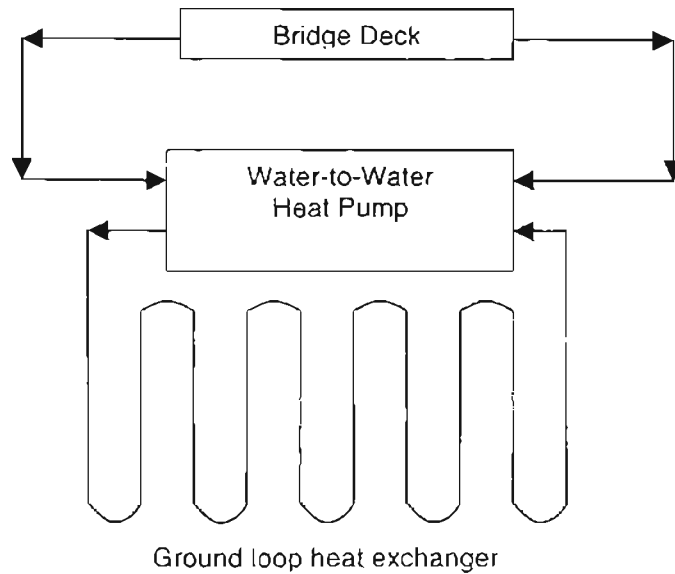
Figure 3.8. *Hybrid ground source heat pump system*

The results of the system simulation, for a duration of 24 hours, are compared against a similar model in TRNSYS with the same set of inputs and parameters. The system performance in both the environment has been presented in Figure 3.9 and 3.10 for comparison. Figure 3.9 shows the temperature of the working fluid (water in this case) at the bridge deck slab inlet and outlet. Similarly, Figure 3.10 shows the temperature of the working fluid at the ground loop heat exchanger inlet and exit.
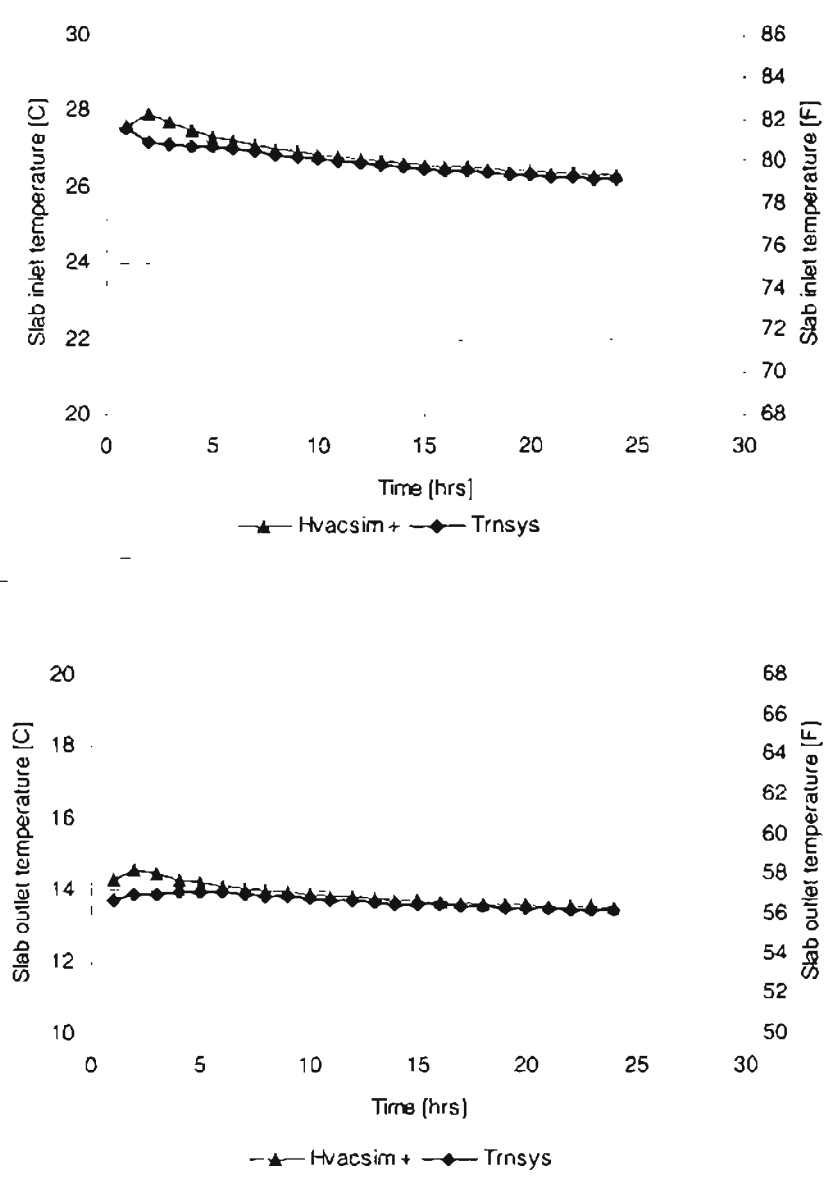
Figure 3.9. *Comparison of TRNSYS and HVACSIM+ results for the bridge deck slab inlet and outlet temperature*

It is evident from the results that, the converted component models work well in HVACSIM+ and results are in close agreement with the TRNSYS system simulation results.
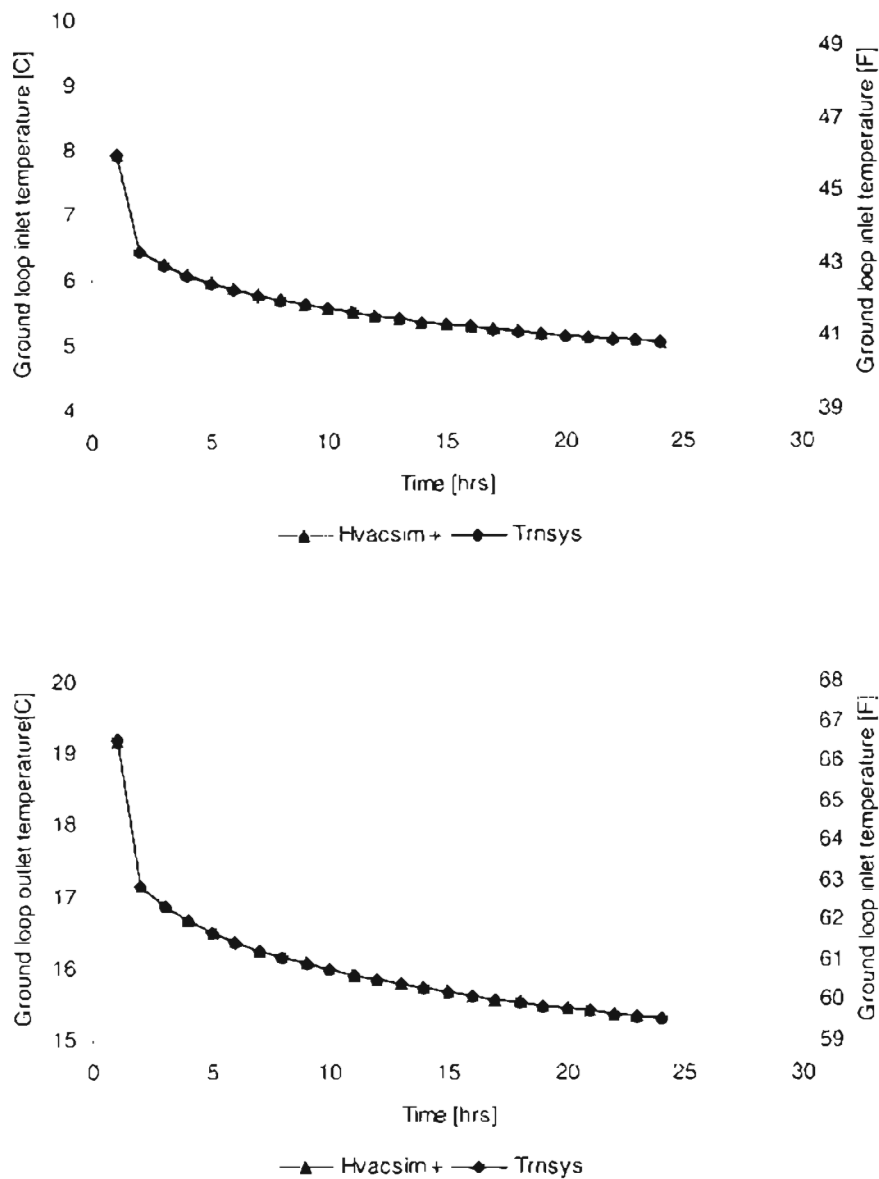
Figure 3.10. *Comparison of TRNSYS and HVACSIM+ results for ground loop heat exchanger temperature at inlet and outlet*

However, even for the same initial values, the simulation results is not in close agreement for the bridge deck inlet and outlet temperature during the starting few hours of the simulation. This is due to the difference in solution algorithms employed by the two simulation environments, which will be addressed in detail in the next chapter. Small time steps can be used during start up or when there are sudden changes in the system

and large time steps when the system has reached steady state, thereby producing more accurate and realistic results. However, this is not possible at present, since the ground loop heat exchanger model is incapable of using variable times. Having implemented the necessary component models in HVACSIM+, the performance of a geothermal heated bridge deck system can now be attempted. This will be described in the following chapters.

Chapter 4

Modeling of Hybrid GSHP Systems in HVACSIM+ for Application to Bridge Decks

4.1 Introduction

As discussed in the previous chapter, the ground loop heat exchanger, water-to-water heat pump, water-to-air heat pump, and the bridge deck models are made compatible with the HVACSIM+ modeling environment. The controller, circulation pump, and "gang" of heat pumps are modeled in HVACSIM+. After having installed all the models, the next step is to integrate the components to represent a physical system using HVACGEN. To establish a satisfactorily working model of the bridge deck, several different systems were configured iteratively. The common problems with the HVACSIM+ user interface, input files, debugging problems, and problems related to the solver SNSQ, encountered during system simulations, the remedial measures taken, a few sample results from the system simulation are discussed in the following sections. In the final section of the chapter a workable system configuration for the bridge deck heating system with provisions for recharge during winter is briefly discussed.

4.2. Problems with HVACSIM+

The motivation behind choosing the HVACSIM+ as the modeling and simulation environment for bridge deck heating systems was its ability to solve a system of simultaneous nonlinear differential algebraic equations using variable order and variable

time step integration methods. However, after having worked on it for considerable amount of time modeling and simulating various system configurations, various problems were encountered. Some of the problems were more significant than others. The problems with the user interface, or the problems encountered during the debugging of system simulations were merely cumbersome and time consuming. More importantly, serious problems were encountered with the simultaneous equation solver SNSQ employed by HVACSIM+. At times, the solver failed to converge, yet gave no indication that it had failed. In this respect, it failed to live up to our expectations. The various problems encountered with using HVACSIM+ have been highlighted in the following sections.

4.2.1 User Interface

The user interface of HVACSIM+ for modeling systems and running system simulation is "primitive", albeit simple. The program interacts with the user using a combination of command and menu-driven system. The menu driven program control has a hierarchy of menus which the user can select by typing one or more characters to direct the program. However, if the user makes an error while configuring a system, there is no way that it can be rectified immediately. The user has to either abort the process and get back to the main menu, or supply arbitrary values to get to the next command prompt. Aborting the process discards all changes that have been made. Once the user returns to the main menu command prompt, he can choose the EDIT command to edit the changes in the system configuration (e.g. input, output, parameter information, or variable indices,

86

or variable initial values or boundary variable indices). This usually requires a lot of time and patience on the user's part.

Building a complex system involving lot of components is very tedious and time consuming with the present user interface. This makes the HVACSIM+ modeling environment highly complicated. It helps for the user to have some experience in modeling of systems in a similar environment such as TRNSYS. Keeping track of the indices of the component input and output variables that constitute the system and establish their connectivity is of utmost importance to represent the system correctly in a physical sense. For example, if the temperature of one component is connected to a flow rate of the other, the system is bound to give wrong results, as it does not make any physical sense.

4.2.2. Input Files

The work file (*.sim) created by HVACGEN from the information supplied by the user, and the definition file (*.dfn) created by SLIMCON, which describe the system configuration, are cryptic and hence difficult to find mistakes in the connectivity of different components. As mentioned earlier, the connectivity of the components is established using indices for the specific category. Repetition or missing indices, or a connectivity of one category with a different category (e.g. mass flow rate with temperature) distorts the whole system configuration. The boundary file posed a similar problem when lot of boundary variables were involved.

87

A discrepancy in the model description in the Typar.dat and the actual component model used to build the executable leads to disastrous simulation results. The number and indices of state variables, designated by SLIMCON to be solved simultaneously by MODSIM, seemed to be ambiguous at first. Though the HVACSIM+ manual helped the author to familiarize with the simulation environment initially, it did not offer much help about how the variables are chosen for being solved simultaneously, the use of the variable freezing option, or the inherent problems associated with the solver. A careful scrutiny of the definition files of different system configurations indicated that a variable is solved for only when it is an output of one component and an input of a different component and is not included as a boundary variable.

4.2.3. Debugging Issues

It is not unusual to encounter problems during system simulations. The results of system simulation may be plausible yet not true. The validity of the system simulation results may be checked against experimental results or field data of such systems. However, it is desirable to first determine if the system simulation is internally consistent. Consider a simple system comprised of a bridge deck and a ground loop operating in recharge mode. The fluid circulating in the system is supposed to absorb heat from the heated bridge deck and recharge the ground. Moreover, the heat absorbed from the system is supposed to be equal to the heat being dumped into the ground when pumping energy and heat loss in the pipes connecting them is considered negligible. In other words, a simple heat balance on the bridge deck side and the ground loop side is enough to indicate if the system is being internally consistent. If it is not, then it requires tracking

the problem to its source, which could be the individual component models or their connectivity in the system, or the solution methodology. However, debugging such a problem requires the simulation to run for over 1-1/2 hours (on Pentium III, 500 MHz machine) until the system starts recharging in summer if a weather data for an annual simulation is used.

HVACSIM+ has an option of running a long system simulation file by small parts. The system could be started where it was discontinued using the information about the variables at the end of the previous run contained in the initialization file. However, this advantage of HVACSIM+ cannot be exploited in systems using components which require information from multiple previous time steps such as the ground loop heat exchanger model. The ground loop heat exchanger model carries information over to the next time step, storing a history of ground loads for computing the exiting fluid temperature and the heat extraction rate to the ground at a particular time step.

Problems related to the solution algorithm and its associated subroutines were much more difficult. The algorithm lacks structure and logical flow. This is quite evident by looking at the source code which contains a plethora of "go to" statements. Moreover, its difficult to comprehend what the variable/array holds by their names. Many work arrays have been used in which a lot of information is overwritten during intermediate calculations. Although it helps reduce the computation burden, it increases the onus during debugging phase. The source code also lacks necessary documentation. The only reprieve during debugging phase was the diagnostic report which could be printed out for a specified duration in system simulation. The diagnostic report can be made to print

information such as the Jacobian, residual information, "hybrid step" size of the optimization algorithm indicating the progress of the iteration, limiting convergence criteria, and intermediate solution vector. Although it is of some help to the user, it is still insufficient to find the source of the problem.

4.2.4. Solver Related Problems

Initially various bridge deck heating system configurations with a combination of bridge deck, ground loop heat exchanger, gang of heat pumps, circulation pumps, T-pieces, diverters, and a controller were configured using HVACGEN. After having exhausted a lot of time and effort trying to refine the component models, modifying the system configurations and studying the effect of critical parameters such as the minimum flow parameters of components, and convergence criteria (specified in the definition file), it was finally decided to abort the complex system configuration and resort to much simpler and workable system. This "fall back" approach created a necessity for a simpler system, which is described in detail below.

The simpler model was intended to shed more light on the working of the existing non-linear simultaneous equation solver SNSQ. Hence, a simple system as shown in Figure 4.1 is comprised of just three components: bridge deck (Type 100), ground loop heat exchanger (Type 139), and controller (Type 540) was configured. The motivation behind configuring such a system was to study the system performance when operated in the recharge mode by doing a simple heat balance on the ground loop and bridge deck sides. The flow rates are fixed parameters in the heat pump and GLHE models. The

90

controller sends a control signal depending on the bridge deck temperature, and snow flag to determine whether there is any flow in the components (1 =flow), no flow in the components (0= no flow), or recharge flow in the components (a fraction; 0.3 in this case). The parameters of components used in the simulation are listed in Table 4.1 and a detailed port diagram is shown in Appendix B
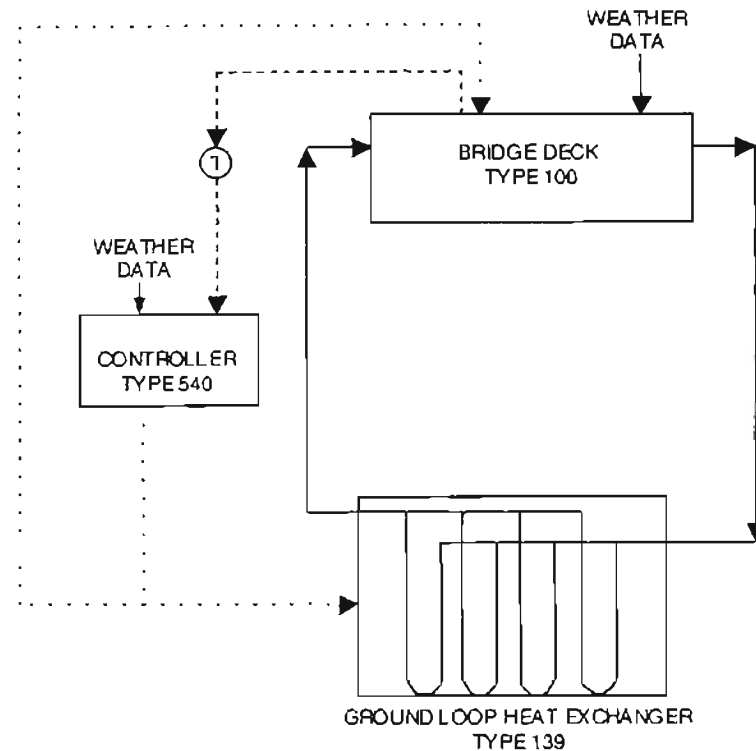
Figure 4.1. *Bridge deck system (recharge mode)*

Reading the flow rate of the components as model parameters removes it from the system of simultaneous equation set. Moreover, reducing the number of simultaneous variables decreases the burden of computation time on the machine, as the computation time is directly proportional to the square of the number of simultaneous equations. Removing the flow rates from the equation helped the system simulation to run smoothly. However, this does not mitigate the whole problem. There were still some discrepancies

during recharge periods. Hence, it was decided to scrutinize the system operation during

recharge mode.

Table 4.1. Bridge deck system parameters (recharge mode)

Parameter No	Bridge Deck TYPE 100	Ground loop heat Exchanger TYPE 139	Controller TYPE 540
1	Length = 200 m (656 ft)	Number of boreholes =250	Lower set point = 0°C (32°F)
2	Width = 12.5 m (40 ft)	Borehole depth =76.2 m (250 ft)	Upper set point = 2.78°C (5°F)
3	Slab orientation = 90°	Borehole radius = 6.351 cm (2.5")	Recharge set point = 32.2°C (90°F)
4	Slab thickness = 0.2032 m (8")	k ground = 0.6923 W/(m K) (0.4BTU/(h-F-ft))	Max. no. of heat pump pairs = 8
5	Pipe spacing = 0.3048 m (12")	Ground vol. heat capacity= 2347 KJ/(m3 K) (35 BTU/F-ft3)	
6	Pipe diameter = 2.667 cm (1.05")	Fluid specific heat capacity = 3.77 (kJ/kg K) (0.9 BTU/lb-K)	
7	Pipe depth = 7.62 cm (3")	Undisturbed ground temperature = 17.2°C (63°F)	
8	Depth to interface material =15 m (50 ft)	Min. flow rate = 5 kg/s	
9	k layer 1 =1.4 W/(m K) (0.81 BTU/(h-F-ft))	k grout = 0.6923 W/(m K) (0.4BTU/(h-F-ft))	
10	k layer 2 =1.4 W/(m K) (0.81 BTU/(h-F-ft))	k pipe- 0.3911 W/(m K) (0.226 BTU/(h-F-ft))	
11	Emissivity coefficient = 0.9	k fluid = 0.6023 W/(m K) (0.348 BTU/(h-F-ft))	
12	Absorptivity coefficient = 0.6	Fluid density = 1024.0 kg/m3 (64 lb/ft3)	
13	Vol. heat capacity 1 =2200 kJ/(m3°K)(33 BTU/F-ft3)	Fluid viscosity = 9.88E-4 N/(s m2) (2.4 lb/ft-h)	
14	Vol. heat capacity 2 =2200 kJ/(m3°K)(33 BTU/F-ft3)	U-tube outer diameter = 2.667 cm (1.05")	
15	k pipe =0.391 W/(m²K) (0.226 BTU/(h-F-ft))	Distance between U-tube legs = 2.54 cm (1")	
16	Pipe wall thickness = 0.24245 cm (0.1")	Pipe wall thickness = 0.241cm (0.1")	
17	Fluid type = 1 (Water)	Maximum flow rate = 58.45 kg/s	
18	Fluid concentration = 42 %		
19	No. of pipe circuits =110		
20	Pipe length = 73.818 m (242 ft)		
21	Finite difference time step =30 seconds		
22	Bottom boundary condition =1(Convective)		
23	Minimum flow rate = 0.1 kg/s		
24	Maximum flow rate = 22.7315 kg/s		
25	Recharge flow rate = 17.535 kg/s		
26	Recharge fraction = 0.3		

In order to reduce the computation burden and simulation run time, weather data

(Oklahoma City –1983) starting from June 15 was used instead of using a whole year. A

heat balance test of the heat transfer rates on ground and bridge deck was conducted.

Figure 4.2 shows the ground loop ExFT, and the heat balance performed on the ground

and bridge heat transfer rates. For the simulation to be correct, the heat balance (or heat

imbalance) should be zero for each hour. Clearly, it is not always zero and, for many

hours, the heat imbalance exceeds 100 kW (341 kBTU/hr).
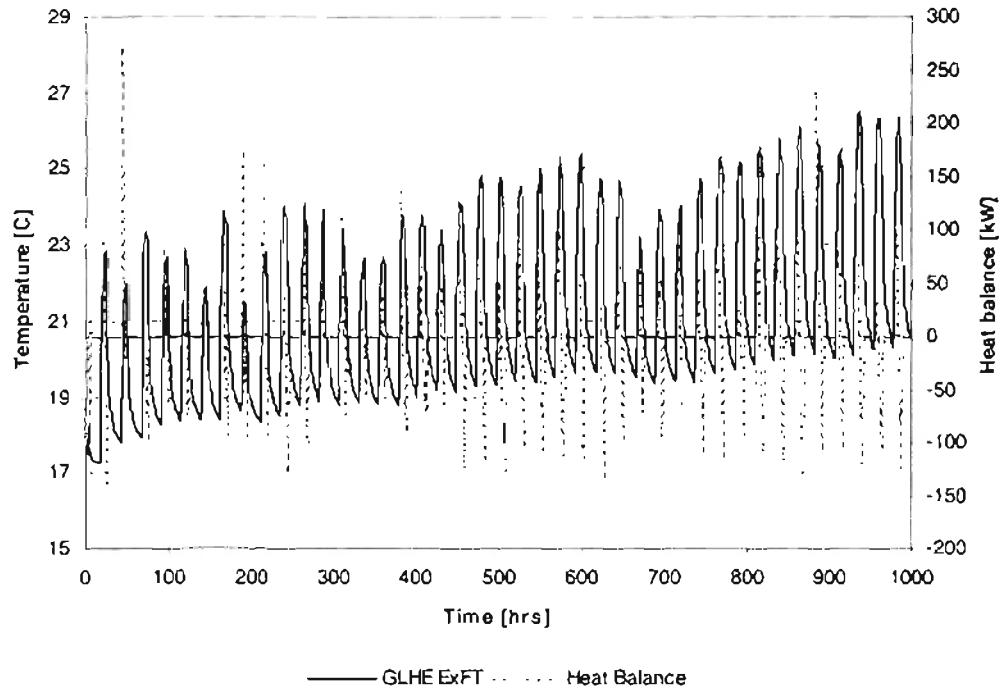
Figure 4.2. *Ground loop ExFT and heat balance during summer recharge [June 15 –July 27]*

Convergence Problems

As shown in Figure 4.2, the system simulation results fail to pass the heat balance test. It is clear that the system simulation encounters convergence problems whenever the system starts to recharge or is about to stop recharging. This is indicated by the warning message "iteration not making good progress" prompted on the screen by the HVACSIM+ solver SNSQ. The solver prompts the error message when the steps taken in gradient direction, while searching for a solution (global minimum) in the domain, exceeds 10. The number of iterations that limit the gradient step bounds (NSLOW1), which the algorithm uses as a criterion for checking the progress of iterations in SNSQ, was changed to 50. Although this improved the solution only marginally and eliminated

the warning message about the progress of iterations from prompting onto the screen, it did not have a significant effect on the solution as such.

A closer investigation of the residuals, printed in the diagnostic report, during the hours when the system was recharging revealed that the solution had failed to converge even though it has satisfied all the stringent convergence criteria. In addition, it gave no warnings on the screen as it used to before when the limiting number of iterations was 10. The heat balance was worse during transients because of the residuals being pretty high (greater than 1). In a system which simulates mainly the temperatures (which are mostly in the range of -10 °C - 60 °C; 14°F - 140°F), a residual greater than 1°C (1.8°C) affects the results significantly. Moreover, in computing the heat transfer rates, where the temperature differential is multiplied by high flow rates, the effect of high residuals is very significant.

The convergence criteria used by SNSQ does not directly consider the magnitude of residuals. The only limiting criterion of the solver to check whether the optimum solution is reached is the step size used by the solution algorithm. The details of the solution algorithm are discussed further below.

Solution Algorithm

The subroutine SNSQ along with its associated subroutines used in HVACSIM+ to solve a set of nonlinear simultaneous equations is based on Powell's hybrid method (Powell, 1970). The hybrid method is a combination of the quasi-Newton method and the gradient method. The use of the "hybrid step", which is obtained as a convex

94

combination of quasi-Newton and scaled gradient reduction methods, facilitates faster convergence of the variables to a solution unlike the successive substitution method. The only limiting criterion of the solver to check whether the optimum solution is reached is the size of the step bound. Instead of recalculating the Jacobian at each iteration, SNSQ approximates the Jacobian during each iteration employing Broyden's rank-one update (Park et. al., 1985). However, the solver recalculates the Jacobian matrix by forward-difference approximation when the rank-one method fails to give satisfactory results. The main disadvantage of hybrid method is that it requires a good initial guess of the variables. Moreover, the convergence criteria used by SNSQ does not directly consider the magnitude of residuals.

A closer investigation of the diagnostic report indicated that higher residuals due to unconverged solution were causing large heat imbalances during transients. Moreover, higher residuals always appeared when the Jacobian was being recalculated. Hence, it was decided to include a successive substitution step, as suggested by Haves and Norford (1995), into SNSQ in an attempt to provide a good starting point for the solution algorithm whenever the starting point provided by the previous time step fails to give satisfactory results. The modification in the solver and its impact on the heat balance results is discussed below.

4.3. Modification in Simultaneous Equation Solver SNSQ

As discussed in the previous section, the existing non-linear simultaneous equation solver SNSQ fails to reduce the Euclidean norm of the residual vector to near zero. Hence, the solution vector has high residuals even though the stringent convergence

criteria are met. A successive substitution step was added to SNSQ just before

recalculating the Jacobian when the updated Jacobian fails to give satisfactory results.

The modified and documented version of SNSQ is given in Appendix D. A flow chart of

the successive substitution step (shaded part) implemented in SNSQ is presented in

Figure 4.3.
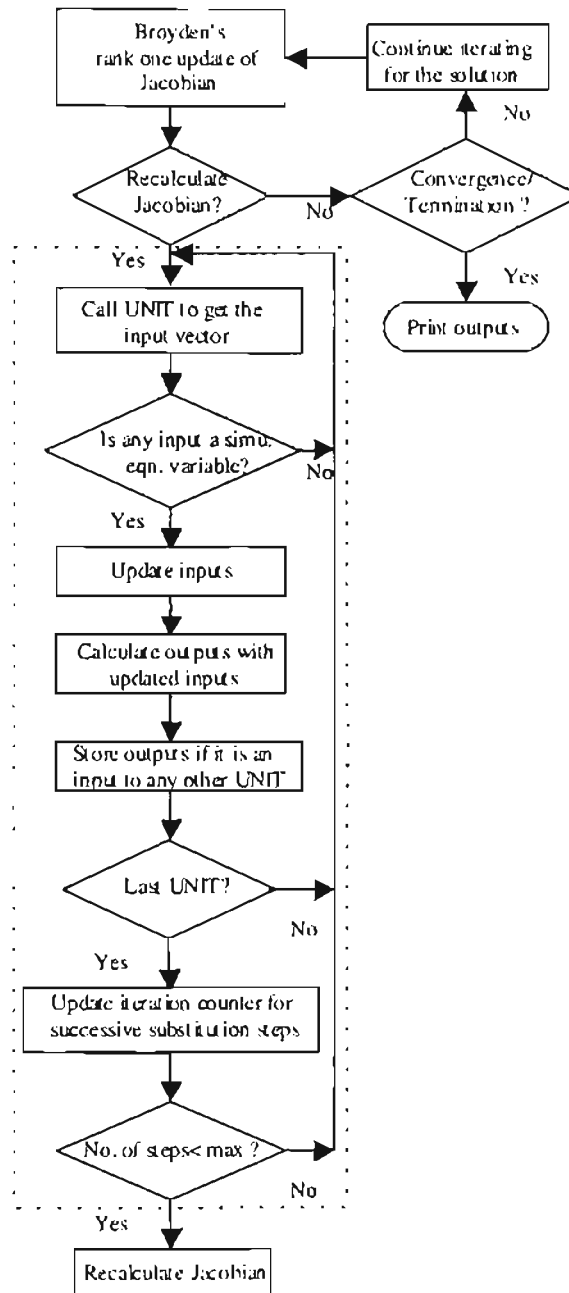
Figure 4.3. *Flow diagram for the successive substitution algorithm in SNSQ*

96

Since the input and output variables of all the units (called state variables) are stored in an array, it is first necessary to know how many and which variables are being solved simultaneously. Of all the state variables, only those inputs that are also outputs of some other component and are not boundary variables are solved simultaneously. Other variables, which may be just an output of interest (e.g., power), are not solved for by SNSQ. While implementing successive substitutions step in SNSQ, each unit is called successively. Each of the units in the system is checked for any output variable being solved by SNSQ. If none of the outputs are solved simultaneously, the unit is skipped. Then, the input vector of each unit is retrieved. If any of the inputs happen to be the output of another component, the output vector overwrites the input variable. Outputs of the unit are computed using the new input vector. If the input of the component happens to be the output of the other component, then the variable value is stored in a temporary array for update during the next iteration of successive substitution. The next unit is called and the procedure is repeated until all the units have been called and their values updated. Different number of iterations was employed in the successive substitution. This means starting from an initial value (supplied by SNSQ), the calculations are proceeded through all the units in the system until the initially assumed values have been recalculated and the recalculated values are successively substituted through all the components in the system. This loop of calculation is executed in order to get a better initial guess for obtaining the solution using the Powell's hybrid conjugate direction method after the Jacobian matrix has been recalculated.

The bridge deck system shown in Figure 4.1 was simulated again with the modifications in the solver SNSQ and the results were obtained for different number of successive substitution steps. The results using the same component parameters, components and system configuration, but employing the modified solver with 2 and 5 successive substitution steps are shown in Figure 4.4 and Figure 4.5 respectively. A few other simulation runs with 3 and 10 successive substitution steps were also tried. System simulation with two successive substitution steps was found by far to be the best among all options for the system configuration analyzed.
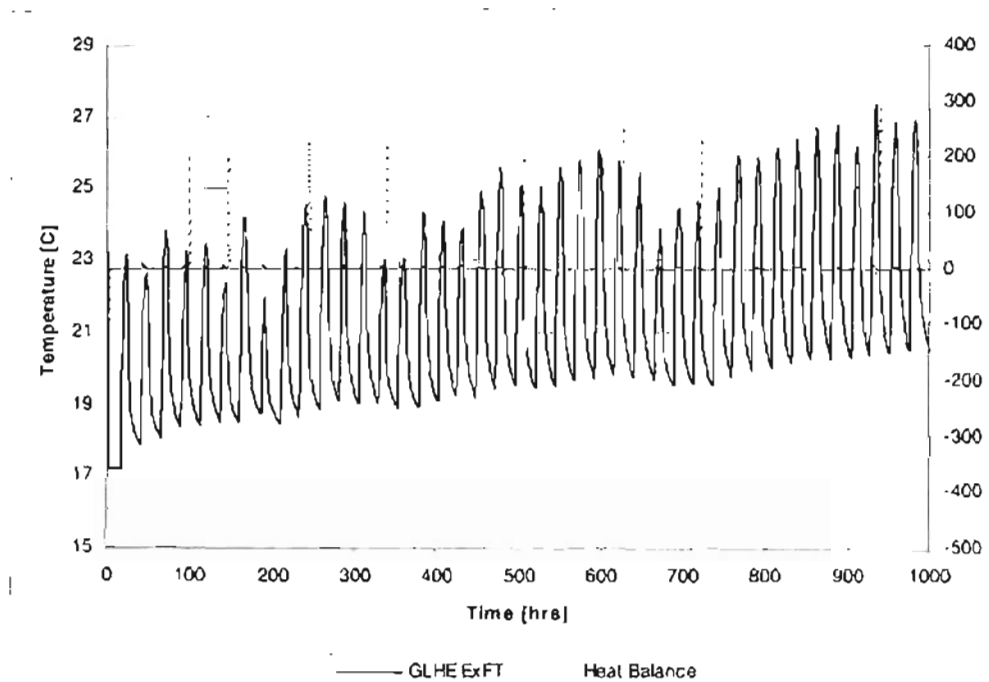
Figure 4.4. *Ground loop ExFT and heat balance during summer recharge with modified solver(Successive substitution steps :2)[June 15 –July 27]*
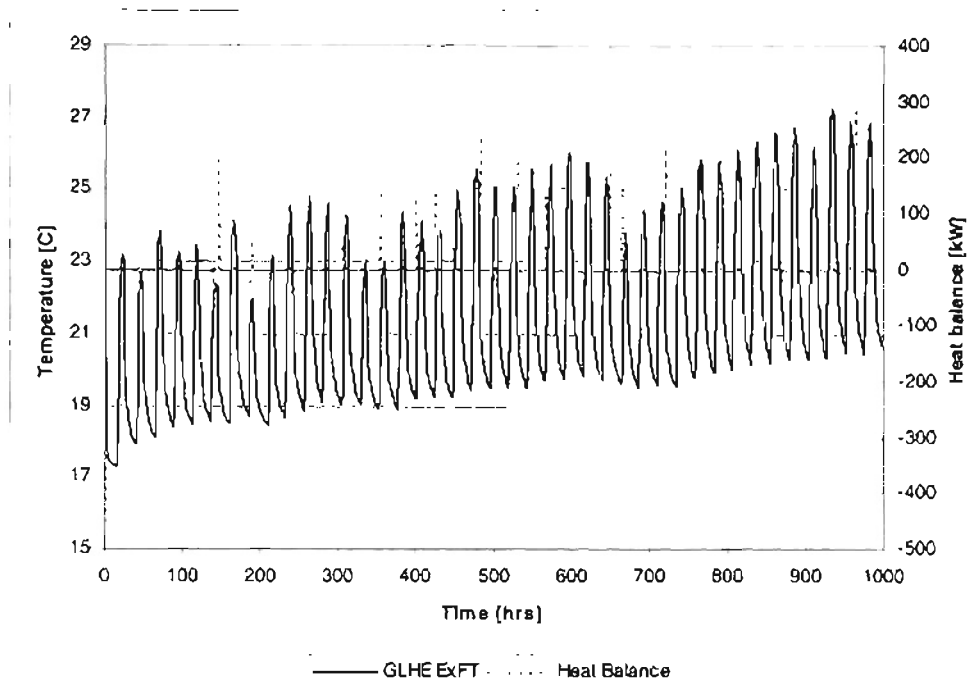
Figure 4.5. *Ground loop ExFT and heat balance during summer recharge with modified solver(Successive substitution steps :5)[June 15 –July 27]*

A comparison of results shown in Figure 4.4 and 4.5 with the one obtained with the old solver (Figure 4.2) indicates marked improvement in heat balance. The absolute value of relative error of the heat imbalance to the heat extracted from the bridge deck exceeds 1% 270, 98, 46, 45, and 44 hours, during the 386 hours when the system is recharging the ground, when 0, 2, 3, 5, and 10 successive substitution steps are used respectively. However, the relative error $[|(Q_{bridge}-Q_{ground})/Q_{bridge}|]$ exceeds 10% only 10 hours (2.5% of the total time in recharge) for two successive substitution steps where as the modified solver with 0, 3, 5, and 10 successive substitution steps exceeds the 10 % relative error for 182, 39, 43, and 26 hours respectively. This indicates that the residuals of the variables have been reduced significantly. However, there are still large imbalances during some of the transient conditions. The effect of using an under-relaxation factor of 0.5 in the successive substitution step was also investigated. This dampened the effect of

substituting an altogether new value of the variable with its value from the previous iteration of the substitution step. This did not iron out the discrepancies in the heat balance, i.e. the residuals were still high during some transient conditions. One possible solution could be using sophisticated "sticky controller" to mitigate some of the discrepancies during the transient stages when the system comes on or off. Another possible solution is to shorten the minimum time step.

4.4. Bridge Deck System with Winter Heating and Summer Recharge

As the final step in the study, a bridge deck heating system with provisions for summer recharge operation was configured with the ground loop heat exchanger, bridge deck, heat pump, controller models already described in chapter 3. The system was necessary to study the performance of a heated bridge deck model with a provision for summer recharge. A detailed description of the component models is provided in Appendix A. The models used were the ground loop heat exchanger (Type 139), the bridge deck (Type 100), the ganged heat pumps (Type 75), two circulation pumps (Type 546), and a bridge deck controller (Type 540). The "full" mass flow rate of each component was declared as parameter instead of being treated as input/output variable as described in section 3.5.2-3.5.5. Flow in each component is activated by a signal from the controller. The controller either shuts off the flow (control signal =0), or operates the component in full capacity (control signal =1) during heating, or activates a fraction of the ground loop flow in the bridge deck (control signal = a fraction between 0 and 1) during recharge mode. The ganged heat pump model is bypassed during recharge and the flow through the bridge deck is directed to the ground for "recharging" the ground, i.e.

picks up the heat from heated bridge deck and stores it in the ground during summer for later use (for snow melting applications in winter). The system schematic is shown in Figure 4.6 and a detailed port diagram is shown in Appendix B, Figure B.2.
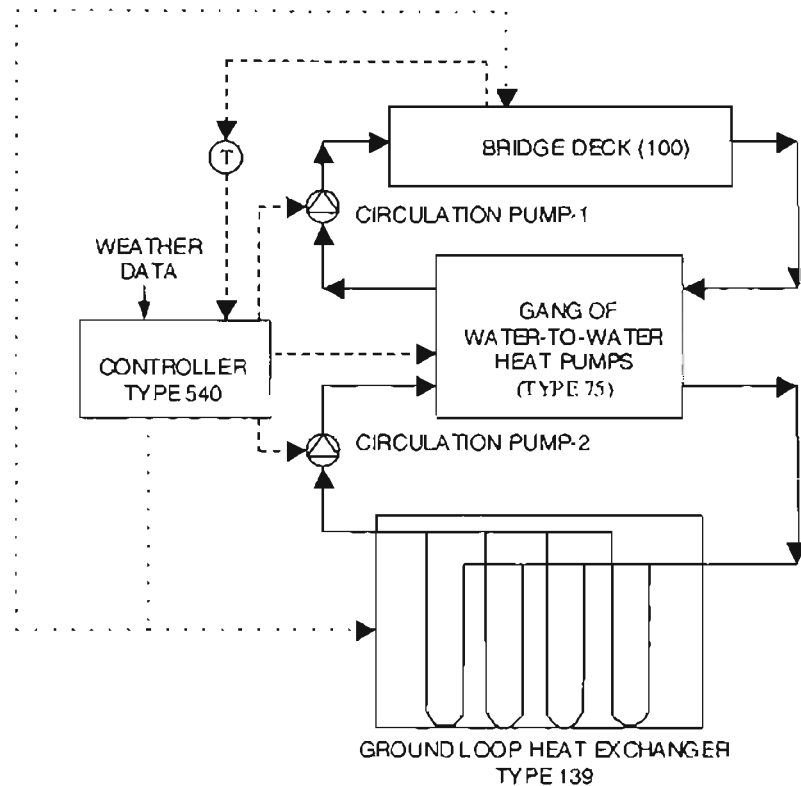
Figure 4.6. *Bridge deck heating system*

A detailed description of the parameters used in system simulation, the control strategies and system simulation results are covered in chapter 5.

4.5. Summary

Numerous problems were encountered while creating a workable bridge deck heating system in HVACSIM+. The "unfriendly" user interface, cryptic input files, and tedious process of configuring and debugging various systems were not the most serious

101

problems encountered. Problems related to convergence were much more time consuming, and are not completely fixed at this point. The author has spent considerable time and effort, with plenty of suggestions from HVACSIM+ users, help from manuals, and published articles, to gain an understanding of the simulation environment within the time available. Due to various constraints, the author has had to accept the solver results, even though the heat balance is less than satisfactory for some hours. In the next section, a geothermal bridge deck heating application is considered and, a simple set point strategy for recharging the ground during summer is investigated.

Chapter 5

Deicing and Recharge Strategies for a Hydronically Heated Bridge Deck that use Hybrid GSHP systems – The Weatherford Bridge Deck Model

5.1. Introduction

In the previous section 4.4, it was explained how a workable bridge deck heating model was configured in the HVACSIM+ simulation environment, the problems faced during system modeling, and the remedial measures taken to circumnavigate the problem. The work described in this chapter is an extension of what was described in section 4.4. The bridge deck heating model depicting the Weatherford bridge deck system is simulated for an year. A detailed description of the Weatherford bridge deck system is given. First, a simple set point strategy for recharging the ground during summer is investigated. Sample simulation results of a days operation in winter and two days operation during summer have been presented. Next, the predicted performance of bridge deck heating system under a few more set point temperatures has been studied and a simple cost analysis performed. This study on the bridge deck heating system is intended for establishing a better understanding of the performance and aiding future design of such systems.

5.2. Weatherford Bridge Deck

The Weatherford bridge is located east of Weatherford, Oklahoma on Interstate Highway 40 (I-40). The bridge spans a county road, a creek, and a railroad. The existing

bridges are scheduled to be replaced by new bridges 215m (705 ft) long by 12m (40 ft) wide. The westbound section of the bridge is intended to be heated by the ground source heat pump system.

5.3. Hybrid System Description

The design procedure for the GSHP system is described in Chiasson and Spitler (2000). The authors used an iterative procedure for finding a suitable combination of number of heat pumps, borehole field size and depth, and minimum entering fluid temperature. The ground loop heat exchanger design tool, GLHEPRO (OSU, 1996), and a system simulation were used for arriving at the final design. The final design of the GSHP system consists of eight pairs of heat pumps of nominal 30-ton (105 kW) capacity and 250 boreholes, each 76 m (250 ft) deep. The weather conditions that are used to arrive at the final design are a constant snowfall rate of 10 in/day (25 cm/day), air temperature of –9.4 °C (15°F), and a wind speed of 22.5 km/hr (14 miles/hr). 42% propylene glycol at a flow rate 22 l/s (350 gpm) is assumed to be the heat exchange fluid circulated through the bridge deck. The flow rate in the ground loop during bridge heating is maintained at 57 l/s (900 gpm). Eight pairs of heat pumps of 30-ton (105kW) nominal capacity represent Water Furnace Spectra SXW360 arranged in parallel on the source side and in series on the load side. A recharge flow of 3/10th of the ground loop flow rate has been used during the summer recharge in the simulation.

The ground loop heat exchanger (Type 139), gang of water-to-water heat pump (Type 75), controller (Type 540). and the bridge deck (Type 100) are utilized to represent

the final design of the bridge deck heating system. The information flow diagram of the system is shown in Appendix B, Figure B.2.

The system is simulated on an hour-by-hour basis for one year. HVACSIM+ is used as the simulation environment. The non-linear simultaneous equation solver (with a successive substitution step) as described in the previous chapter is used in the system simulation.

As discussed earlier in sections 4.2 and 4.3, the solver has problems with convergence and results in high residuals during some transient conditions. The system simulation is internally consistent during most of its operation during recharge. However, the results during winter heating, when there is a change in the number of heat pump pairs being used for subsequent hours, is far from satisfactory for some hours. Due to the limitations of the solver, the system simulation failed to give satisfactory results during some of the hours in heating and recharge operation. The data points that resulted in high relative error (greater than 10%) in heat balance have been eliminated from the electricity cost calculations. Compared to leaving the spurious hours in the calculation, this will reduce the error. (However, the hours that are eliminated have some electricity consumption that will not be accounted for. Therefore, it is estimated that the heating cost calculations may under predict by about 20%.)

5.4. Weather Data

The system is simulated with 1983 Oklahoma City weather data compiled and developed by Ramsey et al (1999) by processing the meteorological data obtained from

the Solar and Meteorological Surface Observation Network (SAMSON) (NCDC 1993).

The SAMSON database covers a longer and more recent period (1961-1990) than its

predecessor Solar and Meteorological (SOLMET) database (1952-1975) and uses

improved measurements and an improved model for estimating solar radiation. The data

set has information about following parameters: direct (beam) solar radiation, total

horizontal solar radiation, dry-bulb and dew point temperatures, precipitation, weather

indicator, wind speed, and cloud cover.

The system simulation required additional information such as sky temperature,

snowfall and rainfall rate, total solar radiation, and solar angle, which were computed

using the available weather information. The solar angle θ (radians) is computed using

the latitude and longitude information for the location and the date and time. The total

solar radiation (W/m^2) is computed using the equation given by Equation (5.1).

$$solar\ radiation_{total} = solar\ radiation_{beam} \times cos\theta + solar\ radiation_{diffuse} \qquad (5.1)$$

The sky temperature T_{sky}(°C) is computed from the dry bulb temperature T_{db} (°C)

and dew point temperature T_{dp}(°C) using the Bliss(1961) model.

$$T_{sky} = (T_{db} + 273.15) + (0.8 + T_{dp}/250.)^{0.25} - 273.15 \qquad (5.2)$$

The raw weather file contains a flag for snowfall (S) and rainfall (R), and the

precipitation rate. The snowfall and rainfall rates (mm of water equivalent/hr) for each

hour are computed by multiplying the snow/rain indicator (1 or 0) with the corresponding

precipitation rate. The snowfall and rainfall rates thus calculated are used in the boundary

files for running the system simulations.

106

A boundary variable file containing an annual weather data starting from April 01, 0:0 hours has been used in the subsequent study. The intention of starting the simulation of the bridge deck heating system from April is to initially recharge the ground from April through November, and study its effect on the heat pump power consumption during months when the system operates under heating mode. This gives a better picture of the effect of recharging the ground on the system heating performance. Running multiple year simulations would have given an even better picture but would have taken more time.

5.5. Control Strategy

A simple control strategy has been employed for the system simulations. However, to study the feasibility of the bridge deck heating system and the impact of recharge on the system design a more sophisticated control strategy will be required. The current control strategy uses the weather information from the boundary file. The snow event is forecasted artificially since the weather information is already available for the whole year. The bridge deck heating system is switched on six hours prior to a snow event and is operated until there is no longer any snowfall. The number of pairs of heat pumps to be operated depends on the bridge surface temperature. One pair of heat pump is used for a surface temperature of 2.78°C (37°F) and above during the heating mode. Eight pairs of heat pumps are used for surface temperature of 0°C (32°F) and below. For surface temperatures between 0°C(32°F) and 2.78°C(37°F), the number of heat pump pairs are linearly controlled. However, since fractional heat pump pairs does not make any sense, the number of heat pump pairs is rounded off to the next highest whole

number. Hence, the numbers of heat pump pairs are controlled step-wise depending on the surface temperature as shown in Figure 5.1.
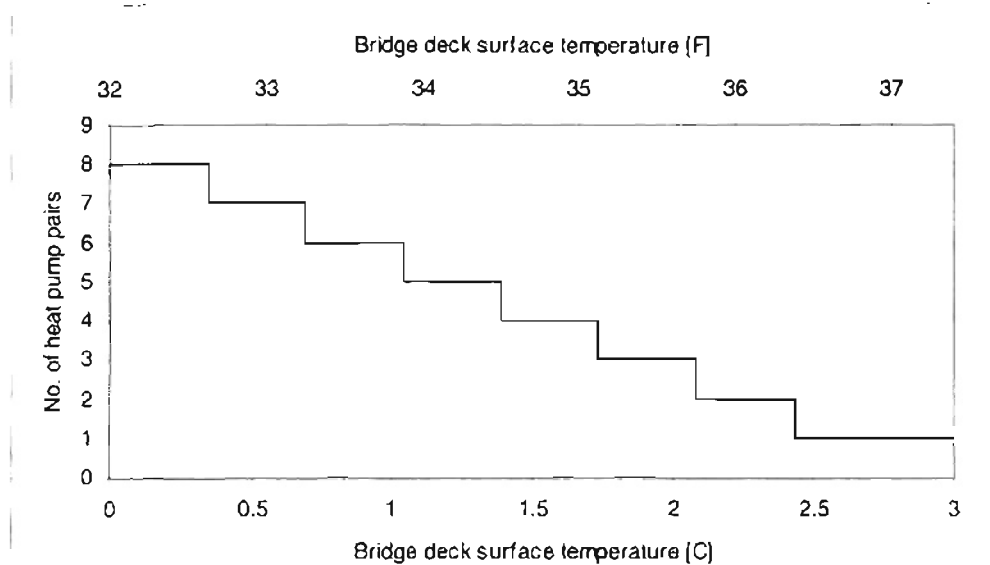
Figure 5.1._Number of heat pump pairs to be operational during heating mode_

The flow through the bridge deck is diverted to the ground loop heat exchanger, bypassing the heat pumps during summer for "recharging" the ground. The controller sends control signals to the pumps, bridge deck, heat pumps, and the ground loop heat exchanger when the bridge deck surface temperature exceeds a user specified set point, 32.22°C (90.0°F) has been used in the study. In section 5.6.2, the effects of using different set points will be investigated.

5.6. System Simulation Results and Discussion

The hydronically heated bridge deck system described in the previous section is simulated with Oklahoma City weather data pertaining to the year 1983. Sample results of the system performance for one day in the winter and two days in the summer are

presented. In addition, annual ground heat extraction /rejection rates, heat pump power consumption, and operating cost of the system for a few set point controls are presented. During winter, the heat pump transfers heat from the ground loop to the bridge deck to heat the bridge deck. During summer operation, the system operates in "recharge" mode as the heat picked up from the bridge deck surface is stored in the ground. The results help gain a better understanding of the hour-by-hour system performance of the bridge deck system. Both the modes of operation of the bridge deck system are yet to be optimized.

5.6.1. Winter Snow Melting

Figure 5.2 (a) and (b) shows the operation of the bridge deck surface temperature, ambient temperature, and snowfall rate on January 1 in SI and IP units respectively. The heat pump comes on 6 hours prior to the snow event at hour 6614 (2 p.m.). Due to relatively mild weather conditions, only one pair of heat pumps is operated through out the snow event from 6614 hours – 6625 hours except during hour 19 (7 p.m.) when another pair is switched on as the bridge deck surface temperature drops below 2.77°C (37°F). The bridge deck surface temperature is maintained above freezing through out the heating period. The surface temperature of the bridge deck drops, even though one pair of heat pump is in operation, after the hour 6615 (3 p.m.). The temperature drop at the bridge deck is more rapid than that of the ambient temperature after 6615 hour (3 p.m.) due to the reduced contribution of the solar radiation towards the bridge deck heating.
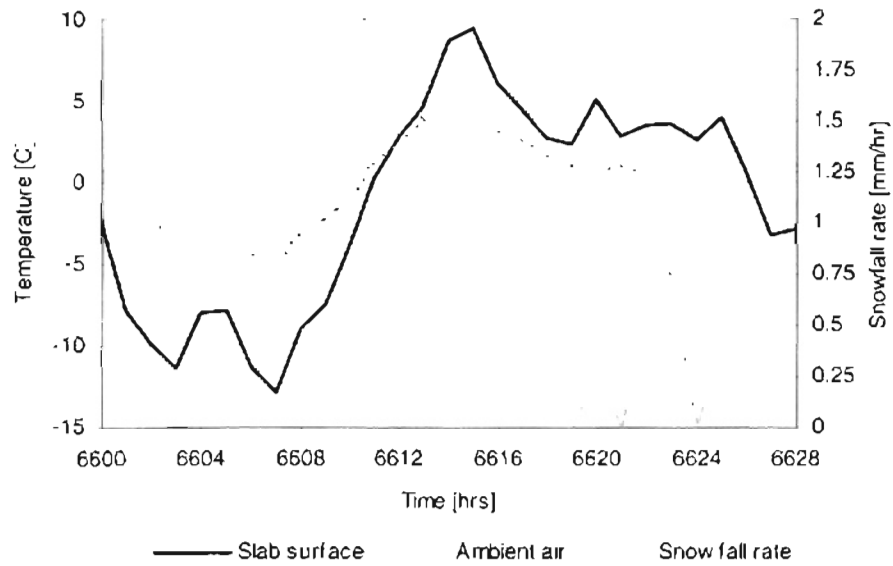
.

Figure 5.2(a). *Slab surface temperature, ambient air temperature, and snowfall rate (January 1) –OKC 1983 (SI)*
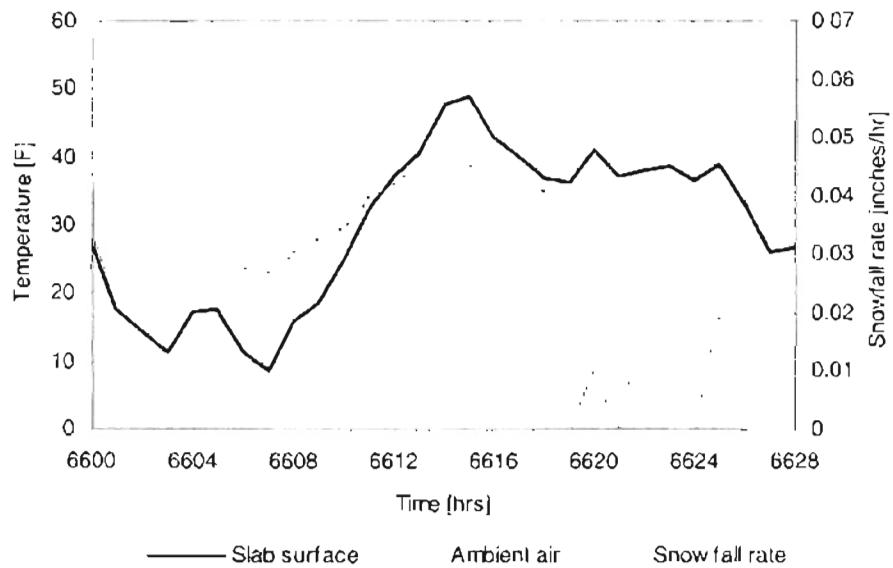
Figure 5.2(a). *Slab surface temperature, ambient air temperature, and snowfall rate (January 1) –OKC 1983(IP)*

Figure 5.3 shows the ground loop entering and exiting fluid temperatures during the heating operation on January 1. It can be seen from Figure 5.3 that the ground loop entering temperature dips as the fluid at the heat pump exit on the source side runs cooler due to a second pair of heat pump being in operation during hour 6619.

Ground loop temperatures
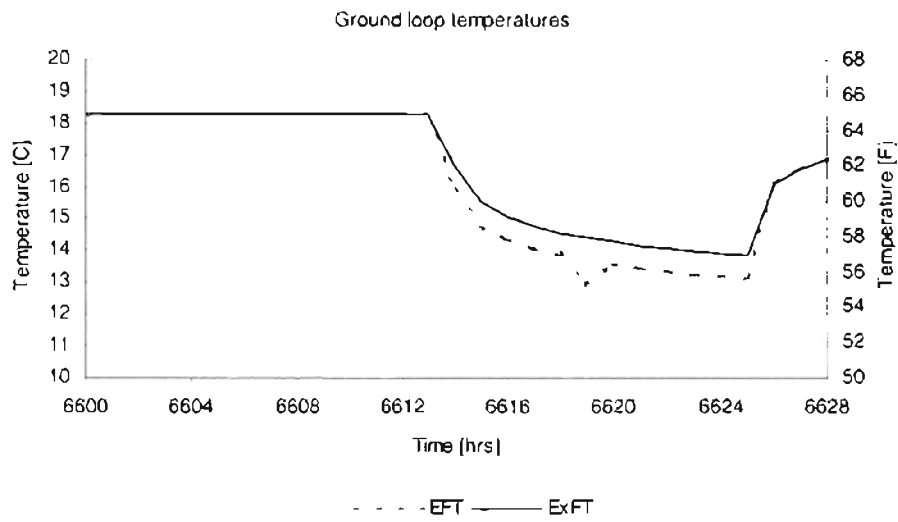
Figure 5.3. *Ground loop heat exchanger entering and exit fluid temperatures (January 1) –OKC 1983*
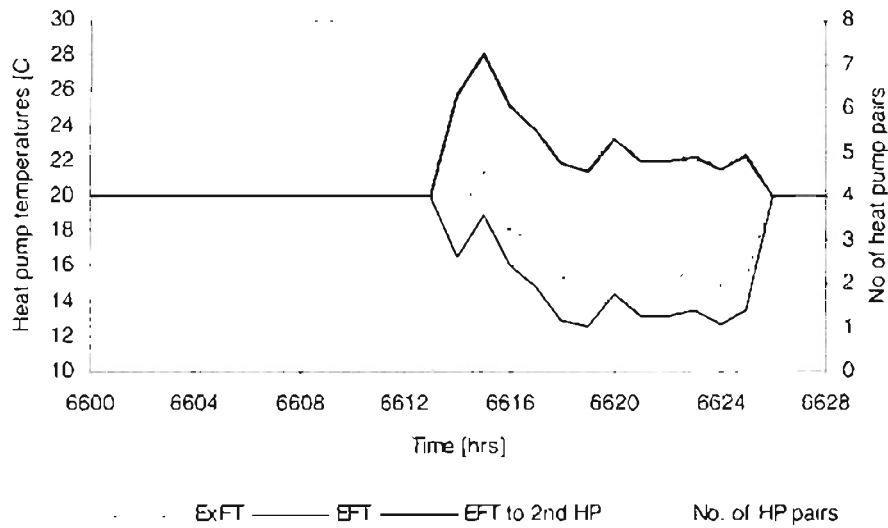
Figure 5.4(a). *Heat pump temperatures on the load side, number of heat pump pairs in operation (January 1)-OKC 1983 (SI)*
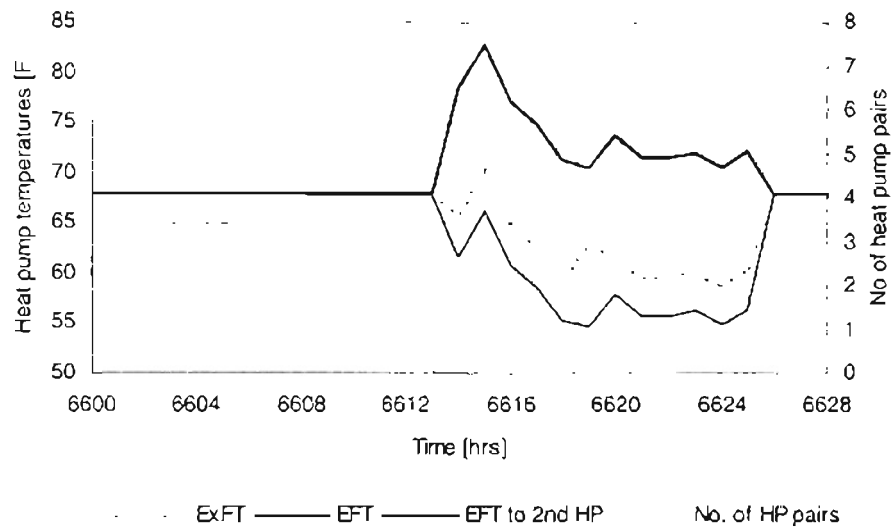
Figure 5.4(b). *Heat pump temperatures on the load side, number of heat pump pairs in operation (January 1)-OKC 1983 (IP)*

Figure 5.4(a) and (b) shows the heat pump fluid temperatures on the load side and the number of heat pump pairs in operation in SI and IP units respectively. The fluid temperatures at the heat pump pairs exit are much lower than that exiting from the first heat pump in the pair. This is due to the mixing of the hot fluid at the exit of the operational pair with much cooler fluid exiting from the non-operational heat pump pairs. The exit fluid temperature of the heat pump pairs that are not in operation is the same as their inlet temperatures. This explains the temperature rise of only a few degrees (2°C-5°C; 3.6°F – 10°F) in the fluid temperature from the "ganged" heat pumps, though the temperature rise across the first heat pump is 8°C – 10°C (14.4°F – 18°F). The EFT to the second heat pump is well within the maximum allowable EFT (48.9°C, 120°F) throughout their operation during such relatively mild weather conditions. The heat pump fluid temperatures are assumed to stay constant at 20°C (68 °F) when the system is neither in heating mode nor in recharge mode.

5.6.2. Summer Recharge

Summer recharge involves storing heat in the ground during the summer for use in the winter. Without summer recharge, over the years of use of the GLHE system, the ground surrounding the ground loop heat exchanger will get colder and colder. This will lead to lower entering fluid temperatures to the heat pump and unsatisfactory performance of the system. The system might not be able to meet the load requirements during periods of severe weather. Hence, it is necessary to put back a part or whole of the heat extracted by diverting the hot fluid in the bridge deck to the ground during summer thereby "recharging" the ground of its depleted thermal energy. This assures that the ground has been recharged of the heat that was extracted during winter.

The results obtained by simulating the GSHP system with provisions for recharging the ground during summer are of some interest. The flow is diverted to the ground when the temperature at the bridge deck exceeds 32.22°C (90°F). The bridge deck surface temperature, ambient air temperature and the solar radiation for a day in mid July are shown in Figure 5.5 (a) and (b). The bridge deck surface temperature starts to rise with the incident solar radiation and ambient air temperature and peaks around 12 noon. The circulation pumps starts pumping the fluid once the surface temperature exceeds the set point at hour 2600(8 a.m.) and starts recharging the ground till the bridge deck surface temperature drops below the set point at hour 2610(6 p.m.). The fluid enters the ground hotter and leaves the ground loop heat exchanger cooler thereby rejecting heat to the ground. The ground loop fluid temperatures are shown in Figure 5.6. It should be noted that the ground loop entering and fluid temperatures are artificially fixed to be the same

113

when the fluid is not being circulated. However, the fluid temperature can be seen to be dropping gradually before and after the recharge. This is because the heat added to the ground loop heat exchanger diffuses into the nearby ground.
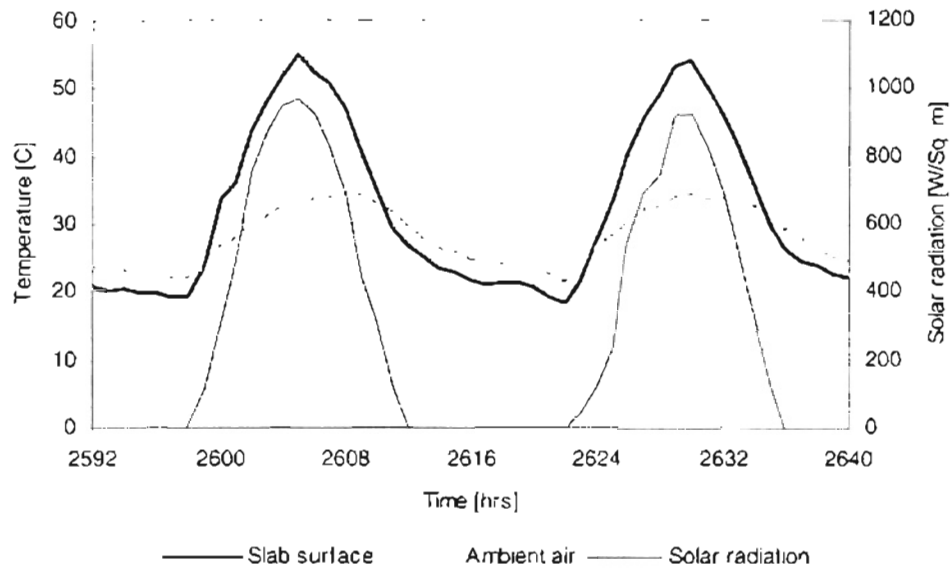
Figure 5.5(a). *Slab surface temperature, ambient air temperature, and solar radiation(July 17-18) -OKC 1983 (SI)*
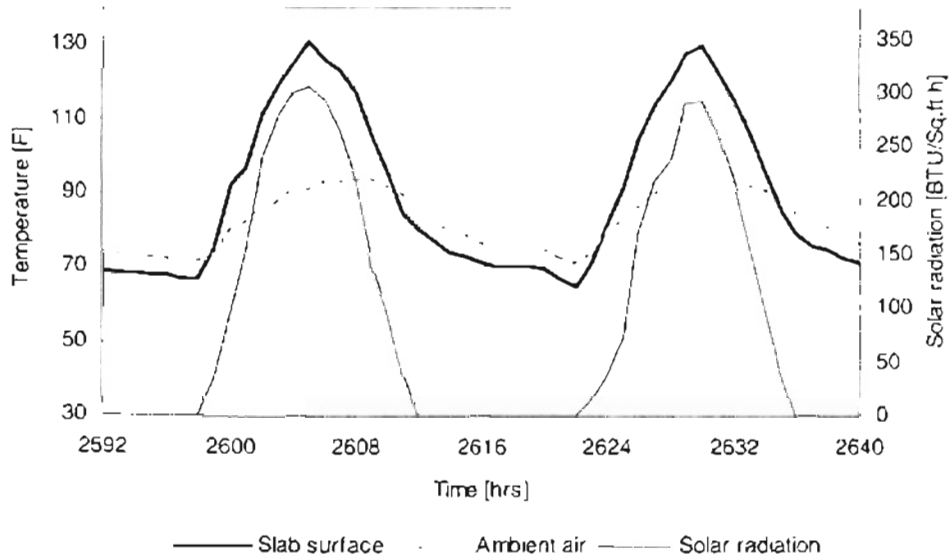
Figure 5.5(b). *Slab surface temperature, ambient air temperature, and solar radiation(July 17-18) -OKC 1983 (IP)*

114
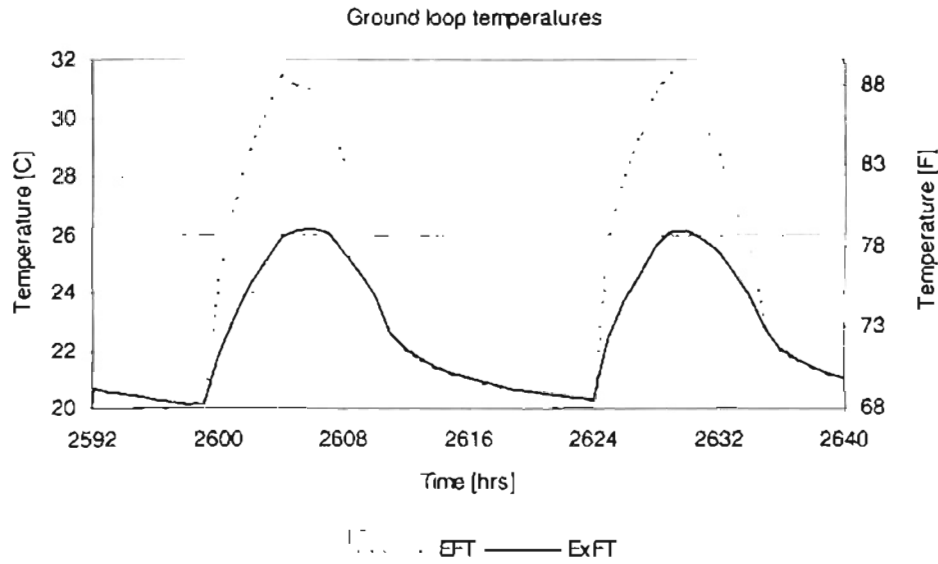
Figure 5.6. *Ground loop heat exchanger entering and exiting fluid temperatures (July 17-18) -OKC 1983*
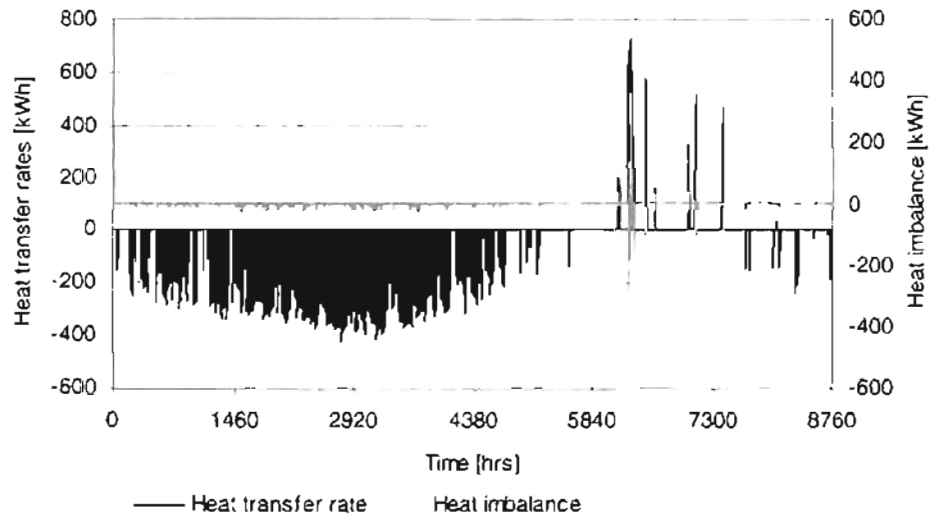
Figure 5.7. *Annual recharge rates and heat imbalance*

A simple heat balance check as indicated by equation (5.3) is performed on the simulated results.

$$Heat\ imbalance = Q_{ground} + Q_{heat\ pump} - Q_{bridge\ deck} \tag{5.3}$$

As discussed earlier, the imbalance should be equal to zero for the simulation to be internally consistent. However, it is evident from the Figure 5.7 that there are marked

115

heat imbalances during the heating period. The heat balance during heating of the bridge deck is far from satisfactory. The relative error between the heat imbalance and the heat transfer rate to the bridge deck is more than ±10% for 23% of the time (27 hours out of 118 hours it operates during heating). During summer recharge, the heat extracted from the bridge deck agrees with the heat rejected to the ground within ±1% for 99% of the time it is used. The reasons have already been discussed in the earlier chapter.

It is necessary to minimize the operating cost for recharging the ground. Recharging the ground for more hours than necessary will increase the operating costs. Reducing the number of hours that the circulation pumps are used during summer will cut down on the operating cost but might prove detrimental to the system performance during winter. It is necessary to find an optimum control strategy to make the HGSHP system economically attractive for bridge deck heating applications. The effect of different control strategies on the system performance can be analyzed by employing system simulation tools. In this study, only a simple set point control strategy has been used. The system was simulated with a few more set points to study the system performance. The additional set points that were analyzed are 35.0°C (95.0°F) and 37.78°C (100°F), which are higher than the one previously used (32.2°C, 90.0°F). The higher the set point, the less frequent the bridge deck surface temperature exceeds it, and the fewer hours the pump is operated. All the system parameters including the flow rate were otherwise identical to the ones used with 32.2°C (90.0°F) set point.

The cost of operating the circulation pumps is of great concern during recharging the ground. The following assumptions have been used for computing the operating cost in this study:

- Electricity cost of $0.07/kWhr

- Circulation pump power of 75 HP (56kW) on the ground loop side and 60 HP (45kW) on the bridge deck side during heating mode

- Circulation pump power of 50 HP (37 kW) during recharge mode

- All data points with relative error $[|(Q_{bridge}-Q_{ground})/Q_{bridge})|]$ greater than 10% have not been considered towards the operating cost calculation for all cases. As a result, 27 data points in heating mode and nearly 20 data points in recharge mode have been eliminated for all cases. This will cause an under prediction in heating electricity consumption of about 20% and an under prediction in pumping electricity consumption of about 2%.

Results obtained from the simulation run for a year period provided deeper insight into the system performance. The summary of the simulation results is shown in Table 5.1. It is noted that the ratio of the net heat rejected to the net heat extracted from the ground is 11.1 for the system with 32.2°C (90.0°F) recharge set point, 10.1 for the system with 35.0°C (95.0°F) set point, and 8.6 for the one with 37.78°C (100°F). The net recharge rate went down by nearly19 % when the recharge set point is increased from 32.2°C (90.0°F) to 37.78°C (100°F). Still the system is far from being optimized for balancing the annual ground loads.

.

Table 5.1. Summary of simulation results for various set points

		Recharge set point temperature C (F)		
		32.2 (90)	35 (95)	37.7 (100)
Operating Hours of the system (Rel Err<10%)	Recharge	1397	1181	969
	Heating	91	91	91
Operating Hours of the system (Rel Err>10%)	Recharge	18	20	18
	Heating	27	27	27
Ground heat transfer rates, kWh	Recharge	311175	283434	252815
	Heating	27927	28133	29285
Ground heat rejection/extraction	Ratio (-)	11	10	9
Heat pump power consumption	kWh	8197	8264	8421
	kBTU	27970	28197	28731
Circulation pump power consumption	kWh	61273	53216	45308
	kBTU	209062	181573	154592
Heat pump operating cost	$	$574	$578	$589
Circulation pump operating cost	$	$4,289	$3,725	$3,172
Total Operating Cost	$	$4,863	$4,304	$3,761

The simulation results indicated that the system with a recharge set point of 32 2°C (90.0°F) operated the circulation pumps for 1415 hours during recharge Also, the systems with recharge set points 35.0°C (95.0°F), and 36 38°C(97.5°F) operated for 1201 and 987 hours, 8% and 15% less than the one with 32.2°C (90.0°F) respectively.
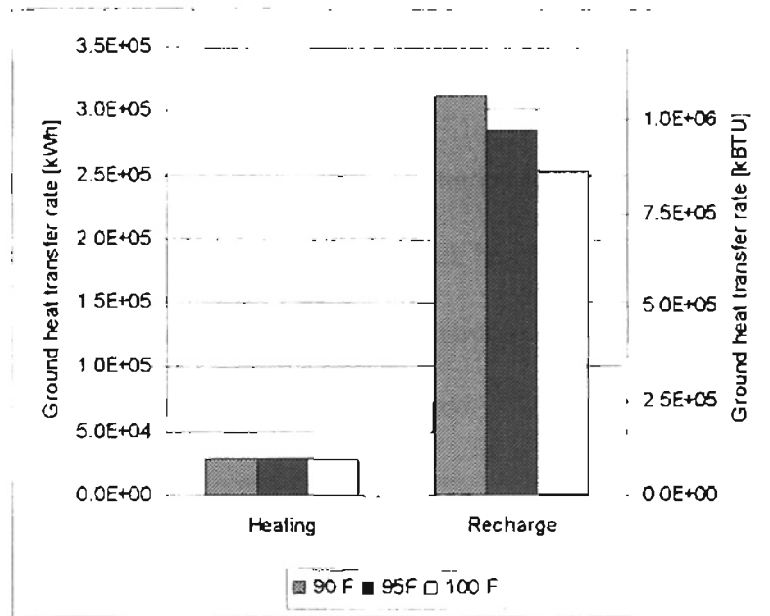
Figure 5.8. *Net heat transfer rates to the ground during recharge and heating*

The net heat rejected or extracted from the ground during recharge and heating is given by Figure 5.8. It is evident from the figure that the net heat rejected to the ground exceeds the heat extracted during winter by a large margin. The heat put back into the ground during summer is approximately 10 times that taken from it during winter. It is possible to run the circulating pump for fewer hours and yet balance the annual load. In addition, the difference in the heat rejected to the ground is not as significant as the difference in operating hours during recharge when the set point is raised from 32.2°C (90.0°F) to 37.7°C (100.0°F). This is because it is possible to extract more heat from the bridge deck at a higher set point than at a lower one. Therefore, the system can be operated at a higher set point for fewer hours thereby cutting down the operating costs with little compromise on the amount of heat rejection to the ground. Hence, further investigation on the effect of different control strategies on the recharge heat transfer rates is required. It is also necessary to strike a balance between increasing the ground temperature and reducing the pumping costs.

5.7. Summary

In this study, a few set point control strategies for recharging the ground have been investigated on the Weatherford bridge deck heating system. Within the limited scope of the study, the following specific conclusions can be drawn:

1. All the set point control strategies used in the study reject much more heat to the ground than is being during heating. A system with a lower set point temperature operates for more hours and rejects more heat to the ground during recharge. The heat pump operating costs goes down for a lower set

119

point as the fluid in the ground loop runs at a higher temperature. However, the pumping energy is much larger than it needs to be.

2. A system operated under a higher set point temperature could be operated for fewer hours thereby reducing the operating cost with less excess recharge.

This work opens a number of areas for further study. The hybrid GSHP systems that were simulated in this work were not optimized and there are still some options to be examined. Some of these include:

1. The system simulation should be made internally consistent by improving upon the solution algorithm used by HVACSIM+. Another option is to use a smaller time step to eliminate the inconsistencies (convergence problems) in system simulations.

2. A long term simulation of the system could give much better understanding of such systems. A life cycle cost of the system based on a long term performance (20-30 years) needs to be examined.

The system modeling and simulation approach is a powerful tool to study and analyze the system performance of several possible designs. The design of a system could be easily modified by changing the design parameters of the components that make the system. Since bridge deck heating systems have high initial cost, their optimum design and operation is of paramount importance. Using the system simulation approach, the trade offs between the GLHE size and number of heat pump pairs, effect of variable flow rates and their related pumping cost, and different control strategies could easily be scrutinized. The work presented in the chapter is just a start towards a better understanding of HGSHP systems and their efficient design.

Chapter 6

Conclusions and Recommendations

6.1. Conclusions

Hybrid ground source heat pump systems have proved to be a successful and energy efficient alternative for heating and cooling applications. A better understanding of such systems is necessary to make them economically attractive. Lack of proper design guidelines is another reason which prevents their wide spread usage. Considerable savings in cost and effort could be realized if the performance of such systems could be easily simulated and analyzed. Various system configurations, component sizes, and different control strategies could be studied using the system simulation approach to arrive at cost efficient design solutions. Both short and long term system performance could be easily simulated using validated numerical models of the system components.

This study uses the simulation approach to analyze the applications of hybrid ground source heat pump systems to buildings and bridges. Chapter 2 addresses the application of an HGSHP system which utilizes a shallow pond as a heat rejecter. This part of the study investigates the influence of a differential control strategy on the design and operation of a hybrid system. In the study, it is shown through a system simulation approach that an optimal design for minimal life cycle cost could be achieved by adjusting the borehole depth and pond loop lengths. This study shows that for buildings with dominant cooling demand and significant heating load, the size of the supplemental heat rejecter is determined by the heating load. However, for highly cooling dominated

buildings significant economic benefits can be realized on a long term irrespective of the size of the supplemental heat rejecter.

Chapter 3 highlights the merits and demerits of two simulation environments: TRNSYS and HVACSIM+. The modeling of components that constitute a hydronically heated bridge deck system is dealt in detail in this chapter. Also, the revisions on the models to improve their accuracy and robustness are described in detail.

Chapter 4 discusses in detail the step-by-step approach in building hybrid GSHP systems for bridge deck heating applications in HVACSIM+. Various problems encountered in modeling the system are dealt with in detail. The draw back of the solution methodology used in HVACSIM+ and the failure of the algorithm to arrive at a solution within specified tolerance limits are discussed. The following conclusions were reached:

1) System modeling is difficult in HVACSIM+ due to the lack of a proper user interface. Modeling of complex systems is extremely laborious with the existing user interface.

2) Although Powell's Hybrid method is employed for solving a set of non-linear simultaneous in HVACSIM+, the algorithm fails to find an exact solution. The magnitudes of residuals are significant during transients. The solution methodology encounters problems, indicating that it has converged when it has not.

3) The results are much better, though still not completely satisfactory, when successive substitution step is used for arriving at better initial guesses

when the solution algorithm recalculates the Jacobian. Use of under relaxation in the substitution step does not have any pronounced effect on the simulation results.

Chapter 5 discusses the performance of hydronically heated bridge deck model that use hybrid ground source heat pumps. The system is simulated and the performance studied in detail for a sample bridge deck located at Weatherford, OK. The simulation results for a few summer recharge set point temperatures are presented. The advantages of using the bridge deck during summer for recharging the ground is quite evident from simulation results. Storing the heat extracted from bridge deck surface during summer raises the ground temperature and makes it available for use in winter for bridge deck heating. However, with the set point temperatures examined, the system recharges much more heat in the summer than is extracted during the winter. Therefore, the circulating pump electricity consumption is much higher than necessary.

6.2. Recommendations

Though the work presented in this thesis is a step towards finding solutions for HGSHP design and operation, its scope is limited. The author suggests research in the following areas to further advance the work:

1) Although HVACSIM+ is a better simulation environment than TRNSYS in some aspects, its user interface needs lot of revamping to make it user "friendly". The present interface makes it extremely cumbersome for modeling complex systems such as the bridge deck heating system. A graphical user interface would make it

more user friendly and considerable amount of time could be saved in modeling systems.

2) At present, the system has been simulated only on an hour-by-hour basis. The effect of using smaller/variable time steps should be studied. It is quite likely that allowing the HVACSIM+ solver to control the time step will improve convergence. However, the load aggregation algorithm used in GLHE is not suitable for such simulations. Hence, the algorithm used in GLHE needs to be revised to enable smaller/variable time steps.

3) Currently, the controller used in the simulation is relatively simple. Using a "sticky" controller could possibly iron out the discrepancies in the simulation result during transients.

4) The present algorithm for nonlinear simultaneous equations fails to find a solution, despite reporting that it has converged. The magnitudes of residuals are significantly high in such cases. Modifying the convergence criteria to check the residual value would be useful. Furthermore, revising or even selecting a different solution algorithm should be considered.

5) Simulation of a bridge deck heating system with recharge during summer requires over four hours on Pentium III, 500 Mhz machine for an annual hour-by-hour simulation. The simulation tool could be more effective when it can be used to study a long term performance of such systems (say 20 years), which would require lot of computation time. The computation time and burden of the system could be significantly reduced if the finite-difference bridge deck model is replaced by a QTF (heat source transfer function) bridge deck model.

6) Use of sophisticated control strategies, different set points, and variable pumping rates need to be analyzed in detail to optimize the bridge deck heating system with summer recharge.

7) Finally, multiple year weather data could be used to predict the system performance for different weather conditions.

REFERENCES

ASHRAE. 1995. *Commercial/Institutional Ground Source Heat Pumps
Engineering Manual*. Atlanta: American Society of Heating, Refrigerating and Air-
Conditioning Engineers, Inc.

ASHRAE. 1996. *ASHRAE Handbook-Systems and Equipment*. Chapter 36.
Atlanta: American Society of Heating, Refrigerating and Air-
Conditioning Engineers, Inc.

BLAST. 1986. BLAST (Building Loads and System Thermodynamics).
Urbana-Champaign : University of Illinois.

Chiasson, A. J. and Spitler J. D. A Modeling Approach to Design of Ground
Source Heat Pump Bridge Deck Heating System. *Proceedings of the Fifth
International Symposium on Snow Removal and Ice Control Technology*,
Raonoke, VA. September 5-8, 2000

Chiasson, A. 1999. Advances in Modeling of Ground-Source Heat Pump Systems. M.S.
Thesis. Oklahoma State University. Stillwater, OK. . (Also available at
http://www.mae.okstate.edu/Faculty/spitler/chiasson_thesis.pdf)

Chiasson, A. D., J. D. Spitler, S. J. Rees, M. D. Smith. 1999. A Model for

Simulating the Performance of a Shallow Pond as a Supplemental Heat Rejecter with Closed-Loop Ground-Source Heat Pump Systems. *ASHRAE Transactions* 106 (2).

Clark, D. R., Hurley, C. W., and Hill, C. R. 1985. Dynamic models for HVAC System Components. *ASHRAE Transactions* 91(1): 737-751

Dennis, J. E. and, Schnabel, R. B. 1983. *Numerical Methods for Unconstrained Optimization and Nonlinear Equations*. New Jersey: Prentice-Hall, Inc.

Donnelly, D., Griffin, R., Nydahl, J., Pell, K. M., Swanson, H. 1982. *Geothermal Heating of Highway Structures*. Transportation Research Board. Record No. 860.

Eskilson, P. 1987. Thermal Analysis of Heat Extraction Boreholes. Doctoral Thesis, University of Lund, Department of Mathematical Physics. Lund, Sweden.

Ferrara, A. A. and Haslett, R. 1975. *Prevention of Preferential Bridge Icing using Heat Pipes*. Report No. FHWA-RD-75-111, Federal Highway Administration.

Gear, C. W. 1971. The Automatic Integration of Ordinary Differential Equations. Comm. *ACM* 14:176-179

Gilbreath, C. S. 1996. Hybrid Ground Source Heat Pump Systems for Commercial Applications. M.S. Thesis. University of Alabama. Tuscaloosa, Alabama.

Haves, P. and L. K. Norford. 1995. ASHRAE 825- RP Final Report. *A Standard Simulation Test Bed for the Evaluation of Control Algorithms and Strategies.*

Hill, C. R.1985. Simulation of a Multizone Air Handler. *ASHRAE Transactions* 91(1): 752-765.

Iwamoto, K., Nagasaka, S., Hamada, Y., Nakamura, M., Ochifuji, K. and K. Nagano. 1998. Prospects of Snow Melting System (SMS) Using Underground Thermal Energy Storage (UTES) in Japan. *Proceedings of the Second Stockton International Geothermal Conference,* Pomona, New Jersey. March 16 – 17, 1998.

Jin, H. 2000. A Parameter Estimation Based Model for Water-to-Water Heat Pumps. Preliminary Report. Oklahoma State University. Stillwater, OK.

Kakac, S., and Yener, Y. 1993. *Heat Conduction.* Washington: Taylor and Francis.

Kavanaugh, S. P. 1998. A Design Method for Hybrid Ground-Source Heat Pumps. *ASHRAE Transactions* 104(2): 691-698.

Kavanaugh, S. P. and K. Raffferty. 1997. *Ground Source Heat pumps: Design of*

Geothermal Systems for Commercial and Institutional Buildings. Atlanta:

American Society of Heating, Refrigerating and Air-Conditioning Engineers.

Komor, Paul. 1997. Space cooling demands from office plug loads. *ASHRAE*

Journal, 39 (12): 41-44.

Lee, R. C., Nydahl, J. E., Pell, K. M., and Sackos, J. T. 1984. *Bridge Deck*

Heating Using Ground Source Heat Pipes. Report No. FHWA-WY-86-002,

Transportation Research Board.

McQuiston, F.C. and Parker, J.D. 1994. *Heating, Ventilating, and Air Conditioning.* New

York: John Wiley & Sons, Inc.

NBS. 1985. *HVACSIM+ Building Systems and Equipment Simulation Program*

Reference. Gaithersburg: National Bureau of Standards.

Ogershok, D., D. Philips. 1999. *National Construction Estimator.* Carlsbad:

Craftsman Book Company.

Park, C., Clark D. E., Kelly G. E. 1985. An Overview of HVACSIM+, a Dynamic

Building/HVAC/Control Systems Simulation Program. *Building Energy Simulation*

Conference, Seattle, Washington. August 21-22, 1985.

Paul, N. D. 1996. The Effect of Grout Thermal Conductivity on Vertical Geothermal Heat Exchanger Design and Performance. M.S. Thesis. South Dakota State University.

Phetteplace, G., W. Sullivan. 1998. Performance of a Hybrid Ground-Coupled Heat pump Systems. *ASHRAE Transactions* 104(1b): 763-770.

Powell, M. J. D. 1970. *A Hybrid Method for Nonlinear Equations in Numerical Methods*. London : P. Rbinowitz, Ed., Gordon and Breach.

Ramsey, J., Hewett, M., Kuehn, T., and Petersen, S. 1999. Updated Design Guidelines for Snow Melting Systems. *ASHRAE Transactions* 105(1): 1055-1065.

SEL. 1997. *TRNSYS Manual, a Transient Simulation Program*. Madison: Solar Engineering Laboratory, University of Wisconsin.

Shonder, J. A., Baxter, V. D., Hughes, P. J., and Thornton J. W. 2000. A Comparison of Vertical Ground Heat Exchanger Design Software for Commercial Applications. *ASHRAE Transactions* 106(1): 831-842.

Singh, J. B., G. Foster. 1998. Advantages of Using the Hybrid Geothermal Option. *Proceedings of the Second Stockton International Geothermal Conference*, Pomona, New Jersey. March 16 – 17, 1998.

Spitler, J.D. and M. Ramamoorthy. 2000. Bridge Deck Deicing using Geothermal Heat Pump. *Proceedings of the Fourth International Heat Pumps in Cold Climates Conference*, Aylmer. Quebec. August 17-18, 2000.

Spitler, J. D., C. Marshall, R. Delahoussaye, and M. Manickam. 1996. *Users Guide of GLHEPRO*. School of Mechanical and Aerospace Engineering. Oklahoma State University. Stillwater, OK

Spitler, J. D. and S. J. Rees. 2000. ASHRAE 1052-RP Progress Report. *Development of an Analytical Verification Test Suite for Whole Building Energy Simulation Programs - Building Fabric.*

Stoecker, W. F. 1989. *Design of Thermal Systems.* New York: McGraw-Hill, Inc.

Wadivkar, O. 1997. An Experimental and Numerical Study of the Thermal Performance of a Bridge Deck De-Icing System. M.S. Thesis. Oklahoma State University, Stillwater, OK. (Also available at http://www.mae.okstate.edu/Faculty/spitler/Wadivkar.pdf)

Yavuzturk, C. 1999. Modeling of Vertical Ground Loop Heat Exchangers for Ground Source Heat Pump Systems. Ph. D. Thesis. Oklahoma State University. Stillwater, OK. (Also available at http://www.mae.okstate.edu/Faculty/spitler/Yavuzturk_thesis.pdf)

Yavuzturk, C., J. D. Spitler. 1999. A Short Time Step Response Factor Model for Vertical Ground Loop Heat Exchangers. *ASHRAE Transactions* 105(2): 475-485.

Yavuzturk, C., J. D. Spitler. 1999. Comparative Study to Investigate operating and Control Strategies for hybrid Ground Source Heat Pump Systems Using a Short Time-Step Simulation Model. *ASHRAE Transactions* 106 (2).

APPENDIXES

APPENDIX A

DESCRIPTION OF COMPONENT MODELS

A.1. TYPE 92: WATER-TO-AIR HEAT PUMP

Component description

This component model simulates the performance of a water-to-air heat pump. Inputs to the model include total load, entering fluid temperature, and fluid mass flow rate. The loads can be read from the boundary file if they are specified as the boundary variable in the definition file. Heating loads are assumed to be positive and cooling loads are assumed to be negative by convention. Other component models supply entering fluid temperature and fluid mass flow rate.

The model uses quadratic curve-fit equations to manufacturer's catalog data to compute the heat of rejection in cooling mode, heat of absorption in heating mode, and the heat pump power consumption. Outputs provided by the model include exiting fluid temperature, power consumption, and fluid mass flow rate for availability to the next component.

Nomenclature

a = curve- fit coefficient	(--)
b = curve- fit coefficient	($/^\circ$C)
c = curve- fit coefficient	($/^\circ$C^2)
cp = specific heat of fluid	(kJ/(kg-C)
d = curve- fit coefficient	(--)
e= curve- fit coefficient	($/^\circ$C)
f = curve- fit coefficient	($/^\circ$C^2)
lowerc = lower T_{in} limit of heat pump in cooling mode	($^\circ$C)
lowerh = lower T_{in} limit of heat pump in heating mode	($^\circ$C)
mdott= mass flow rate of fluid	(kg/s)
PD = piston displacement	(m^3/s)
minflow = minimum mass flow rate of fluid below which the heat	

pump does not operate		(kg/s)
Pcons = power consumption		(kW)
q_{abs} = heat absorbed by heat pump in heating mode		(kW)
q_c = cooling load		(kW)
q_h = heating load		(kW)
q_{rej} = heat rejected by heat pump in cooling mode		(kW)
q_{total} = total load		(kW)
T_{in} = entering fluid temperature		(°C)
T_{out} = exiting fluid temperature		(°C)
u = curve- fit coefficient		(--)
upperc = upper T_{in} limit of heat pump in cooling mode		(°C)
upperh = upper T_{in} limit of heat pump in heating mode		(°C)
v = curve- fit coefficient		(--)
w = curve- fit coefficient		(--)
x = curve- fit coefficient		(--)
y = curve- fit coefficient		(--)
z = curve- fit coefficient		(--)

Mathematical Description

The basic function of this model is to determine the heat of absorption or rejection of a heat pump for each time step in a system simulation given a heating or cooling load, an entering fluid temperature, and a mass flow rate. Since these data are typically available in calalogs supplied by heat pump manufacturers, this model uses a quadratic curve fit to the ratio q_{abs}/q_h (in heating mode) or the ratio q_{rej}/q_c (in cooling mode) as a function of T_{in} to compute q_{abs} or q_{rej}.

The heat rejected or absorbed is then computed by:

$$q_{rej} = q_c [a + b(T_{in}) + c(T_{in}^2)] \qquad (A.1.1).$$

$$q_{abs} = q_h [u + v(T_{in}) + w(T_{in}^2)] \qquad (A.1.2).$$

By sign convention of q_c and q_h, q_{rej} is a negative value and q_{abs} is a positive value. Power consumption is computed by the same approach:

135

$$\text{Pcons} = | \, q_c \, [d + e(T_{in}) + f(T_{in}^2)] \, | \qquad (A.1.3).$$

$$\text{Pcons} = q_h \, [x + y(T_{in}) + z(T_{in}^2)] \qquad (A.1.4).$$

The parameters lowerc, upperc, lowerh, and upperh, and minflow are used to prevent the model from computing a value for q_{rej}, q_{abs}, or Pcons beyond the limits of the catalog data. If T_{in} is above or below user supplied limits or if the mass flow rate is less than minimum flow rate, the heat rejection, heat absorption, and the power consumption are set to zero.

The outlet fluid temperature T_{out} is computed by:

Cooling mode $\qquad T_{out} = T_{in} - q_{rej}/(\text{mdott } c_p) \qquad (A.1.5).$

Heating mode $\qquad T_{out} = T_{in} - q_{abs}/(\text{mdott } c_p) \qquad (A.1 6).$

Component Configuration
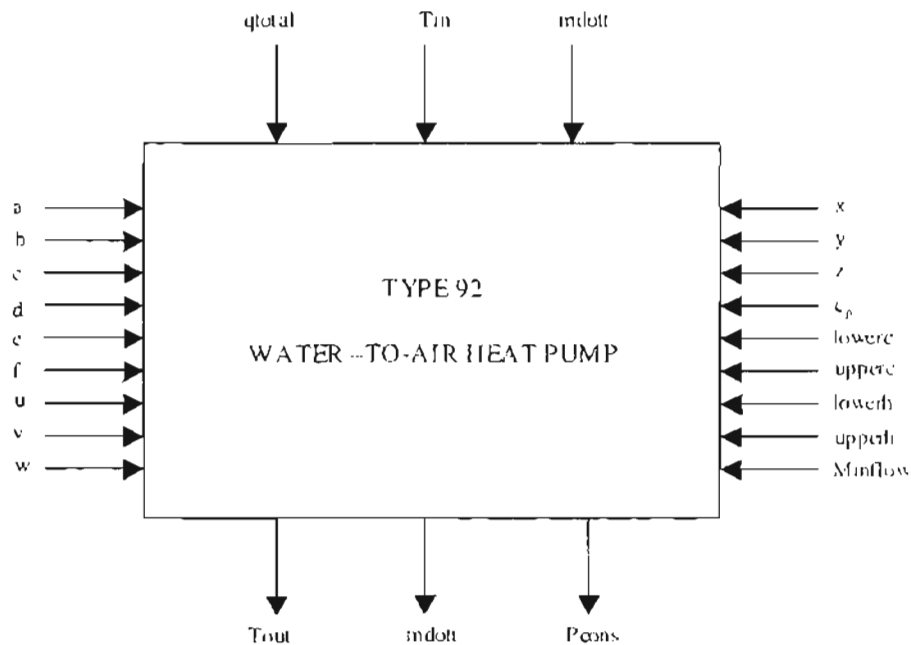
A.2. TYPE 71: WATER-TO-WATER HEAT PUMP

Component description

This component model simulates the performance of a steady state water-to-water vapor compression cycle heat pump. Inputs to the model are condenser and evaporator entering fluid temperature and fluid mass flow rates. Other component models supply the entering fluid temperatures and mass flow rates. A detailed description of the model can be found in Jin (2000).

The parameter estimation based model uses the thermodynamic laws of mass, and energy conservation. Outputs provided by the model include power consumption, condenser and evaporator exiting fluid temperature and fluid mass flow rate for availability to the next component. The optimal value of parameters is obtained separately using a multi-variable optimization routine from the manufacturers' catalog data. The parameters are specific for heating and cooling mode of a heat pump of certain make. The estimated parameters include piston displacement, clearance factor, load side UA, source side UA, a proportional loss factor accounting for the electro-mechanical loss of the compressor, constant part of the electromechanical loss, pressure drop across the suction and discharge valves, and superheat temperature.

Nomenclature

C = Clearance factor	(-)
Cp = specific heat of fluid	(kJ/(kg-C)
h = enthalpy	(kJ/(kg)
$\dot{m}_l$ = load side mass flow rate	(kg/s)
$\dot{m}_r$ = refrigerant mass flow rate	(kg/s)
$\dot{m}_s$ = source side mass flow rate	(kg/s)
$Minflow$ = Minimum mass flow rate of the heat pump	(kg/s)
$P_{suction}$ = suction pressure	(kPa)
$P_{discharge}$ = discharge pressure	(kPa)

137

T_{SH} = superheat (C)
T_c = condensing temperature (C)
T_{min} =Minimum entering fluid temperatures (C)
T_{max} =Minimum entering fluid temperatures (C)
TL_i = load side entering fluid temperature (C)
TL_o= load side exiting fluid temperature (C)
TS_i = source side entering fluid temperature (C)
TS_o= source side exiting fluid temperature (C)
V_{cd} = specific volume of saturated vapor at condensing pressure(m^3/kg)
V_{ev} = specific volume of saturated vapor at evaporating pressure(m^3/kg)
V_{sh} = specific volume of superheated vapor from evaporator (m^3/kg)
W = heat pump power consumption (kW)
W_{loss} = constant part of the electromechanical losses (kW)
Q_l = load side heat transfer rate (kW)
Q_s = source side heat transfer rate (kW)
ε_l = thermal effectiveness of the heat exchanger on load side (-)
ε_s = thermal effectiveness of the heat exchanger on source side (-)
η = electromechanical loss factor proportional to power consumption (-)
ΔP = pressure drop across suction and discharge valves (kPa)

Mathematical description

The model computes the heat transfer in the condenser and evaporator, power consumption, exit fluid temperatures on the condenser and evaporator using the mass flow rates and entering fluid temperatures on the load and source sides and the user supplied parameters as described below.

The model will be described below for heating mode operation; cooling mode is similar, though the parameters are estimated separately for cooling mode.

The load side and source side effectiveness of the heat exchanger is determined using the relationship (A.2.1) and (A.2.2).

$$\varepsilon_s = 1 - e^{(\frac{-UA_s}{m_s Cp})}$$ (A.2.1)

$$\varepsilon_l = 1 - e^{(\frac{-UA_l}{m_l Cp})}$$ (A.22)

138

Where, UA_s and UA_l represent the overall heat transfer coefficient of the source and load sides respectively and $\dot{m}_l$ and $\dot{m}_s$ are the mass flow rate of the fluid on the load and source sides and Cp is specific heat capacity of the fluid.

The evaporating and condensing temperatures of the heat pump are computed using the effectiveness calculated using equations (1) and (2). The evaporating temperature T_e and condensing temperature T_c are computed using equation (3) and Equation (4).

$$T_e = TS_i - \frac{Q_s}{\varepsilon_s \dot{m}_s Cp} \tag{A.2.3}$$

$$T_c = TL_i + \frac{Q_l}{\varepsilon_l \dot{m}_l Cp} \tag{A.2.4}$$

TS_i and TL_i indicate the source side and load side entering fluid temperatures. And, Q_s and Q_l are source side and load side heat transfer rates. Guess values of Q_s and Q_l are used during the first iteration. The heat transfer rates are updated after every iteration until the convergence criteria are met. The suction pressure $P_{suction}$ and discharge pressure $P_{discharge}$ of the compressor is computed from the evaporator and condenser temperatures as shown in equations (A.2.5) and (A.2.6).

$$P_{suction} = P_e - \Delta P \tag{A.2.5}$$

$$P_{discharge} = P_i + \Delta P \tag{A.2.6}$$

Where, ΔP represents the pressure drops across the suction and discharge valves of the compressor respectively. The pressure drop is again a predetermined parameter for specific model of heat pump.

The refrigerant mass flow rate is found using the relation given by (A.2.7)

$$\dot{m}_r = \frac{PD}{Vsuc}\left[1 + C + C\left(\frac{P_{discharge}}{P_{suction}}\right)^{\frac{1}{\gamma}}\right] \tag{A.2.7}$$

Where γ is the isentropic exponent and V_{suc} is the specific volume of at suction pressure.

The power consumption of the compressor for an isentropic process is computed. The actual power consumption is the sum of electromechanical losses W_{loss} and the isentropic work times the loss factor η. The condenser side heat transfer rate Q_l is then the sum of power consumption W and the heat transfer rate in the evaporator Q_s.

For a given set of inputs, the computation is repeated with the updated heat transfer rates until the heat transfer rate of the evaporator and condenser converge within a specified tolerance.

For heating mode, the evaporator acts as the source side and the condenser acts as the load side. The load and source sides of the heat pump are reversed during the cooling cycle. Hence, parameters obtained for cooling mode should be used to simulate the performance of the heat pump in cooling mode.

Component configuration
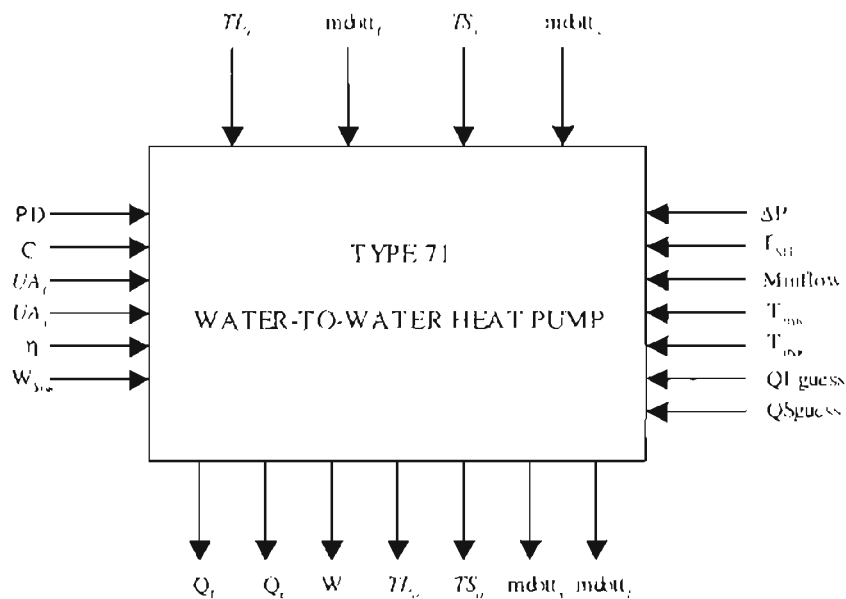
A.3. TYPE 74: GANG OF WATER-TO-WATER HEAT PUMPS

Component description

This model simulates the performance of "N" pairs of serially connected water-to-water heat pumps. The two heat pumps in a pair have their source side in parallel and load side in series. The model inputs are entering fluid temperatures and mass flow rates to the gang of heat pumps on the load and source side, and a control signal dictating the number of heat pump pairs in operation at any given time during the simulation.

A positive integer N denotes the maximum number of heat pump pairs in the gang. Depending upon the control signal input to the heat pump, the model computes the exit fluid temperatures of the gang on the load and source sides accounting for the mixing of fluid streams from the heat pump in operation and those that are not in use (A future refinement might be to allow for systems that shut off the flow to heat pumps not switched on). The other outputs of the model are cumulative heat pump power consumption, and the entering fluid temperature to the second heat pump in the pair. The second heat pump in the pair is shut off when the entering fluid temperature to the second heat pump, which is the exiting fluid temperature from the first heat pump, exceeds a user specified limit.

Nomenclature

$Flow_1$ = total mass flow rate through the heat pump pairs in use on load side (kg/s)
$Flow_2$ = total mass flow rate through the heat pump pairs not in use on load side (kg/s)
$Flow_3$ = total mass flow rate through the heat pumps in use on source side (kg/s)
$Flow_4$ = total mass flow rate through the heat pumps not in use on source side (kg/s)
HP_{power} = power consumption of a heat pump pair in the gang   (kW)
$\dot{m}_l$ = load side mass flow rate through each heat pump   (kg/s)
$\dot{m}_s$ = source side mass flow rate through each heat pump   (kg/s)
$\dot{m}total_l$ = total load side mass flow rate to the gang of heat pumps   (kg/s)

$\dot{m}total_s$ = source side mass flow rate to the gang of heat pumps (kg/s)

N = Number of heat pump pairs in use (-)

N_{max} = Maximum number of heat pump pairs in the gang (-)

N = Number of heat pump pairs operational (-)

T_{min} =Minimum entering fluid temperature ($^\circ$C)

T_{max} =Minimum entering fluid temperature ($^\circ$C)

TL_HP2_i = Load side entering fluid temperature to the 2nd heat pump ($^\circ$C)

TL_i = load side entering fluid temperature of the gang ($^\circ$C)

TL_o= load side exiting fluid temperature of one heat pump pair ($^\circ$C)

TS_i = source side entering fluid temperature ($^\circ$C)

TS_o= source side exiting fluid temperature of one heat pump pair ($^\circ$C)

Mathematical description

The computation methodology of one heat pump in the pair is similar to that

described for Type 71. Flow through each heat pump on the load side is given by (A.3.1)

$$\dot{m}_l = \frac{\dot{m}total_l}{N_{max}}$$

(A.3.1)

Where N_{max} is the maximum number of heat pump pairs that constitute the gang.

Flow through each heat pump on the source side is given by (A.3.2)(since the source

sides are arranged in parallel, the total flow is divided equally between the two)

$$\dot{m}_l = \frac{\dot{m}total_l}{2N_{max}}$$

(A.3.2)

If none of the heat pump pair are operational or if the entering fluid temperatures

do not lie within the limits supplied by the user, the heat pump power consumption is set

to zero and the exit fluid temperatures set at the same value as the inlet temperatures.

Otherwise, heat pump power consumption and exit fluid temperatures on the load and

source sides are computed using $\dot{m}_l$ and $\dot{m}_s$ as described in Type 71. If the exit fluid

temperatures on the load side from the first heat pump exceed Tmax, then the second heat

pump is bypassed. The source side entering fluid temperature to the second heat pump is

the same as that of first one in the pair since their source sides are in parallel. Else the

142

computation is repeated to find the exit fluid temperatures from the second heat pump and its power consumption.

The power consumed by the gang of heat pumps is the cumulative power consumption of the heat pumps in use as given by (A.3.3).

$$Total\ power\ consumption = N \times HP_{power} \tag{A.3.3}$$

Where HP_{power} is the power consumption of a pair of heat pumps.

Flow through the operational heat pump pairs is computed as follows:

$$Flow_1 = \dot{m}_1 \times N \tag{A.3.4}$$

$$Flow_2 = \dot{m}total_1 - Flow_1 \tag{A.3.5}$$

The load side exit fluid temperature computed after mixing streams is then given by equation (A.3.6).

$$Load\ side\ outlet\ temperature = (Flow_1 \times TL_o + Flow_2 \times TL_i)/ \dot{m}total_1 \tag{A.3.6}$$

The source side exit fluid temperature for the gang of heat pumps is computed in a similar manner using equations (A.3.7), (A.3.8), and (A.3.9).

$$Flow_3 = \dot{m}_1 \times N \times HP_{number} \tag{A.3.7}$$

$$Flow_4 = \dot{m}total_1 - Flow_3 \tag{A.3.8}$$

$$Source\ side\ outlet\ temperature = (Flow_3 \times TS_o + Flow_4 \times TS_i)/ \dot{m}total_. \tag{A.3.9}$$

Where HP_{number} is two if both the heat pumps in a pair are in use. If the second heat pump in the pair is not used due to high fluid inlet temperature HP_{number} is taken as one. T_o is the average of heat pumps exit fluid temperatures on the source side.

143

Component configuration

Component diagram — TYPE 74 GANG OF WATER-TO-WATER HEAT PUMPS

Top inputs: TL_i, $\dot{m}$total$L$, TS_i, $\dot{m}$total$S$, N

Left inputs: PD, C, UA_l, UA_s, η, $W_{b,o}$, ΔP

Right inputs: T_{SH}, N_{max}, Minflow, T_{min}, I_{max}, QLguess, QSguess

Bottom outputs: W, TL_o, TS_o, TL_HP2, $\dot{m}$total$L$, $\dot{m}$total$S$

144
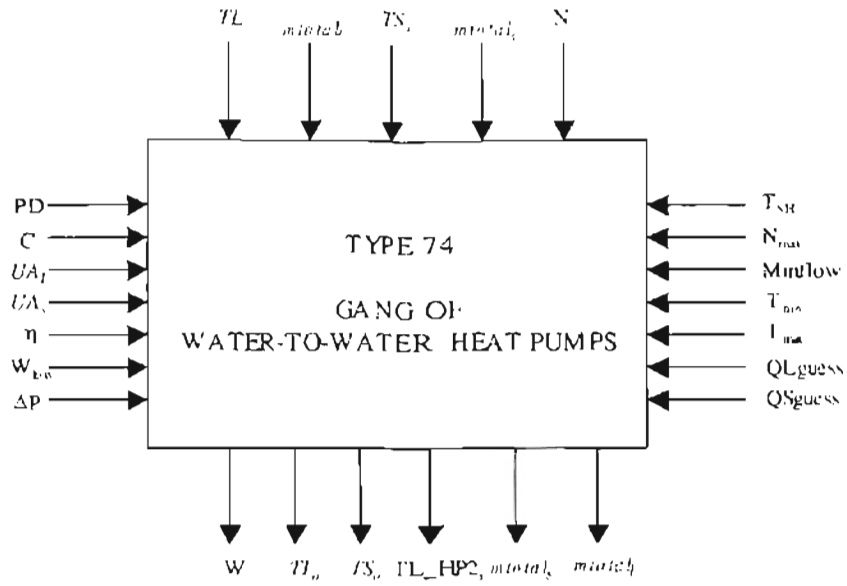
A.4. TYPE 75: GANG OF WATER-TO-WATER HEAT PUMPS

Component description

Type 75 follows the gang of heat pump model Type 74 in almost all aspects. The difference between the two types is that the flow rates in Type 74 are read into the model as user specified parameters, and the flow is activated by a control signal, which is a model input. The control signal γ can take values between 0 and 1. The flow on the source side and load side is obtained by multiplying the flow parameters with the control signal. Hence, the heat pump is shut off when γ is 0 and is operating at its full capacity when γ is 1.

The parameters that are additional to the ones used in Type 74 are the flow rates in source and load side, and recharge fraction R_f. During recharge mode, when the recharge fraction is equal to the control signal, the heat pump is bypassed. The mass flow rate on the load side should be equal to the maximum flow rate on the bridge deck, where as the source side should be equal to the flow through the ground loop.

Operation of the heat pump during heating and recharge mode can be easily understood by looking at the schematic diagram of the heat pump during the two modes of operation given below.
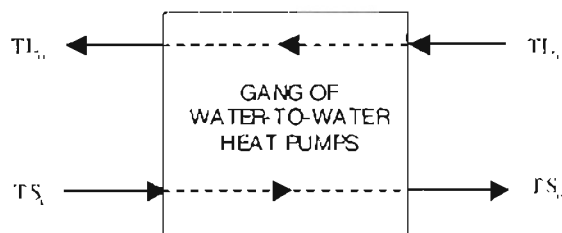
Figure 1. Heating mode

The operation during heating mode is similar to the one explained in Type 71 and Type 74.
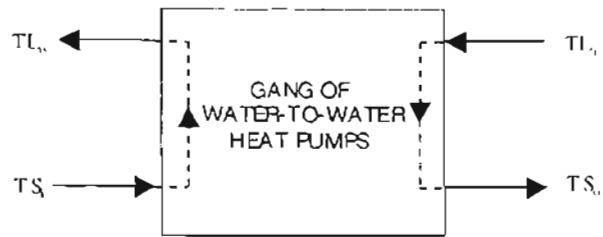
Figure 1. Recharge mode

Use of diverters and T-pieces can be avoided, while achieving the same effect, i.e. bypassing the heat pump during recharge mode, using Type 75. The heat pump is bypassed by fixing the source side outlet temperature equal TS_o to the load side inlet temperature TL_i and load side outlet temperature TL_o to the source side inlet temperature TS_i internally in the model.

Component configuration.

146
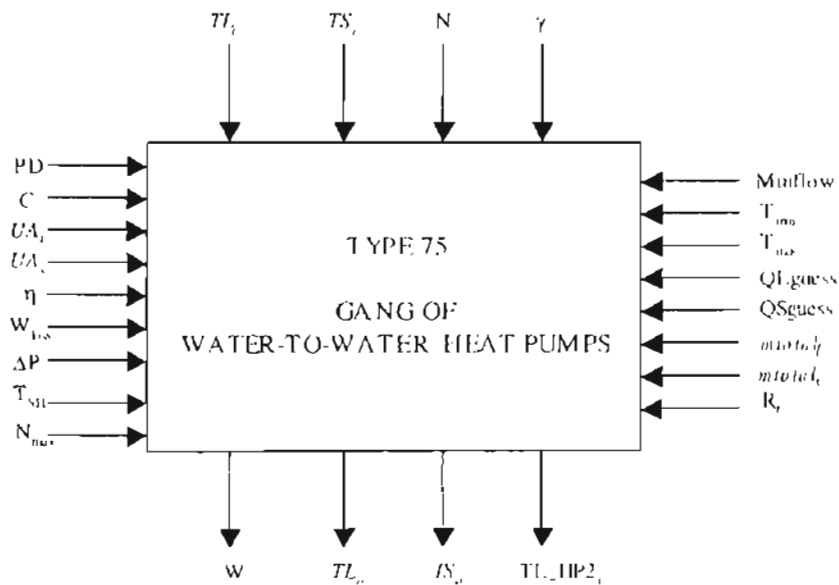
A.5. TYPE 136: GROUND LOOP HEAT EXCHANGER

Component description

The ground loop heat exchanger (GLHE) model considered here is that described by Yavuzturk and Spitler (1999), which is an extension of the long-time step temperature response factor model of Eskilson (1987). It is based on dimensionless, time-dependent temperature response factors known as "g-functions", which are unique for various borehole field geometries. In order to compute the average temperature of the borehole field for each time step, the time-dependent building loads profile is decomposed into unit pulses and superimposed in time using the corresponding temperature response factors. The model includes a load aggregation algorithm that significantly reduces computation time.

Inputs to the model are the mass flow rate and entering fluid temperature. The outputs from the model include exit fluid temperature, mass flow rate (for use to other components), average borehole fluid temperature, and heat transfer rate to the ground normalized to borehole depth. The parameters include the number of boreholes, depth of each borehole, borehole radius, thermal conductivity of the ground, specific heat capacity of the heat exchange fluid, undisturbed ground temperature, borehole thermal resistance, and a minimum flow parameter.

Nomenclature

C_{ground} = volumetric heat capacity of ground $(J/(m^3 K))$
C_{fluid} = specific heat capacity of fluid $(J/(kgK))$
$Gfnc$ = gfnc(i) holds the i'th value of the g-function   (-)
$Gfunc$ = value of the g-function for the time step   (-)
H = borehole length over which heat extraction takes place (m)
K = thermal conductivity of the ground $(W/(mK))$

$\dot{m}$ = mass flow rate of fluid   (kg/s)
Minflow = minimum mass flow rate   (kg/s)
N_b = number of boreholes   (-)
R_b = thermal resistance of the borehole   ($^{\circ}$K per W/m)
$R_{borehole}$ = borehole radius   (m)
RQ = thermal resistance to the heat extraction step   ($^{\circ}$K per W/m)
RQ_{long} = thermal resistance to the aggregated heat extraction step($^{\circ}$K per W/m)
t = current simulation time   (s)
TF = average fluid temperature   ($^{\circ}$C)
Tin = inlet fluid temperature   ($^{\circ}$C)
T_{om} = undisturbed ground temperature   ($^{\circ}$C)
T_{out} = outlet fluid temperature   ($^{\circ}$C)
t_s = steady-state time   (s)
QN = normalized heat extraction rate for ith hour   (W/m)

Mathematical Description

The g-function value for each time step is pre-computed and stored in an array for later

use. The outlet fluid temperature and ground load is found using an iterative procedure

mentioned below. At the beginning of each time step, an initial ground load is computed

with an initial guess value of outlet fluid temperature equal to the undisturbed ground

temperature at that time. The initial ground load, which has been normalized to the active

borehole length, is given by (A.5.1).

$$QN_i = \dot{m} \ C_{fluid}(T_{om}\text{-}T_{in})/(H \ N_b) \tag{A.5.1}$$

The outlet fluid temperature is computed from average fluid temperature using equation
(2)

$$T_{out} = TF + \frac{QN_i \cdot H \cdot N_b}{2\dot{m}C_{fluid}} \tag{A.5.2}$$

The average fluid temperature TF is computed using the relation :

$$TF = T_{om} + \sum_{i=1}^{n} \frac{(QN_i - QN_{i-1})}{2 \cdot \pi \cdot k} g\left(\frac{t_n - t_{i-1}}{t_s}, \frac{R_{borehole}}{h} \right) \tag{A.5.3}$$

The iteration is repeated until the change in outlet fluid temperature between iterations is

less than a pre-specified tolerance limit.

148

To reduce the computation time and burden, the superposition of ground loads from the earlier time steps is aggregated into 'blocks' using a load aggregation algorithm. The load aggregation algorithm keeps track of all hourly ground loads up to the current time-step. An average ground load is then computed for user-definable 'blocks' of time (for example, if the ground loads are given in hourly time steps then 730 hours worth of hourly loads may be averaged over this time period to represent one aggregate load for the 730-hour time block).

Component Configuration
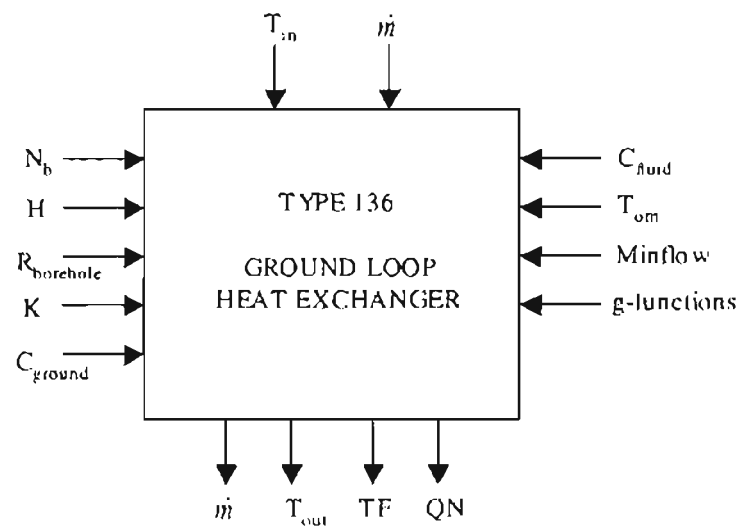
A.6. TYPE 138: GROUND LOOP HEAT EXCHANGER

Component description

The ground loop heat exchanger model (Type 136) has borehole thermal resistance as a parameter. However, the borehole thermal resistance varies with the mass flow the circulating fluid. Type 138 is essentially the same as Type 136, except that the borehole thermal resistance is not read in as a parameter. Instead, it is calculated using a subroutine "BORERES" in Type 138. Since borehole thermal resistance is critical to predict the heat transfer characteristics of the ground, Type 138 can be used for situations when the mass flow rate is not constant through out the simulation period.

The model requires the user to supply values for thermal conductivity of the pipe, ground, and the circulating fluid, the density and viscosity of the fluid, outer diameter of U-tube piping, distance between the U-tube legs, and pipe wall thickness in addition to the parameters mentioned in Type 136. These parameters are used to calculate the borehole thermal resistance depending upon the flow through the borehole.

Nomenclature

d_i = inner diameter of the U-tube pipe   (m)
$h_{c,i}$ = convection coefficient $(W/m^2 \, {}^\circ K)$
k_{pipe} = pipe thermal conductivity $(W/m \, {}^\circ K)$
k_{grout} = grout thermal conductivity $(W/m \, {}^\circ K)$
k_{fluid} = fluid thermal conductivity $(W/m \, {}^\circ K)$
Nu = Nusselt number   (-)
r_o = outer radius of the U-tube pipe   (m)
r_i = inner radius of the U-tube pipe   (m)
$Pipe_t$ = wall thickness of the U-tube   (m
Pr = Prandtl number   (-)
Re = Reynolds number   (-)
R_b = borehole thermal resistance $({}^\circ K \text{ per } W/m)$
R_{cond} = conductive resistance $({}^\circ K \text{ per } W/m)$
R_{conv} = convective resistance $({}^\circ K \text{ per } W/m)$
R_{grout} = resistance of the grout $({}^\circ K \text{ per } W/m)$

X_{tube} = distance between t legs of the U-tube   (m)
β_i, β_0 = shape factors   (-)
v = fluid viscosity   (N s/ m^2)
ρ = fluid density   (kg/ m^3)

The procedure for computing the borehole thermal resistance is explained below. The borehole thermal resistance is calculated using equation (A.6.1).

$$R_b = R_{cond} + R_{conv} + R_{grout} \tag{A.6.1}$$

R_{cond} is the conductive resistance is computed using Fourier's relation (2)

$$R_{cond} = \frac{\log\left(\frac{r_o}{r_i}\right)}{4\pi \, k_{pipe}} \tag{A.6.2}$$

Where r_o is the outer radius of the pipe, r_i is the pipe inner radius, and k_{pipe} is the pipe thermal conductivity. The convective resistance is computed as follows.

$$R_{conv} = \frac{1}{2\pi \, d_i \, h_{c.i}} \tag{A.6.9}$$

Where d_i is the pipe inner diameter, and $h_{c.i}$ is the convection coefficient inside the pipe computed using Dittus-Boelter correlation.

$$h_{c.i} = Nu \, K_{fluid}/d_i \tag{A.6.10}$$

Nusselt number Nu is computed from Prandtl number, Pr and Reynolds number, Re as shown below

$$Nu = 0.23 \, Re^{0.8} \, Pr^{0.35} \tag{A.6.11}$$

Resistance due to the grout, R_{grout} is calculated using the following relation

$$R_{grout} = \frac{1.}{k_{grout} \beta_0 \left(R_{borehole}/r_o\right)^{\beta_i}} \tag{A.6.12}$$

Where β_i and β_0 are the resistance shape factor coefficients (Paul 1996) whose value depends on the U-tube shank spacing inside the borehole

151

Component configuration

TYPE 138

GROUND LOOP
HEAT EXCHANGER

Inputs (top): T_n, $\dot{m}$

Inputs (left): N_b, H, $R_{borehole}$, K, C_{ground}, C_{fluid}, T_{am}, Minflow

Inputs (right): K_{grout}, K_{pipe}, K_{fluid}, ρ_{fluid}, ν_{fluid}, d_{outer}, X_{tube}, $Pipe_t$, g-functions

Outputs (bottom): $\dot{m}$, T_{out}, TF, QN

152
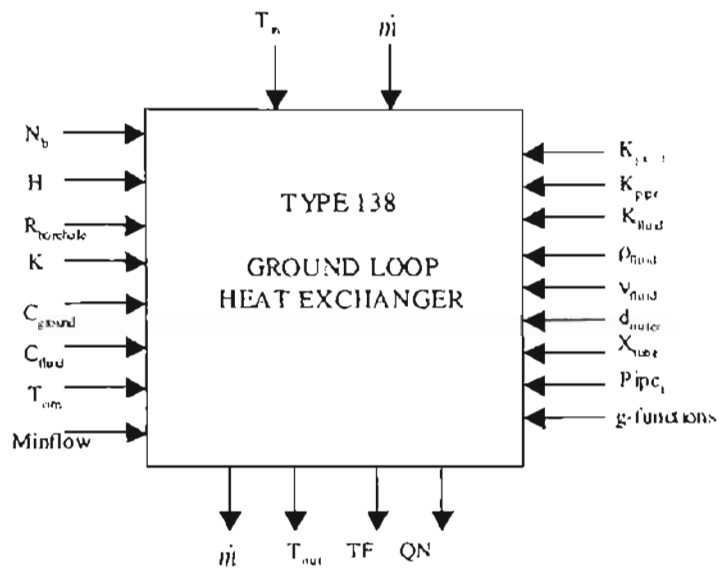
A.7. TYPE 139: GROUND LOOP HEAT EXCHANGER

Component description

The difference between ground loop heat exchanger Type 138 and Type 139 is that the flow rate in Type 138 has been made a parameter in Type 139. Instead, the model takes a control signal or a flow indicator as input, thereby removing mass flow rates from input and outputs.

The inputs to the model include inlet fluid temperature and a control signal. The outlet fluid temperature, average borehole temperature, and the normalized heat extraction rate constitute the model outputs. In addition to the parameters used in Type 138, the maximum flow rate on the ground loop is taken as a parameter. The model can still accommodate variable flow rates since the maximum flow rate is multiplied with the flow indicator to compute the flow through the ground loop at any instant. Rest of the model resembles Type 138 basically. The control signal C takes values between 0 and 1, 0 indicating no flow through the ground loop and 1 indicating the maximum flow $\dot{m}$.

Component configuration
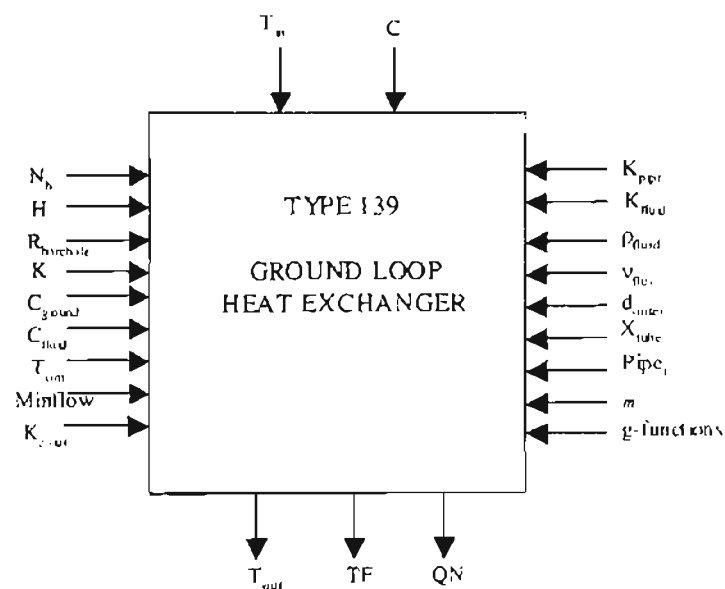
A.8. TYPE 540: BRIDGE DECK CONTROLLER

Component description

This component is specifically meant for controlling the hydronically heated

bridge deck system. The controller controls the number of heat pump pairs to be operated

during a snow event depending upon the bridge deck surface temperature linearly. The

component also sends a control signal to the circulation pump to control the flow rate.

The control signal can vary between 1 (maximum flow) and 0 (no flow).

The inputs to the model are a flag indicating the snow event and bridge deck

surface temperature. The outputs are two control signals meant for the circulation pump

and the heat pump. The model takes the lower and upper limits of the bridge deck surface

temperature, recharge set point temperature, maximum number of heat pump pairs in the

system, and a recharge fraction.

Nomenclature

C_1 = First control signal output (Flow fraction) (-)
C_2 = Second control signal output (Number of heat pump pairs to be used)
R_f = recharge fraction (-)
$Snowflag$ = snow indicator (-)
T_{surf} = bridge deck surface temperature (°C)
T_{surf_upper} = surface temperature upper limit (°C)
T_{surf_lower} = surface temperature lower limit (°C)
$T_{surf\_recharge}$ = recharge temperature (°C)
N_{max} = Maximum number of heat pump pairs in the system (-)

Mathematical description

The model sends a control signal to the circulation pump. When the snow indicator is

equal to 1, the model sends a control signal to the pump C_1 equal to 1. Also, if the bridge

deck surface temperature T_{surf} is greater than T_{surf_upper} during the snow event ($Snowflag = 1$), then C_l is equal to 1. If T_{surf} less than the lower limit temperature T_{surf_lower} then the model sends an output to the heat pump C_2 equal to the maximum number of heat pump pairs N_{max}. For any value of T_{surf} between the two set point temperatures, the number of heat pumps to be used is calculated linearly using the relation (A.8.1) given below.

$$C_2 = \frac{N_{max}\left(T_{surf\_upper} - T_{surf}\right)}{\left(T_{surf\_upper} - T_{surf\_lower}\right)} \tag{A.8.1}$$

The number of heat pumps is rounded off to the next highest integer when C_2 has a fractional value.

When T_{surf} exceeds $T_{surf\_recharge}$ during recharge mode, the control signal to the pump C_l is equal to the recharge fraction supplied by the user (usually lies between 0 and 1). And the control signal C_2 to the heat pump is zero indicating no heat pump is operational during recharge.

Component configuration
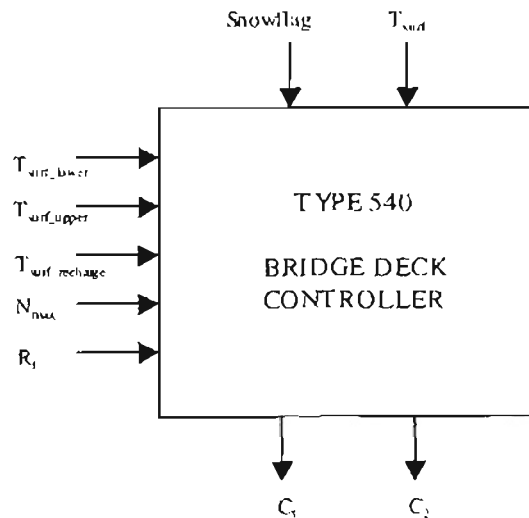
A.9. TYPE 546: PUMP

Component description

This model computes the outlet mass flow rate using a variable control signal (between 0 and 1) and a user specified maximum flow capacity. The model also computes the power consumption and the rise in fluid temperature using the parameters; pressure drop across the pump and pump efficiency. The model assumes that all of the pump power is converted into fluid thermal energy and goes on to increase the temperature of the fluid. Also, the parameter R_f is used to operate only one pump during recharge mode when more than one pump of the same model are used in the simulation.

The inputs to the model include mass flow rate, temperature, and control signal. The outputs from the model are exit mass flow rate, exit fluid temperature, and the power consumption.

Nomenclature

C = control signal variable (between 0 and 1)	(-)	
Mode = simple (1) or any other mode	(-)	
$\dot{m}_{in}$ = inlet pump flow rate	(kg/s)	
$\dot{m}_{max}$ = maximum pump capacity	(kg/s)	
$\dot{m}_{out}$ = mass flow rate at pump outlet	(kg/s)	
$Minflow$ = Minimum flow rate	(kg/s)	
P = pump power consumption	(kW)	
R_{fl} = recharge fraction	(-)	
Tin = temperature at the inlet	(°C)	
$Tout$ = outlet temperature	(°C)	
ΔP = pressure drop across the pump	(kPa)	
η = pump efficiency	(-)	
ρ = density of the fluid	(kg/m^3)	

Mathematical description

Mode 1 depicts the simple pump model. More sophisticated could be later added later on in the same type and differentiated by Mode number

The pump flow rate as determined by the control signal C is given by equation (A.9.1).

$$\dot{m}_{out} = C\dot{m}_{max} \qquad \text{(A.9.1)}$$

The pump power consumption and the temperature rise across the pump are computed using relation (A.9.2) and (A.9.3) respectively.

$$P = \frac{\Delta P \dot{m}_{out}}{\rho \cdot \eta} \qquad \text{(A.9.2)}$$

$$T_{out} = T_{in} + \Delta P \left(\frac{\frac{1}{\eta} - 1}{\rho \cdot \eta} \right) \qquad \text{(A.9.3)}$$

If two pumps are to be used is a simulation and only one is supposed to be operational during recharge mode, then R_f is specified a value (between 0 and 1) for the pump which will have an outlet flow rate equal to the intended recharge flow rate when multiplied by the pumps maximum capacity. For the pump that is not in use, R_f should be equal to 0. During recharge mode, for the pump that is not in use, the outlet flow rate is the same as the inlet flow rate.

Component configuration
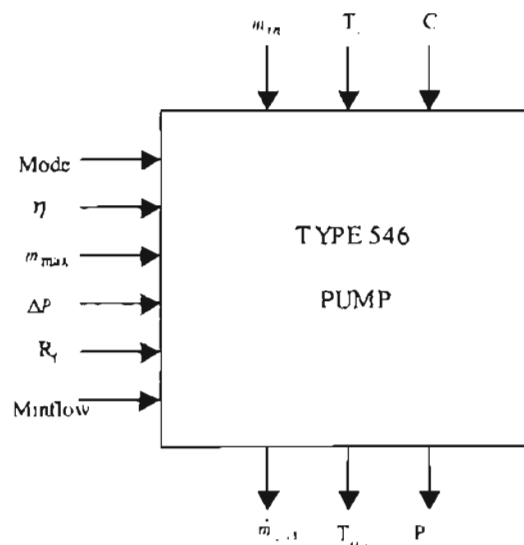
A.10. TYPE 547: PUMP

Component description

The model is a slight variation of Type 546 except that the mass flow rate has been removed from the inputs and outputs. This model is intended for the purpose of using it with bridge deck (Type 100), ground loop heat exchanger (Type 139), and water-to-water heat pump (Type 75). Just as the Type 546, this model computes the power consumption and temperature rise of the fluid across the pump using pressure drop and pump efficiency.

The inputs to the model include temperature, and control signal. The outputs from the model are exit fluid temperature, and the power consumption. A few more parameters have been added like the pressure drop during recharge mode, recharge flow rate. The parameter 'Mode' has been changed to 'Pump No.' for the purpose of identifying the pump that needs to be operational during recharge mode when several pumps of the same model are used in the simulation.

Nomenclature

C = control signal variable (between 0 and 1)   (-)
$Mode$ = simple (1) or any other mode   (-)
N = pump number   (-)
$\dot{m}_{in}$ = inlet pump flow rate   (kg/s)
$\dot{m}_{max}$ = maximum pump capacity   (kg/s)
$\dot{m}_{recharge}$ = recharge flow rate   (kg/s)
$\dot{m}_{out}$ = mass flow rate at pump outlet   (kg/s)
$Minflow$ = Minimum flow rate   (kg/s)
P = pump power consumption   (kW)
R_{fl} = recharge fraction   (-)
T_{in} = temperature at the inlet   (°C)
T_{out} = outlet temperature   (°C)
ΔP = Effective pressure drop across the pump   (kPa)
ΔP_1 = pressure drop across the pump during heating   (kPa)
ΔP_2 = pressure drop across the pump during recharge   (kPa)

η = pump efficiency (-)
ρ = density of the fluid (kg/m^3)

Mathematical description

The pump flow rate as determined by the control signal C is given by equation (1).

$$\dot{m}_{out} = C\dot{m}_{max} \tag{A.10.1}$$

The pump power consumption and the temperature rise across the pump are computed

using relation (A.10.2) and (A.10.3) respectively.

$$P = \frac{\Delta P \dot{m}_{out}}{\rho \cdot \eta} \tag{A.10.2}$$

$$T_{out} = T_{in} + \Delta P \left(\frac{\frac{1}{\eta} - 1}{\rho \cdot \eta} \right) \tag{A.10.3}$$

If two pumps are to be used is a simulation and only one is supposed to be operational

during recharge mode. During bridge deck heating, ΔP is equal to ΔP_1 for both the

pumps. During recharge, the pump that has a pump number N equal to 1 and a pressure

drop ΔP_2 equal to 0 is not used. No power is consumed for the pump not used.

Component configuration

159
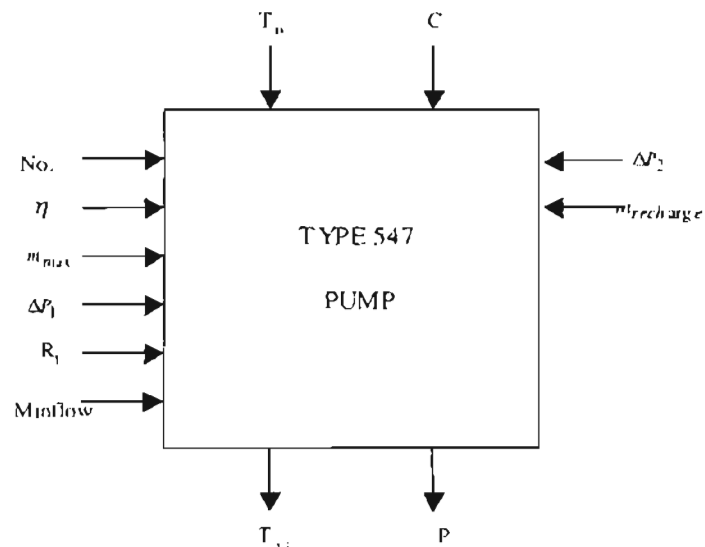
A.11. TYPE 104: T-PIECE

Component description

This model calculates the outlet flow rates and temperatures of a mixing T-piece. The model is fairly simple but plays a significant role in the thermal system simulations and computes the mixing of two fluid streams at different temperatures. The inputs to the model are the temperatures and mass flow rates at the inlet. The model outputs are flow rate and temperature computed after the mixing of the inlet streams. A "dummy" parameter has been specified, since HVACSIM+ does not permit models without parameters!

Nomenclature

$\dot{m}1_{in}$ = inlet flow rate at 1		(kg/s)
$\dot{m}2_{in}$ = inlet flow rate at 2		(kg/s)
$\dot{m}_{out}$ = outlet flow rate		(kg/s)
$T1_{in}$ = temperature of the inlet fluid at 1		(°C)
$T2_{in}$ = temperature of the inlet fluid at 1		(°C)
T_{out} = temperature of the exit fluid temperature		(°C)

Mathematical description

The outlet mass flow rate is equal to the sum of the inlet flow rates given by (A.11.1).

$$\dot{m}_{out} = \dot{m}1_{in} + \dot{m}2_{in} \qquad (A.11.1)$$

The temperature T_{out} of the fluid after mixing of streams 1 and 2 is given by equation (A.11.2)

$$T_{out} = \left(\frac{\dot{m}1_{in}T1_{in} + \dot{m}2_{in}T2_{in}}{\dot{m}_{out}} \right) \qquad (A.11.2)$$

If $\dot{m}_{out}$ happens to add up to zero, then the outlet fluid temperature is computed as an average of $T1_{in}$ and $T2_{in}$ instead of using equation 2.

Component configuration
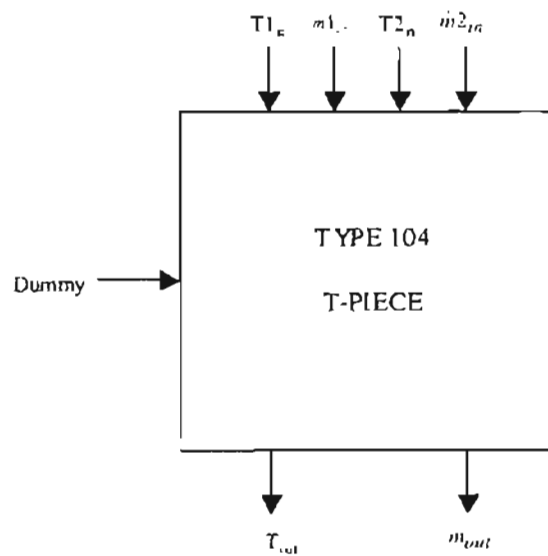
A.12. TYPE 105: DIVERTER

Component description

This model simulates the operation of a flow diverter, which splits a stream of fluid into proportionally two different streams depending upon the control signal. Inputs to the model are mass flow rate and temperature at the inlet, and the variable control signal. The model outputs are flow rates and temperatures of the two streams. A dummy parameter has been specified, since HVACSIM+ does not permit models without parameters!

Nomenclature

C = control signal variable (between 0 and 1) (-)
$\dot{m}1_{out}$ = exit flow rate at 1 (kg/s)
$\dot{m}2_{out}$ = exit flow rate at 2 (kg/s)
$\dot{m}_{in}$ = inlet flow rate (kg/s)
T_{in} = temperature of the inlet fluid (°C)
$T1_{out}$= temperature of the outlet fluid at 1 (°C)
$T2_{out}$= temperature of the outlet fluid at 2 (°C)

Mathematical description

The outlet mass flow rates at the two outlets of the diverter are given by equations (1) and (A.12.2)

$$\dot{m}1_{out} = (1\text{-}C)\ \dot{m}_{in} \qquad (A.12.1)$$

$$\dot{m}2_{out} = C\ \dot{m}_{in} \qquad (A.12.2)$$

When control signal C takes value of 1, the entire incoming flow is diverted to the second outlet. And, the entire flow is diverted to first outlet when C takes a vale of 0. Otherwise, the flow is proportionately split between the two outlets. The temperature T_{out} of the fluid remains the same as the inlet temperature T_{in} irrespective of all cases.

162

Component configuration
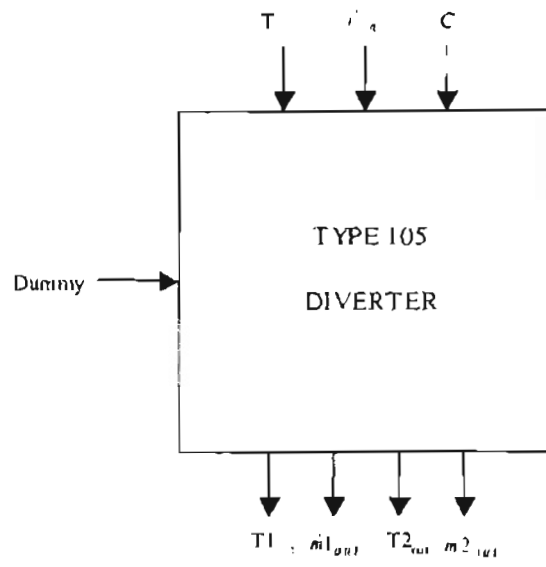
A.13. TYPE 99: Bridge Deck Heating Model

Component Description

This component model simulates heat transfer mechanisms within a hydronically-heated bridge deck. The heat transfer mechanisms within the bridge deck slab include several environmental factors as well as convection due to the heat transfer fluid. The heat transfer fluid in this model can be either pure water or an antifreeze solution. The fluid is carried by a series of pipes positioned in parallel circuits which are embedded in the slab. This model was developed to simulate the performance of a bridge deck de-icing system.

The different modes of heat transfer include at the top surface of the bridge include the effects of solar radiation heat gain, convection heat transfer to the atmosphere, thermal or long-wave radiation heat transfer, sensible heat transfer to snow, heat of fusion required to melt snow, and heat of evaporation lost to evaporating rain or melted snow. Heat transfer at the bottom surface of the bridge includes convection heat transfer to the atmosphere and heat transfer due to radiation to the ground. Weather data are supplied by the user at a desired time interval and read from the boundary file. Heat transfer mechanisms within the pavement slab include conduction through the pavement material and convection due to flow of the heat transfer fluid through the embedded pipes.

Because of symmetry and small temperature differences between adjacent pipes (and neglecting edge effects), the model domain is reduced to a width equivalent to one-half of the pipe spacing as shown in Figure 3. In the y direction, the domain corresponds to the

top and bottom of the slab. In the x direction, the domain corresponds to a distance from the center-line of a pipe to half the distance to the adjacent pipe. The model uses a default square nodal spacing equal to the pipe radius.
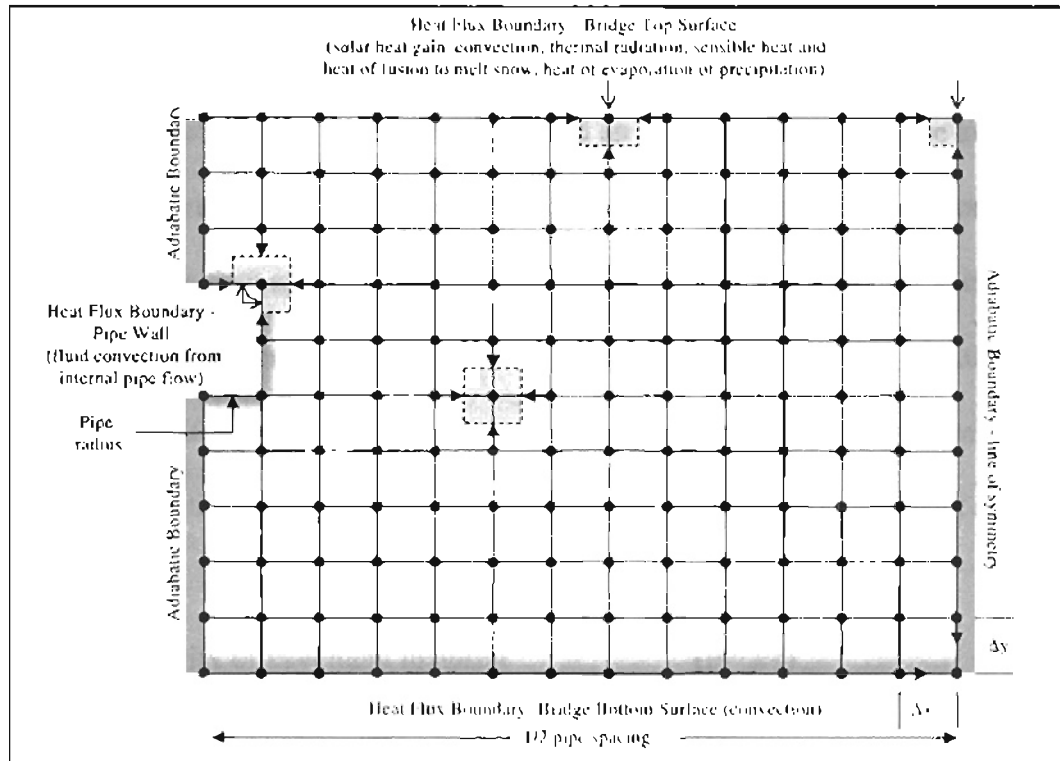
Figure 3. Model domain showing the finite-difference grid and boundary conditions. Shaded squares show example control volumes for different types of grid node geometries. Arrows show the direction of heat flow used to derive the finite-difference equations for each node type; open arrowheads denote an exterior flux and closed arrowheads denote conduction between adjacent nodes. Note $\Delta x = \Delta y$.

As shown in Figure 3, boundary conditions are of two types: (1) a flux boundary at top surface nodes and at nodes surrounding the pipe location and (2) an adiabatic boundary at all other boundary nodes. The finite-difference equation for all nodes is obtained by the energy balance method for a control volume about the nodal region (i.e. using a "node-centered" approach) assuming all heat flow is into the node.

An iterative procedure is used to determine the temperature of the fluid at the pipe boundary surface. This temperature is equivalent to average fluid temperature T_{avg}, where T_{avg} is the average of the inlet and outlet fluid temperatures for the current time step. Therefore, the model is assumed to be representative of an average condition in the pavement slab. The total fluid flow rate is first divided by the number of flow circuits to obtain the flow rate per circuit. T_{avg} is then assigned an ititial value equal to the average of the inlet temperature at the current time step and the outlet temperature at the previous time step. The code is then executed iteratively, computing new temperatures at each node and new outlet fluid temperatures until a default convergence criterion of 0.001 °C is achieved for T_{avg}. It is assumed that the average top surface temperature for the cross-section approximates the average top surface temperature for the entire pavement area.

Nomenclature

α	= thermal diffusivity of pavement material	(m^2/s)
α_{solar}	= solar absorptivity coefficient	(--)
Δt	= time step	(s)
ε	= emmissivity coefficient	(--)
ν	= viscosity of heat exchange fluid	(N-s/m^2)
ρ_{pv}	= density of pavement material	(kg/m^3)
ρ_{fl}	= density of heat exchange fluid	(kg/m^3)
σ	= Stephan-Boltzmann constant = 5.67×10^{-8} W/m^2-K^4	

circuit	= number of flow circuits	(--)
conc	= volume of GS-4 in solution if used	(%)
$c_{p\,fl}$	= heat capacity of heat exchange fluid	(J/(kg-°C))
$c_{p\,pv}$	= heat capacity of pavement material	(J/(kg-°C)
delta	= x and y grid spacing	(m)
fall	= snowfall rate	(mm of water equivalent per hr)
Fo	= Fourier Number	(--)
Fluid	= fluid type (1=water, other value=GS-4 antifreeze solution)	
h_c	= convection heat transfer coefficient at pavement top surface	(W/m^2-°C)
h_{fg}	= heat of evaporation	(J/kg)
h_{pipe}	= convection heat transfer coefficient for fluid	(W/m^2-°C)
k_{fl}	= thermal conductivity of heat exchange fluid	(W/(m-°C))
k_{pipe}	= thermal conductivity of pipe material	(W/(m-°C))

k_{pv} = thermal conductivity of pavement materials   (W/(m-°C))
length = pavement length   (m)
Minflow = minimum flow parameter   (kg/s)
mdot = fluid mass flow rate   (kg/hr)
mdott = fluid mass flow rate per flow circuit   (kg/s)
Nu = Nusselt Number   (--)
P_a = vapor pressure of moist air   (kPa)
P_s = vapor pressure of water at surface   (kPa)
pipdep = pipe depth below surface   (m)
pipdia = pipe diameter   (m)
pipsp = pipe spacing   (m)
Pr = Prandtl Number   (--)
$P_{(x,y)}$ = temperature at node (x,y) at previous time step   (°C)
q''_{convs} = convection heat flux from pavement surface   (W/m^2)
q''_{emis} = thermally emmitted radiation heat flux from pavement surface   (W/m^2)
q''_{evapr} = heat of evaporation (mass transfer) for rain   (W/m^2)
q''_{evaps} = heat of evaporation (mass transfer) for melted snow(W/m^2)
q''_{fluid} = fluid convection heat flux per unit length of pipe   (W/m^2/m)
q_{fluid} = fluid convection heat transfer   (W/m)
$q_{transfer}$ = total amount of heat transferred to pavement surface(kJ/hr)
q''_{rad} = solar radiation heat flux   (W/m^2)
q''_{snow} = sensible heat plus heat of fusion required to melt snow(W/m^2)
q''_{total} = total heat flux at pavement top surface   (W/m^2)
rad = solar radiation incident on the pavement surface   (W/m^2)
rain = rain indicator (1 OR 0)
Re = Reynold's Number   (--)
RH = relative humidity   (%)
snow = snowfall indicator (1 OR 0)
t = time
T = temperature   (°C)
T_{amb} = ambient air temperature   (°C)
T_{avg} = average fluid temperature   (°C)
thick = pavement thickness   (m)
T_{in} = inlet fluid temperature   (°C)
T_{film} = average of pavement top surface temperature and
air temperature for evaporation calc.   (°C)
T_{out} = outlet fluid temperature   (°C)
T_{sky} = sky temperature   (°C)
T_{top} = average pavement top surface temperature   (°C)
$T_{(x,y)}$ = temperature at node (x,y) at current time step   (°C)
U = overall heat transfer coefficient for fluid   (W/m^2-°C)
wallt = pipe wall thickness   (m)
width = pavement width   (m)
wind = wind speed   (m/s)

Mathematical Description

The governing equation of model is the two-dimensional (2-D) form of the transient heat diffusion equation:

$$\frac{\partial^2 T}{\partial x^2} + \frac{\partial^2 T}{\partial y^2} = \frac{\partial T}{\partial t} \frac{1}{\forall} \qquad \text{(A.13.1)}.$$

Nodal Finite-Difference Equations

Appearing in all nodal equations is the finite-difference form of the Fourier number:

$$Fo = \frac{\alpha \Delta t}{(\Delta x)^2} \qquad \text{(A.13.2)}.$$

One disadvantage of the forward difference approximation method is that the solution is not unconditionally stable. For a 2-D grid, the stability criterion is:

$$Fo \leq \tfrac{1}{4} \qquad \text{(A.13.3)}.$$

For the prescribed values of α and Δx, the appropriate timestep can be determined. This model sets Δx equal to the pipe radius. Consequently, a timestep of approximately 30 seconds is required for stability for a model using typical thermal properties of concrete pavement and ¾-inch diameter pipe.

Nodal equations are described below for different geometries. Symbols are as in Figure 2. y is positive downward and x is positive to the right.
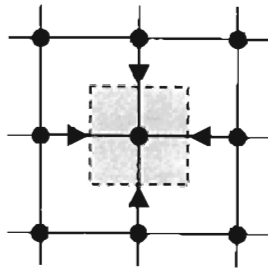
$$T_{(x,y)} = Fo(P_{(x,y-1)} + P_{(x-1,y)} + P_{(x+1,y)} + P_{(x,y+1)}) + (1-4Fo)P_{(x,y)} \tag{A.13.4}$$

Node Geometry 1 – Interior Node:

Node Geometry 2 – Exterior Corner Node With Adiabatic and Flux Boundaries:
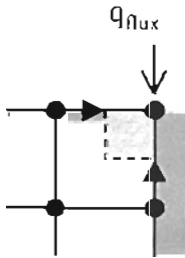
$$T_{(x,y)} = 2Fo(P_{(x-1,y)} + P_{(x,y+1)} + q_{flux}delta/k_{pv}) + (1-4Fo)P_{(x,y)} \tag{A.13.5}$$

Node Geometry 3 – Node at Plane Surface With Flux Boundary:
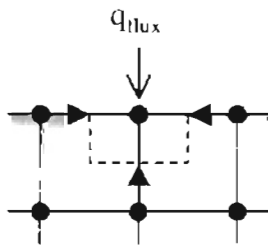
$$T_{(x,y)} = Fo(2P_{(x,y+1)} + P_{(x-1,y)} + P_{(x+1,y)} + 2q_{flux}delta/k_{pv}) + (1-4Fo)P_{(x,y)} \tag{A.13.6}$$

Node Geometry 4 – Node at an Interior Corner With Flux Boundaries (i.e. pipe corner nodes):

169
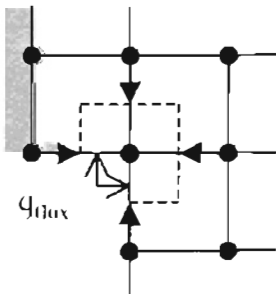
Surface Heat Transfer Equations

$$T_{(x,y)} = 2/3Fo(P_{(x-1,y)} + P_{(x,y+1)} + 2P_{(x,y-1)} + 2P_{(x+1,y)} +$$
$$2q_{flux}delta/k_{pv}) + (1-4Fo)P_{(x,y)} \qquad (A.13.7)$$

To provide the finite-difference equations with the appropriate heat flux term (q_{flux}) at the boundaries, several heat transfer mechanisms are considered in the model. These mechanisms are: (1) solar radiation heat gain, (2) convection heat transfer due to external flow, (3) thermal radiation heat transfer, (4) heat lost to melting of snow, (5) heat lost to evaporation of rain and melted snow, and (6) convection heat transfer due to internal pipe flow. Each of these mechanisms is described below.

Solar Radiation Heat Gain

Solar radiation heat gain is the amount of solar radiation absorbed by the pavement slab:

$$q''_{rad} = \alpha_{solar} \, rad \qquad (A.13.8).$$

Convection Heat Transfer Due to External Flow

This heat transfer mechanism accounts for convective heat transfer at the top surface of the pavement. The model uses a convection model based on work done by Wadivkar (1997). The convection coefficient is a function of wind speed:

if (wind<4.88) then

$$h_c = 5.678(0.775 + 0.35(wind/0.304)) \qquad (A.13.9a)$$

else $h_c = 5.678(0.775+0.35(wind/0.304)^{0.78})$ \qquad (A.13.9b)

$$q''_{conve} = h_c(P_{(x,y)} - T_{amb}) \qquad (A.13.10)$$

Thermal Radiation Heat Transfer

This heat transfer mechanism accounts for heat transfer due to thermal or long-wave radiation at the pavement surface:

$$q''_{emis} = \varepsilon\sigma \, (P_{(x,y)}{}^4 - T_{sky}{}^4) \tag{A.13.11}.$$

where $P_{(x,y)}$ and T_{sky} are in Kelvin.

Heat Lost to Melting of Snow

The model uses algorithms from ASHRAE (1995) to determine the amount of heat lost to melting of snow. The heat required to melt snow is a function of air temperature and snowfall rate. It is the amount of sensible heat needed to raise the temperature of the snow to 0 C plus the heat of fusion. Per unit area, the heat required to melt snow at a given snowfall rate is:

$$q''_{snow} = snow(92.6fall + 0.578fall(0-T_{amb})) \tag{A.13.12}.$$

Heat Lost to Evaporation of Rain and Melted Snow

The model uses snow-melt algorithms from ASHRAE (1995) to determine the amount of heat lost to evaporating water on the pavement surface:

$$q''_{evapr} = snow(h_{fg} \, (0.005*wind*3.6 + 0.022)(P_s-P_a)) \tag{A.13.13}.$$

$$q''_{evaps} = rain(h_{fg} \, (0.005*wind*3.6 + 0.022)(P_s-P_a)) \tag{A.13.14}.$$

P_s and P_a are computed from Kishore and Joshi (1984) as follows:

$$P_s = 0.1333224*(exp(18.403-(3885/(T_{top}+ 230)))) \tag{A.13.15}.$$

$$P_a = RH*0.1333224*(exp(18.403-(3885/(T_{amb}+ 230)))) \tag{A.13.16}.$$

h_{fg} is computed from a curve-fit equation to standard tabulated data for water:

$$h_{fg} = -2.3932T_{film} + 2502.1 \tag{A.13.17}.$$

Total Heat Flux at Pavement Surface

The total heat flux at the pavement top surface is:

$$q''_{total} = q''_{rad} + q''_{convs} - q''_{emis} - q''_{snow} - q''_{evaps} - q''_{evapr}$$ (A.13.18).

The total heat flux at the pavement bottom surface is convection only.

Convection Heat Transfer Due to Internal Pipe Flow

To determine the convection heat transfer due to internal pipe flow, the thermal
properties of the fluid are first computed as a function of T_{in}. If the heat transfer fluid is
water (if the input variable "fluid" = 1), thermal properties are computed from a curve-fit
equation to standard tabulated data for water. If the heat transfer fluid is an antifreeze
solution, thermal properties are computed from equations described by Wadivkar (1997)
for GS-4 solution. The following equations are used to obtain the thermal properties of
water:

$$v = 3E\text{-}7T_{in}^2 - 4E\text{-}5T_{in} + 0.0017$$ (A.13.19a).

$$\rho_n = 0.0045\, T_{in}^2 + 0.0228\, T_{in} + 999.62$$ (A.13.20a).

$$k_n = -7E\text{-}6\, T_{in}^2 + 0.0018\, T_{in} + 0.5695$$ (A.13.21a).

$$c_{p\,n} = 0.0223\, T_{in}^2 - 1.7843\, T_{in} + 4211.9$$ (A.13.22a).

The following equations are used to obtain the thermal properties of an antifreeze
solution:

$$v = (\exp(-0.135\, T_{in} + 2.62E\text{-}4\, T_{in}^2 + 0.172*0.506*conc - 5.64E\text{-}4)*(\, T_{in}$$

$$*0.506*CONC + 17.5)*0.001$$ (A.13.19b).

(for in T_{in} degrees Kelvin).

$$\rho_n = (-0.000226\, T_{in} + 0.00606*0.506conc + 0.99)*1000$$ (A.13.20b).

$$k_n = (0.000717*T_{in} + 0.00085*0.506*conc + 1.8/0.506/conc + 0.107)*1.73$$ (A.13.21b).

$$c_{p\,n} = (-6.77E\text{-}3*0.506*conc + 1.4E\text{-}4*T_{in} + 1.01)*4186.8$$ (A.13.22b).

Next, the following dimensionless numbers are computed so that the pipe convection coefficient can be obtained:

$$Re = 4mdott/(\pi \text{ pipdia } v) \tag{A.13.23}$$

$$Pr = v \, c_{p\,fl} / k_{fl} \tag{A.13.24}$$

$$Nu = 0.023Re^{0.8}Pr^x \quad \text{(Dittus-Boelter equation)} \tag{A.13.25}$$

where $x = 0.3$ if $T_{in} > T_{top}$

else $x=0.4$

$$h_{pipe} = Nu \, k_{fl}/\text{pipdia} \tag{A.13.26}$$

The overall heat transfer coefficient for the fluid can then be computed:

$$U = \frac{1}{\text{wallt}/k_{pipe} + 1/h_{pipe}} \tag{A.13.27}$$

Finally, the fluid heat flux (per unit length of pipe) for use in the finite-difference equations is computed as:

$$q''_{fluid} = U(T_{avg} - P_{(x,y)}) \tag{A.13.28}$$

As previously mentioned, T_{avg} is determined iteratively. T_{avg} is the average of the inlet and outlet fluid temperatures of a flow circuit. On the first iteration of a timestep, T_{avg} is assigned the average of T_{in} at the current time step and T_{out} at the previous time step. The new outlet fluid temperature is computed as:

$$T_{out} = T_{avg} - (q_{fluid}(\text{width*length/pipsp} + \text{length})/\text{circuit})/ (mdott* c_{p\,fl}) \tag{A.13.29}$$

where q_{fluid} is the heat flux computed by equation 27 multiplied by the nodal area and multiplied by 2 to correct for a full pipe diameter. q_{fluid} is computed as:

$$q_{fluid} = 2U \, (\text{delta}/2(T_{avg} - T1) + \text{delta}(T_{avg} -T2) + \text{delta} (T_{avg} -T3) + \text{delta} (T_{avg} -T4)$$
$$+ \text{delta} /2(T_{avg} -T5)) \tag{A.13.30}$$

where T1 to T5 represents nodal temperatures around the pipe surface in clockwise order

starting at the node at the top of the pipe (see Figure 2).

The total amount of heat exchanged by the fluid is computed as:

$$q_{transfer} = mdot(T_{in} - T_{out}) \, c_p \, n \, / 1000 \tag{A.13.31}$$

Component configuration
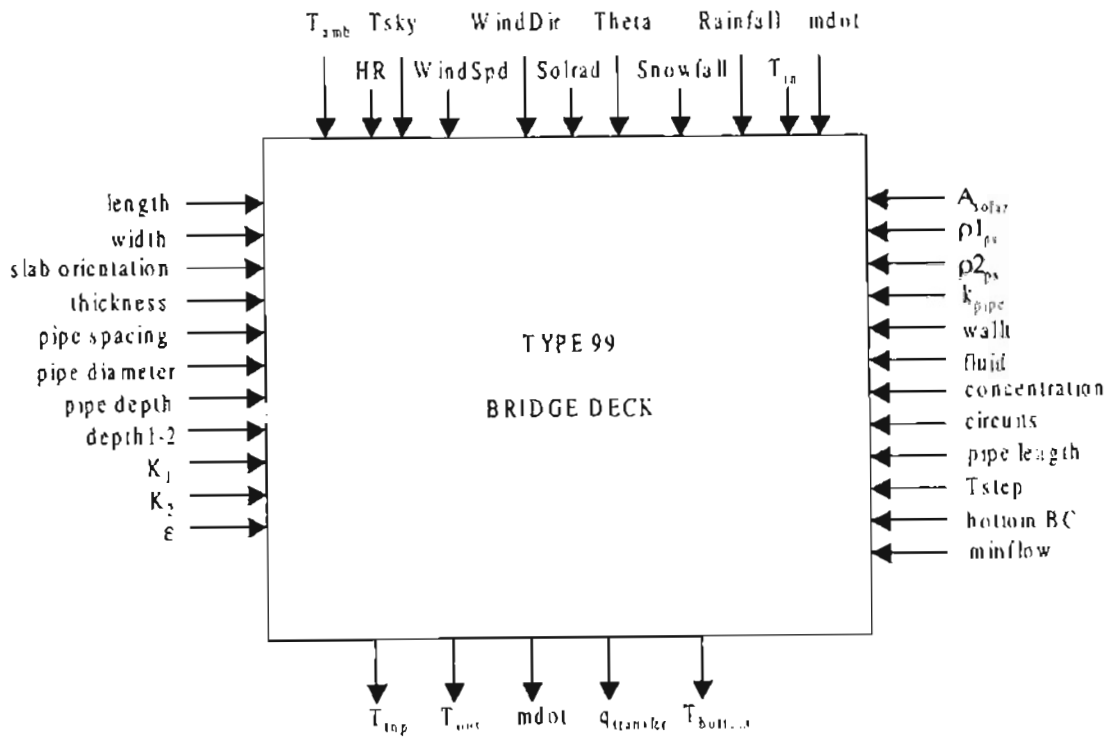
A.14. TYPE 100: BRIDGE DECK

Component description

Type 100 is a slight variation of Type 99 in a sense that Type 100 has flow rates inbuilt as flow rates. The flow is activated in the model by an input control signal unlike the earlier bridge deck model. The flow in the bridge deck is obtained a product of control signal C and the maximum flow rate.

Additional parameters to Type 100 include the mass flow rates (kg/s), the recharge flow rate(kg/s) and a recharge fraction R_f (a number between 0 and 1). The recharge fraction has been added as a parameter to check whether the bridge deck is used in the simulation in recharge mode or heating mode. If the control signal is equal to the recharge fraction parameter specified by the user, then the flow rate through the bridge deck is equal to recharge flow. Else, the flow rate through the model is a product of control signal (usually between 0 an 1) and the maximum mass flow rate specified. Bridge deck Type 100 resembles Type 99 in all other respects.

Nomenclature

C = control signal or flow indicator (between 0 and 1)   (-)
R_f = recharge fraction   (-)
$mdot$ = maximum mass flow rate during heating   (kg/s)
$mdot_{recharge}$= maximum mass flow rate during recharge   (kg/s)

175

Component configuration

TYPE 100

BRIDGE DECK

Inputs (top): T_{amb}, Tsky, WindDir, Theta, Rainfall, C, HR, WindSpd, Solrad, Snowfall, T_{in}

Inputs (left): length, width, slab orientation, thickness, pipe spacing, pipe diameter, pipe depth, depth 1-2, K_1, K_2, ϵ

Inputs (right): A_{sct}, $p1_{ps}$, $p2_{ps}$, k_{pis}, wall t, fluid, concentration, circuits, pipe length, Tstep, bottom BC, minflow, maxdt, R_t, maxdt$_{...}$

Outputs (bottom): T_{top}, T_{out}, $q_{transfer}$, T_{bottom}

****
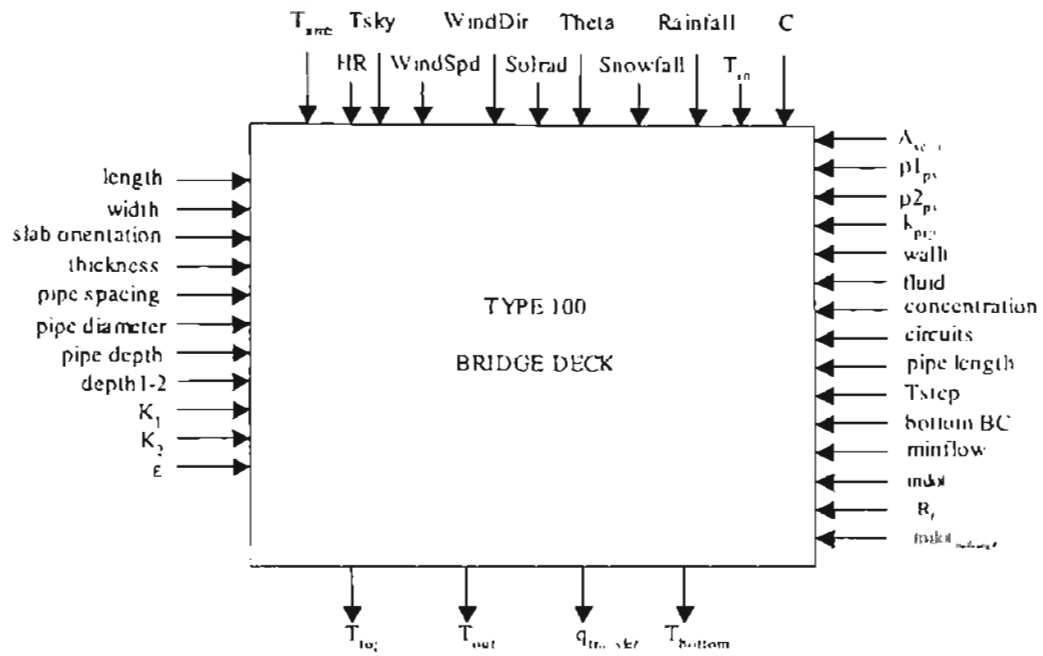
139 'GROUND LOOP HEAT EXCHANGER WITH VARIABLE RESISTANCE AND
FLOW PARAMETER '
 6 0 2 3 17 ! Numbers of SAVED, Diff. Eq., XIN, OUT, PA
 3 'Tin'   'The inlet fluid temperature' 'C'
 4 'FLOW INDICATOR'
#
 3 'Tout'   'The outlet fluid temperature''C'
 3 'TF'   'The average fluid temperature' 'C'
 7 'QN'   'The ground load' 'KW'
#
 1 'NB'
 2 'H'
 3 'RADb'
 4 'K'
 5 'Cground'
 6 'Cfluid'
 7 'Tom'
 8 'MINFLOW'
 9 'k_grout'
10 'k_pipe'
11 'k_fluid'
12 'rho_fluid'
13 'Nu_fluid'
14 'PipeD_Outer'
15 'Dist_UTube'
16 'Pipe_T'
17 'MAX FLOW RATE'
****

APPENDIX B

INFORMATION FLOW DIAGRAM OF SYSTEMS
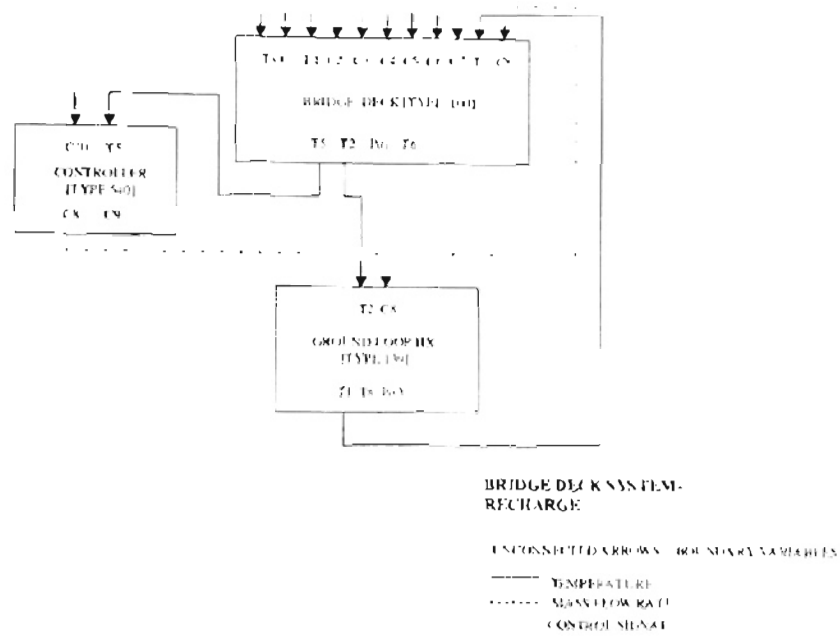
Figure B.1. *Bridge deck system- recharge*
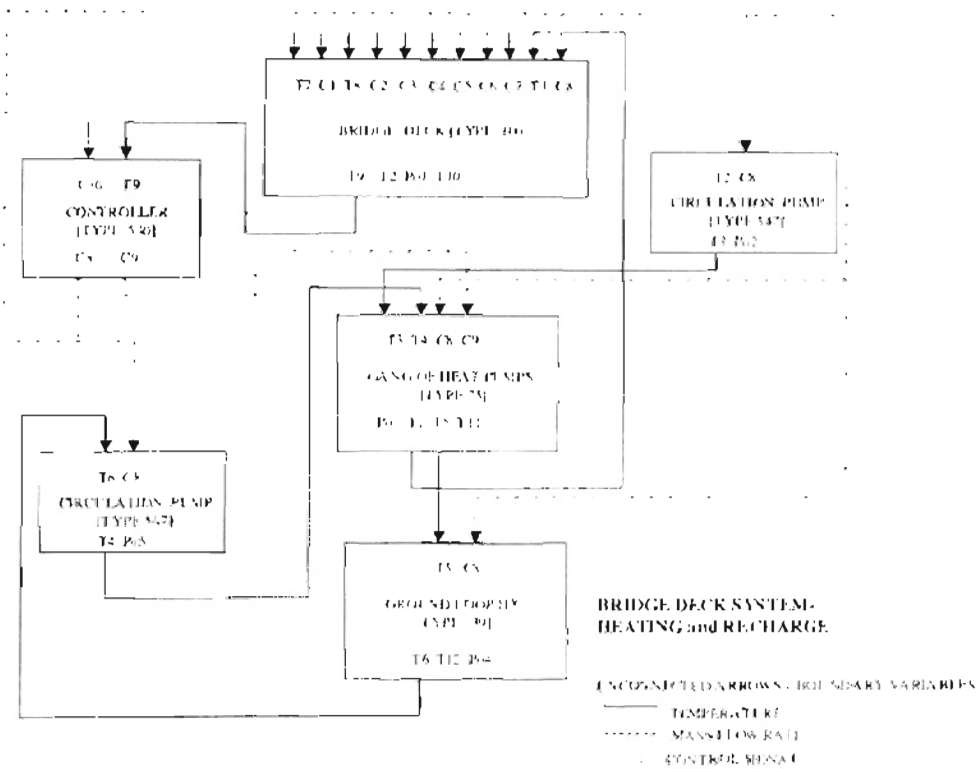
Figure B.2. *Bridge deck system- heating & recharge*

APPENDIX C

SYSTEM SUMMARY FILES
C.1. Bridge deck system -recharge

```
***** PROGRAM MODSIM *****
a MODular SIMulation program
```

BRIDGE DECK-PUMP-GLHE (FOR RECHARGE MODE ONLY)

1 SUPERBLOCKS   1 BLOCKS   4 UNITS

21 STATE VARIABLES:
 8 TEMP 10 CTRL   3 POWR

INITIAL STATE VECTOR:

TEMP:
```
   20.0000      20.0000      20.0000      0.00000      0.00000
   0.00000      0.00000      0.00000
```

CTRL:
```
   0.00000      0.00000      0.00000      0.00000      0.00000
   0.00000      0.00000      0.00000      0.00000      0.00000
```

POWR:
```
   0.00000      0.00000      0.00000
```

10) TIME DEPENDENT BOUNDARY VARIABLES:
TEMP 4 TEMP 5 CTRL 1 CTRL 2 CTRL 3 CTRL 4 CTRL 6 CTRL 7
CTRL 5 CTRL 10

ERROR TOLERANCES: RTOLX, ATOLX, XTOL, TTIME:
   1.00000E-04   1.00000E-05   2.00000E-04   1.0000

***** SUPERBLOCK 1 *****

SUPERBLOCK SIMULTANEOUS EQUATION UNFREEZING OPTION, IFZOPT = 0
SUPERBLOCK INPUT SCAN OPTION, INSOPT = 0

10 REPORTED VARIABLES:
TEMP 1 TEMP 2 TEMP 3 TEMP 6 TEMP 7 TEMP 8 CTRL 8 POWR 1
POWR 2 POWR 3

0 SIMULTANEOUS EQUATIONS; VARIABLES:

***** BLOCK 1 *****

5 SIMULTANEOUS EQUATIONS; VARIABLES:
TEMP 1 CTRL 8 TEMP 2 TEMP 3 TEMP 6

UNIT 1   TYPE100

11 INPUTS:
TEMP 4 CTRL 1 TEMP 5 CTRL 2 CTRL 3 CTRL 4 CTRL 5 CTRL 6

CTRL 7 TEMP 1 CTRL 8

 4 OUTPUTS:
TEMP 6 TEMP 2 POWR 1 TEMP 7

PARAMETERS:
    200.00   12.500   90.000   0.20320   0.30480
    2.66700E-02   7.62000E-02   15.000   1.4000   0.40000
    0.90000   0.60000   2.20000E+06 2.20000E+06 0.39100
    2.42454E-03   1.0000   42.000   110.00   73.818
    30.000   1.0000   0.10000   22.732   17.535
    0.30000

UNIT 2   TYPE547

 2 INPUTS:
TEMP 2 CTRL 8

 2 OUTPUTS:
TEMP 3 POWR 2

PARAMETERS:
    1.0000   0.80000   22.732   50.000   0.30000
    1.0000   100.00   17.535

UNIT 3   TYPE139

 2 INPUTS:
TEMP 3 CTRL 8

 3 OUTPUTS:
TEMP 1 TEMP 8 POWR 3

PARAMETERS:
    250.00   76.200   6.35100E-02 0.69230   2.34700E+06
    3768.3   17.220   5.0000   0.69230   0.39110
    0.60230   998.20   9.87975E-04 2.66700E-02 2.54000E-02
    2.41300E-03   58.450

UNIT 4   TYPE540

 2 INPUTS:
CTRL 10 TEMP 6

 2 OUTPUTS:
CTRL 8 CTRL 9

PARAMETERS:
    0.0000   2.7777   32.222   8.0000   0.30000

TMIN =   3600.000 TMAX =   3600.000 TSTOP = 3600000.000

     ***** PROGRAM MODSIM *****

C.2. Bridge deck system – heating and recharge
a MODular SIMulation program

BRIDGE DECK WITH RECHARGE (FLOW AS INBUILT PARAMETERS)

1 SUPERBLOCKS   1 BLOCKS   6 UNITS

27 STATE VARIABLES:
12 TEMP   10 CTRL   5 POWR

INITIAL STATE VECTOR:

TEMP:
```
    20.0000      20.0000      20.0000      20.0000      20.0000
    20.0000      0.00000      0.00000      0.00000      0.00000
    0.00000      0.00000
```

CTRL:
```
    0.00000      0.00000      0.00000      0.00000      0.00000
    0.00000      0.00000      0.00000      0.00000      0.00000
```

POWR:
```
    0.00000      0.00000      0.00000      0.00000      0.00000
```

10 TIME DEPENDENT BOUNDARY VARIABLES:
TEMP 7 TEMP 8 CTRL 1 CTRL 2 CTRL 3 CTRL 4 CTRL 6 CTRL 7
CTRL 5 CTRL 10

ERROR TOLERANCES: RTOLX, ATOLX, XTOL, TTIME:
```
    1.00000E-04   1.00000E-05   2.00000E-04    1.0000
```

***** SUPERBLOCK 1 *****

SUPERBLOCK SIMULTANEOUS EQUATION UNFREEZING OPTION, IFZOPT = 0
SUPERBLOCK INPUT SCAN OPTION, INSOPT = 0

16 REPORTED VARIABLES:
TEMP 1 TEMP 2 TEMP 3 TEMP 4 TEMP 5 TEMP 6 TEMP 9 TEMP 12
TEMP 11 CTRL 8 CTRL 9 POWR 1 POWR 2 POWR 3 POWR 4 POWR 5

0 SIMULTANEOUS EQUATIONS; VARIABLES:

***** BLOCK 1 *****

9 SIMULTANEOUS EQUATIONS; VARIABLES:
TEMP 1 CTRL 8 TEMP 2 TEMP 3 TEMP 4 CTRL 9 TEMP 5 TEMP 6
TEMP 9

UNIT 1   TYPE100

11 INPUTS:
TEMP 7 CTRL 1 TEMP 8 CTRL 2 CTRL 3 CTRL 4 CTRL 5 CTRL 6
CTRL 7 TEMP 1 CTRL 8

4 OUTPUTS:
TEMP 9 TEMP 2 POWR 1 TEMP 10

PARAMETERS:
```
200.00      12.500      90.000      0.20320      0.30480
2.66700E-02  7.62000E-02  15.000      1.4000      0.40000
0.90000      0.60000      2.20000E+06  2.20000E+06  0.39100
2.42454E-03  1.0000      42.000      110.00      73.818
30.000      1.0000      0.10000      22.732      17.535
0.30000
```

UNIT 2   TYPE547

2 INPUTS:
TEMP 2 CTRL 8

2 OUTPUTS:
TEMP 3 POWR 2

PARAMETERS:
```
1.0000      0.80000      22.732      50.000      0.30000
1.0000      100.00      17.535
```

UNIT 3   TYPE 75

4 INPUTS:
TEMP 3 TEMP 4 CTRL 8 CTRL 9

4 OUTPUTS:
POWR 3 TEMP 1 TEMP 5 TEMP 11

PARAMETERS:
```
2.03640E-02  1.80000E-03  25.515      19.730      1.6039
2.0377      48.074      19.533      8.0000      5.0000
0.0000      47.000      100.00      80.000      22.732
58.450      0.30000
```

UNIT 4   TYPE139

2 INPUTS:
TEMP 5 CTRL 8

3 OUTPUTS:
TEMP 6 TEMP 12 POWR 4

PARAMETERS:
```
250.00      76.200      6.35100E-02  0.69230      2.34700E+06
3768.3      17.220      5.0000      0.69230      0.39110
0.60230      998.20      9.87975E-04  2.66700E-02  2.54000E-02
2.41300E-03  58.450
```

UNIT 5   TYPE547

2 INPUTS:
TEMP 6 CTRL 8

2 OUTPUTS:
TEMP 4 POWR 5

PARAMETERS:
```
    2.0000      0.80000      58.450      50.000      0.30000
    1.0000      0.0000       17.535
```

UNIT 6   TYPE540

 2 INPUTS:
CTRL 10   TEMP 9

 2 OUTPUTS:
CTRL 8 CTRL 9

PARAMETERS:
```
    0.0000      2.7777       32.222      8.0000      0.30000
```

TMIN =   3600.000 TMAX =   3600.000 TSTOP =31536000.000

***** END OF FILE ENCOUNTERED ON BOUNDARY CONDITION FILE AT TIME

APPENDIX D

MODIFIED SNSQ

```
***********************************************************************
C
        SUBROUTINE SNSQ1(FCN,JAC,IOPT,N,X,FVEC,FJAC,LDFJAC,XTOL,MAXFEV,
     &                   ML,MU,EPSFCN,DIAG,MODE,FACTOR,NPRINT,INFO,NFEV,
     &                   NJEV,R,LR,QTF,WA1,WA2,WA3,WA4,IBLK,ISBLK)
C
C -------------------------------------------------------------------
C
C       SNSQ1 : This program is essentially same as SNSQ.
C               Called by subroutine BLOCK. Calls FDJAC2, while SNSQ calls
C               FDJAC1. Note that the argument of FCN has IBLK and ISBLK.
C
C               The original program was written by K.L. Hiebert
C
C               A minor modification was made by C. R. Hill and C. Park
C               August 13, 1984
C
C               Updated for writing diagonastic information by D.C.,
C               March 8, 1985
C
C               Modified by P. Haves, Oxford Univ., U.K. to include
C               simulation times in warning/error messages
C               April 12, 1989
C
C               Modified by Mahadevan Ramamoorthy, Oklahoma State Univ,to
C               include a successive substitution step (as suggested by
P.Haves) before recalcuating the jacobian if the solution method fails
to find a solution This provides a better initial guess for the hybrid
conjugate gradient method September 17, 2000
C
C       (The documention of this SNSQ routine resides elsewhere.
C          See SNSQ.DOC )
C
C
C
***********************************************************************
C
        EXTERNAL FCN
***********************************************************************
C       Included for using common block data in successive substitution:
M. Ramamoorthy
    INCLUDE 'hvacsim.par'
***********************************************************************
        LOGICAL JEVAL,SING
        INTEGER  IWA(1)
        REAL     X(N),FVEC(N),DIAG(N),FJAC(LDFJAC,N),R(LR),QTF(N),WA1(N),
     &           WA2(N),WA3(N),WA4(N)
***********************************************************************
C       Input, output and other arrays dimensioned for use in successive
substitution
        DIMENSION XIN(MINOIU),OUT(MINOIU),LOUT(MINOIU),KOUT(MINOIU),
     .XOLD(N)
```

184

```fortran
**************************************************************************
      COMMON    /FILES/ IFILE1,IFILE2,IFILE3,IFILE4,IFILE5,IFILE6,INP
      COMMON    /CHRONO/ TIME,TSTEP,TTIME,TMIN,ITIME
**************************************************************************
C     common blocks of data for use in successive substitution
      COMMON    /BLOCKS/ IBLOCK(MAXBLK,MUNTIB),NUNITS(MAXBLK),NBLOCK
      COMMON    /CONECT/ IN(MAXUNT,MINOIU),IOUT(MAXUNT,MINOIU),
     &                   NIN(MAXUNT),NOUT(MAXUNT)
      COMMON    /SOLVE/  ISOLVE(MAXBLK,MSEQIB),NSOLVE(MAXBLK)
**************************************************************************
C
      DATA      ONE,P1,P5,P001,P0001,ZERO
     &          /1.0E0,1.0E-1,5.0E-1,1.0E-3,1.0E-4,0.0E0/
C
      EPSMCH = R1MACH(4)
      XNORM=0.
C
      INFO = 0
      IFLAG = 0
      NFEV = 0
      NJEV = 0


C     Check the input parameters for errors.
C
      IF (IOPT .LT. 1 .OR. IOPT .GT. 2 .OR.
     &    N .LE. 0 .OR. XTOL .LT. ZERO .OR. MAXFEV .LE. 0
     &    .OR. ML .LT. 0 .OR. MU .LT. 0 .OR. FACTOR .LE. ZERO
     &    .OR. LDFJAC .LT. N .OR. LR .LT. (N*(N + 1))/2) GO TO 300
      IF (MODE .NE. 2) GO TO 20
      DO 10 J = 1, N
         IF (DIAG(J) .LE. ZERO) GO TO 300
   10    CONTINUE
   20 CONTINUE

C
C     Evaluate the function at the starting point
C     and calculate its norm.
C
      IFLAG = 1
      CALL FCN(N,X,FVEC,IFLAG,IBLK,ISBLK)
      NFEV = 1
      IF (IFLAG .LT. 0) GO TO 300
      FNORM = ENORM(N,FVEC)
C
C     Initialize iteration counter and monitors.
C
      ITER = 1
      NCSUC = 0
      NCFAIL = 0
      NSLOW1 = 0
      NSLOW2 = 0
C
C     Beginning of the outer loop.
C
```

```
   30 CONTINUE

          JEVAL = .TRUE.
C
C         Calculate the Jacobian matrix.
C
          IF (IOPT .EQ. 2) GO TO 31
C
C         User supplies Jacobian.
C
C*            CALL JAC(N,X,FVEC,FJAC,LDFJAC,IFLAG)
C*            NJEV = NJEV+1
              GO TO 32
C
C         Code approximates the Jacobian.
C
   31         IFLAG = 2
              CALL
FDJAC2(FCN,N,X,FVEC,FJAC,LDFJAC,IFLAG,ML,MU,EPSFCN,WA1,
      &                 WA2,IBLK,ISBLK)
              NFEV = NFEV + MINO(ML+MU+1,N)
C**DEBUG
       IF(NPRINT.EQ.2) THEN
          WRITE(IFILE3,666) TIME/3600.
  666    FORMAT(' JACOBIAN AT HOUR:',F8.1)
          DO 13 I=1,N
   13    WRITE(IFILE3,667) (FJAC(I,J),J=1,N)
  667    FORMAT(1X,1P5G15.6)
       ENDIF
C**END DEBUG
C
   32      IF (IFLAG .LT. 0) GO TO 300
C
C          Compute the QR factorization of the Jacobian.
C

           CALL QRFAC(N,N,FJAC,LDFJAC,.FALSE.,IWA,1,WA1,WA2,WA3)
C
C          On the first iteration and if mode is 1, scale according
C          to the norms of the columns of the initial Jacobian.
C
           IF (ITER .NE. 1) GO TO 70
           IF (MODE .EQ. 2) GO TO 50
           DO 40 J = 1, N
              DIAG(J) = WA2(J)
              IF (WA2(J) .EQ. ZERO) DIAG(J) = ONE
   40      CONTINUE
   50      CONTINUE
C
C          On the first iteration, calculate the norm of the scaled X
C          and initialize the step bound delta.
C
           DO 60 J = 1, N
              WA3(J) = DIAG(J)*X(J)
   60      CONTINUE
           XNORM = ENORM(N,WA3)
           DELTA = FACTOR*XNORM
```

```
            IF (DELTA .EQ. ZERO) DELTA = FACTOR
    70      CONTINUE
C
C
C           Form (Q transpose)*FVEC and store in QTF.
C
            DO 80 I = 1, N
               QTF(I) = FVEC(I)
    80      CONTINUE
            DO 120 J = 1, N
               IF (FJAC(J,J) .EQ. ZERO) GO TO 110
               SUM = ZERO
               DO 90 I = J, N
                  SUM = SUM + FJAC(I,J)*QTF(I)
    90         CONTINUE
               TEMP = -SUM/FJAC(J,J)
               DO 100 I = J, N
                  QTF(I) = QTF(I) + FJAC(I,J)*TEMP
   100         CONTINUE
   110      CONTINUE
   120      CONTINUE
C
C
C           Copy the triangular factor of the QR factorization into R.
C
            SING = .FALSE.
            DO 150 J = 1, N
               L = J
               JM1 = J - 1
               IF (JM1 .LT. 1) GO TO 140
               DO 130 I = 1, JM1
                  R(L) = FJAC(I,J)
                  L = L + N - I
   130         CONTINUE
   140      CONTINUE
            R(L) = WA1(J)
            IF (WA1(J) .EQ. ZERO) SING = .TRUE.
   150      CONTINUE
C
C
C           Accumulate the orthogonal factor in FJAC.
C
            CALL QFORM(N,N,FJAC,LDFJAC,WA1)
C
C
C           Rescale if necessary.
C
            IF (MODE .EQ. 2) GO TO 170
            DO 160 J = 1, N
               DIAG(J) = AMAX1(DIAG(J),WA2(J))
   160      CONTINUE
   170      CONTINUE
C
C
C           Beginning of the inner loop.
C
   180      CONTINUE
C
C
C           If requested, call FCN to enable printing of iterates.
C
            IF (NPRINT .LE. 0) GO TO 190
            IFLAG = 0
```

```
              IF (MOD(ITER-1,NPRINT) .EQ. 0)
          &                   CALL FCN(N,X,FVEC,IFLAG,IBLK,ISBLK)
              IF (IFLAG .LT. 0) GO TO 300
    190       CONTINUE
C
C
C             Determine the direction P.
C
              CALL DOGLEG(N,R,LR,DIAG,QTF,DELTA,WA1,WA2,WA3)
C
C             Store the direction P and X + P. Calculate the norm of P.
C
              DO 200 J = 1, N
                 WA1(J) = -WA1(J)
                 WA2(J) = X(J) + WA1(J)
                 WA3(J) = DIAG(J)*WA1(J)
    200          CONTINUE
              PNORM = ENORM(N,WA3)
C
C             On the first iteration, adjust the initial step bound.
C
              IF (ITER .EQ. 1) DELTA = AMIN1(DELTA,PNORM)
C
C             Evaluate the function at X + P and calculate its norm.
C
              IFLAG = 1
              ISET=0
              CALL FCN(N,WA2,WA4,IFLAG,IBLK,ISBLK)
              NFEV = NFEV + 1
              IF (IFLAG .LT. 0) GO TO 300
              FNORM1 = ENORM(N,WA4)
C
C             Compute the scaled actual reduction.
C
              ACTRED = -ONE
              IF (FNORM1 .LT. FNORM) ACTRED   ONE - (FNORM1/FNORM)**2
C
C             Compute the scaled predicted reduction.
C
              L = 1
              DO 220 I = 1, N
                 SUM = ZERO
                 DO 210 J = i, N
                    SUM = SUM + R(L)*WA1(J)
                    L = L + 1
    210             CONTINUE
                 WA3(I) = QTF(I) + SUM
    220          CONTINUE
              TEMP = ENORM(N,WA3)
              PRERED = ZERO
              IF (TEMP .LT. FNORM) PRERED = ONE - (TEMP/FNORM)**2
C
C             Compute the ratio of the actual to the predicted
C             reduction.
C
              RATIO = ZERO
              IF (PRERED .GT. ZERO) RATIO = ACTRED/PRERED
C
```

```fortran
C                   Update the step bound.
C
                    IF (RATIO .GE. P1) GO TO 230
                        NCSUC = 0
                        NCFAIL = NCFAIL + 1
                        DELTA = P5*DELTA
                        GO TO 240
      230           CONTINUE
                        NCFAIL = 0
                        NCSUC = NCSUC + 1
                        IF (RATIO .GE. P5 .OR. NCSUC .GT. 1)
     &                      DELTA = AMAX1(DELTA,PNORM/P5)
                        IF (ABS(RATIO-ONE) .LE. P1) DELTA = PNORM/P5
      240           CONTINUE
C
C
C                   Test for successful iteration.
C
                    IF (RATIO .LT. P0001) GO TO 260
C
C                   Successful iteration. Update X, FVEC, and their norms.
C
                    DO 250 J = 1, N
                        X(J) = WA2(J)
                        WA2(J) = DIAG(J)*X(J)
                        FVEC(J) = WA4(J)
      250           CONTINUE
                    XNORM = ENORM(N,WA2)
                    FNORM = FNORM1
                    ITER = ITER + 1
      260           CONTINUE
C
C                   Determine the progress of the iteration.
C
                    NSLOW1 = NSLOW1 + 1
                    IF (ACTRED .GE. P001) NSLOW1 = 0
                    IF (JEVAL) NSLOW2 = NSLOW2 + 1
                    IF (ACTRED .GE. P1) NSLOW2 = 0
C
C                   Test for convergence.
C
                    IF (DELTA .LE. XTOL*XNORM .OR. FNORM .EQ. ZERO) INFO = 1
C**DEBUG
          IF(NPRINT.EQ.2) THEN
                    XTNORM=XTOL*XNORM
                    WRITE(IFILE3,668) DELTA,XTNORM
      668           FORMAT(' DELTA, XTNORM AT CONVERGENCE TEST:',1P2G15.6)
          ENDIF
C**END DEBUG
                    IF (INFO .NE. 0) GO TO 300
C
C                   Tests for termination and stringent tolerances.
C
                    IF (NFEV .GE. MAXFEV) INFO = 2
                    IF (P1*AMAX1(P1*DELTA,PNORM) .LE. EPSMCH*XNORM) INFO = 3
                    IF (NSLOW2 .EQ. 5) INFO = 4
C                   IF (NSLOW1 .EQ. 10) INFO = 5    ! iteration changed to 50
for better results :M.R, 09/17/2000
```

189

```
              IF (NSLOW1 .EQ. 50) INFO = 5
              IF (INFO .NE. 0) GO TO 300
C
C             Criterion for recalculating Jacobian.
C
              IF (NCFAIL .EQ. 2) GO TO 290
C
C             Calculate the rank one modification to the jacobian
C             and update QTF if necessary.
C
              DO 280 J = 1, N
                 SUM = ZERO
                 DO 270 I = 1, N
                    SUM = SUM + FJAC(I,J)*WA4(I)
  270            CONTINUE
                 WA2(J) = (SUM - WA3(J))/PNORM
                 WA1(J) = DIAG(J)*((DIAG(J)*WA1(J))/PNORM)
                 IF (RATIO .GE. P0001) QTF(J) = SUM
  280         CONTINUE
C
C             Compute the QR factorization of the updated Jacobian.
C
              CALL R1UPDT(N,N,R,LR,WA1,WA2,WA3,SING)
              CALL R1MPYQ(N,N,FJAC,LDFJAC,WA2,WA3)
              CALL R1MPYQ(1,N,QTF,1,WA2,WA3)
C
C             End of the inner loop.
C
              JEVAL = .FALSE.
              GO TO 180
  290      CONTINUE
```

```
*********************************************************************
C     This part of the program does a successive substitution before
recalculating the Jacobian Matrix providing a better initial guess and
dislodges the variables from  the local minima or if the solution fails
to converge
CCCCCCCCCCCCCCCCCCCCCCCCCCCCCCCCCCCCCCCCCCCCCCCCCCCCCCCCCCCCCCCCCCCCCCCC
C     No of equation solved simultaneously (No of variables which are
inputs of one component and
C     output of the other component)
   NEQS=NSOLVE(IBLK)

C     Not done for initial time step
   IF(time.ne.0) THEN
C     Begin outer loop: No of iterations or successive substitutions
   DO 81 M=1,5 ! 5 is the number of successive substitutions
C     Inner loop : Calls each unit in the block

       DO 71  J=1,NUNITS(IBLK)
       IU=IBLOCK(IBLK,J)
       NLOUT=0

C     Check each unit for outputs which are solved simultaneously.
       DO 33   L=1,NOUT(IU)
          DO 21   K=1,N
            IF(IOUT(IU,L).EQ.ISOLVE(IBLK,K)) THEN
```

```
                NLOUT=NLOUT+1
                LOUT(NLOUT)=L
                KOUT(NLOUT)=K
                GOTO 33
            ENDIF
21        CONTINUE
33        CONTINUE
C     Skip unit if no outputs are solved simultaneously.
      IF(NLOUT.GT.0) THEN
C     Gets the input vector for the particular component type
          CALL INPUTS(IU,XIN)
C     If Input of one component is the output of the other Type
C     The output overwrites the input
          DO 41   KK=1,NSOLVE(IBLK)
            DO 41    L=1,NIN(IU)

            IF(IN(IU,L).EQ.ISOLVE(IBLK,KK))THEN
              XIN(L)=X(KK)
          ENDIF
41        CONTINUE

C     Call to the Type number to get the outputs
          CALL SELECT(IU,XIN,OUT)
C     If the input of one Type is the output of the other, store it in
temporary
C     array X for use in Call to the next component type
          DO 61   KK=1,NLOUT
            L=LOUT(KK)
            K=KOUT(KK)
          X(K)=OUT(L)
61        CONTINUE
      ENDIF


71     CONTINUE ! end of inner loop
81 CONTINUE ! end of outer loop
      ENDIF
C     The successive substitution ends here   : Mahadevan Ramamoorthy
09/17/2000
************************************************************************
*********
C          End of the outer loop.
C
          GO TO 30
   300 CONTINUE


C     Termination, either normal or user imposed.
C
      IF (IFLAG .LT. 0) INFO = IFLAG
      IFLAG = 0
      IF (NPRINT .GT. 0) CALL FCN(N,X,FVEC,IFLAG,IBLK,ISBLK)
      IF (INFO .LT. 0) PRINT 1000, TIME, IBLK          ! 3/1/96
      IF (INFO .EQ. 0) PRINT 2000, TIME, IBLK
      IF (INFO .EQ. 2) PRINT 3000, TIME, IBLK
      IF (INFO .EQ. 3) PRINT 4000, TIME, IBLK
      IF (INFO .GT. 4) then
      PRINT 5000, TIME, IBLK
```

[19]

```fortran
       WRITE(IFILE3,669) TIME/3600.
 669    FORMAT(' ITERATION NOT MAKING GOOD PROGRESS AT HOUR:',F8.1)
     ENDIF

C
1000  FORMAT(' TIME = ',F8.1,' SNSQ - EXECUTION TERMINATED BECAUSE',
     &                        ' USER SET IFLAG NEGATIVE.')
2000  FORMAT(' TIME = ',F8.1,' SNSQ - INVALID INPUT PARAMETER.')
3000  FORMAT(' TIME = ',F8.1,' SNSQ - TOO MANY FUNCTION EVALUATION.')
4000  FORMAT(' TIME = ',F8.1,' SNSQ - XTOL TOO SMALL.',
     &                        '  NO FURTHER IMPROVEMENT POSSIBLE.')
5000  FORMAT(' TIME = ',F8.1,' SNSQ - ITERATION NOT MAKING GOOD',
     &                        ' PROGRESS.','IBLK=',I3)    ! 3/1/96
C
     RETURN
     END
C
********************************************************************
```

VITA

Mahadevan Ramamoorthy \

Candidate for the Degree of

Master of Science

Thesis: APPLICATIONS OF HYBRID GROUND
SOURCE HEAT PUMP SYSTEMS TO
BUILDINGS AND BRIDGE DECKS.

Major Field: Mechanical Engineering

Biographical:

Personal : Born in Trichendur, Tamil Nadu, on Feb 28, 1974, to Harihar
Ramamoorthy and Devasena.

Education: Received Bachelor of Engineering in Mechanical Engineering from
Government College of Technology, Coimbatore, India in June 1996. Completed
the requirements for the Master of Science degree with a major in Mechanical
Engineering at Oklahoma State University in May, 2001

Experience: Worked as a Technical Officer at Hindustan Lever Ltd., Foods Division,
Coimbatore June 1996 to August 1997. Employed by Oklahoma State University,
Department of Mechanical Engineering as a graduate teaching assistant from
August 1998 to May 1999 and subsequently as a research assistant from June
1999 to December 2000.

Professional Memberships: American Society of Heating, Refrigerating, and Air
Conditioning Engineers, Inc.